28 February 1966

Report 6101
Volume I

Copy No. 53

(Title -- Unclassified)

CONCEPTUAL DESIGN STUDY REPORT
HYPERSONIC RAMJET RESEARCH ENGINE PROJECT

VOLUME I: ANALYSES

THE Marquardt CORPORATION

[redacted]

28 February 1966

Report 6101
Volume I

Copy No. 55

(Title -- Unclassified)

CONCEPTUAL DESIGN STUDY REPORT
HYPERSONIC RAMJET RESEARCH ENGINE PROJECT

VOLUME I: ANALYSES

[redacted]

[redacted]

28 February 1966

Report 6101
Volume I

(Unclassified Title)

CONCEPTUAL DESIGN STUDY REPORT
HYPERSONIC RAMJET RESEARCH ENGINE PROJECT

VOLUME I: ANALYSES

By T.G. Piercy

Prepared under Contract NAS 1-5117
THE MARQUARDT CORPORATION
Van Nuys, California

for

NATIONAL AERONAUTICS AND SPACE ADMINISTRATION
Langley Research Center

FOREWORD

This Conceptual Design Study Report was prepared in compliance with NASA Statement of Work L-4947, Hypersonic Ramjet Research Engine Project - Phase I, Conceptual and Preliminary Design, dated 15 April 1965, including Addendum No. 1, dated 26 April 1965. Substantiating data and analyses are included in the appendixes to this report (Volume II).

ACKNOWLEDGMENT

The Marquardt Corporation acknowledges the assistance of the Office of the Program Manager for the Hypersonic Ramjet Research Engine Project at the Langley Research Center. The quick response to questions of interpretation of the Statement of Work and the answers supplied to questions concerning the X-15 and its operation greatly aided the contractor in establishing an orderly procedure for conducting these studies. Contributions of the following personnel toward the material incorporated in this report are also acknowledged: Messrs. J. Bendot, J. Hawke, R. I. Ozawa, M. Mandel, A. Martelluci, L. Morretti, A. Marino, and H. Stein.

TABLE OF CONTENTS

TABLE OF CONTENTS (Continued)

TABLE OF CONTENTS (Continued)

LIST OF TABLES

LIST OF FIGURES

LIST OF FIGURES (Continued)

LIST OF FIGURES (Continued)

LIST OF FIGURES (Continued)

CONCEPTUAL DESIGN STUDY REPORT

HYPERSONIC RAMJET RESEARCH ENGINE PROJECT

VOLUME I: ANALYSES

By T. G. Piercy

1.0 SUMMARY

Analyses and studies leading to the selection of an engine concept to be further studied and refined during the preliminary design portion of the Hypersonic Ramjet Research Engine Project are described.

Based upon Marquardt's previous ramjet and Scramjet component and engine studies and test experience, six baseline engine configurations were defined, each of which is believed to be capable of meeting minimum performance, operational and safety requirements. In developing the engine concept, studies were made of the performance requirements and functional relationships of the inlet, combustor, and nozzle components. Ramjet cycle analyses were conducted to define the potential performance of each engine concept. Structural and cooling concepts and development requirements were studied to a depth necessary to insure a sound basis for the engine concept selection. Also, each engine concept was reviewed as to its compatibility with the X-15A-2 and the goals for maximum safety for the X-15 and its pilot.

In reviewing the requirements and guidelines for this work, two areas were considered as deserving special attention. A requirement early recognized was that of providing adequate engine performance over the required speed range. At low speeds, air flow spillage must be minimized and internal contraction must be small to prevent choking of the inlet and to readily permit inlet starting. On the other hand at the higher speeds, additional contraction is required to meet the performance requirements. These requirements have been approached from two ways, namely, the use of variable geometry to match spillage and contraction requirements, and the use of thermal compression with low contraction ratio fixed geometry inlets. Secondly, in developing criteria for the engine concept selection, it was recognized that the selected ramjet engine should provide as much research flexibility in design and operation as possible such that it might provide a maximum of research data to aid the design of future practical airbreathing hypersonic ramjet engines. The engine selection criteria therefore included performance, flexibility, and structural aspects including cooling, development requirements, and the applicability to practical flight configurations.

The recommended engine configuration resulting from these studies employs thermal compression to obtain performance levels exceeding the minimum performance goals in a fixed geometry low contraction ratio engine geometry. Highly swept leading edges reduce leading edge heat load and aid in promoting inlet starting at the low Mach numbers required. The basic inlet is square

in cross section, and a single contoured centerbody is employed to provide non-uniform aerodynamic compression which is integrated with the distributed fuel injector pattern of the combustor. Functional flexibility goals are reflected in the engine's capability of operation over the entire flight envelope of the X-15A-2, in its ability to be operated in a subsonic combustion mode in the lower speed ranges, and in its incorporation of replaceable leading edges on the inlet cowl and centerbody tip.

Supporting analyses and experimental test results, together with general substantiating material are included in the appendixes (Volume II) of this report.

2.0 INTRODUCTION

NASA has taken an admirable step toward the development of the hypersonic ramjet engine by its sponsorship of the Hypersonic Ramjet Research Engine Project. System studies have increasingly been concerned with hypersonic lifting vehicles for applications to various long range earth-to-earth and earth-to-orbit missions as well as to military missions in the earth's atmosphere requiring great speed with economy of operation. The high specific impulse of the hypersonic ramjet engine makes it especially attractive as a source of propulsive thrust for these missions.

As correctly noted by NASA, there is a substantial background in component research in relation to hypersonic airbreathing propulsion, indicating attractive performance potentials above Mach 6 with supersonic combustion and below Mach 6 with subsonic combustion. However, this research has not as yet culminated in the design and test of a single flightweight hypersonic ramjet engine system possessing the predicted flexibility and performance over the speed range shown to be of interest in some mission analyses and system studies. The engine system tests that have been conducted, while yielding valuable experience and design information, have been restricted to simple cold wall boilerplate type construction with tests at specific Mach number-temperature conditions.

Phase I of the Hypersonic Ramjet Research Engine Project encompasses the analyses and studies leading to the selection and definition of the best possible research engine, the development of the preliminary design of the selected engine concept, and the preparation of a development plan for that engine. The engine will be test flown under the X-15A-2 research airplane over a Mach range of 3 to 8 and at altitudes ranging from 50,000 to 122,000 feet. In addition to meeting certain minimum performance and safety requirements, it is recognized that the selected ramjet engine should provide as much research flexibility in terms of design and operation as possible so that it may provide needed research data to aid the design for future airbreathing hypersonic ramjet engines. This report presents the results of studies and analyses leading to the selection of the best possible research engine.

3.0 GUIDELINES AND EARLY MARQUARDT DECISIONS

The general guidelines for the development of a research oriented hypersonic ramjet engine are summarized in Table I. The engines will be tested underneath the X-15A-2 airplane at speeds ranging from Mach 3 to Mach 8 and at altitudes from 50,000 to 122,000 feet. The flight boundaries of the X-15A-2 airplane are shown in Figure 4 of Appendix A to the Statement of Work (L-4947).

The NASA Statement of Work (L-4947) specifies that the contractor shall select a design-Mach number-altitude profile for his engine within the flight envelope of the X-15A-2 and on or above the line B-B (Paragraph 4.1). However, it is requested that the engine be operational over a 15,000-foot range over this design Mach number altitude profile (Paragraph 4.1.3). As shown in Figure 1-A, a Marquardt objective will be to make the engine operational over the entire X-15A-2 flight envelope to increase the engine's research flexibility.

It is also a Marquardt objective to provide research flexibility through versatility of combustor operating mode. The Statement of Work requires supersonic combustion at speeds from Mach 6 to 8, with a special requirement for supersonic combustion at Mach 5 to provide correlation between ground test facility and flight test results. As shown in Figure 1-B, the engine will be designed for supersonic combustion capability over the entire X-15A-2 flight envelope. Supersonic combustion at the higher speeds will utilize thermal compression, or distributed heat release, to produce acceptable performance levels, with low contraction typical of fixed geometry inlets. Dual mode capability is also an objective. The extent of the flight envelope for which subsonic combustion will be tested will be determined during the preliminary design activities of this Phase I program.

The Statement of Work directs that the contractor assume the engine to be outside of the flow field of the X-15A-2 for basic analyses and preliminary design. Performance requirements for this uniform free stream flow field in terms of internal thrust coefficient and fuel specific impulse are shown in Figure 2. However, the engine shall be capable of operation at angles of attack as much as plus or minus 4.5° and shall accept the nonuniformity of the X-15A-2 flow field for as much as 10° without greatly compromising the performance. Installed performance will be predicted for a minimum of four conditions for the engine selected for preliminary design.

The allowable spread in maximum inlet capture area is 1.76 to 3.14 sq ft. An early decision was made to design to the minimum allowable capture area of 1.76 sq ft. This decision was based upon a desire to minimize engine fuel flow and to minimize engine weight, and is further discussed in Section 5.1.1.7 of this report. Also an early decision was made to utilize the maximum allowable nozzle exit area of twice the inlet capture area. This gives a higher internal thrust at the expense of some increase in external drag.

X-15A airplane requirements and the information contained in Appendix A of the NASA Statement of Work are summarized in Table II for reference purposes. The information covered includes engine installation, engine attachment, engine operation, and the flight test aspects of the hypersonic ramjet experiment.

4.0 ENGINE SELECTION CRITERIA

Criteria for selection of an engine concept (upon which to initiate preliminary design activities) were established early to carry out meaningful comparative studies. Nine items are listed in Paragraph 5.1.2 of NASA Statement of Work (L-4947) to be included in the engine comparative studies.

The method of approach which was adopted is indicated in the diagram that follows. Several configurations were defined and screened during an engine concept definition activity. Only those configurations judged capable of meeting the minimum NASA requirements were selected as candidates. The candidate engine concepts were then examined and compared from three primary points of view, namely, engine performance and operational flexibility, mechanical and structural design including the engine cooling aspects, and the relative development requirements. Interrelations between each of the three categories were necessarily examined. Out of this comparison, based upon appropriate weighting factors, an engine concept was selected.

Table III presents a breakdown of the major items considered under the performance, design, and development categories of the engine concept selection criteria.

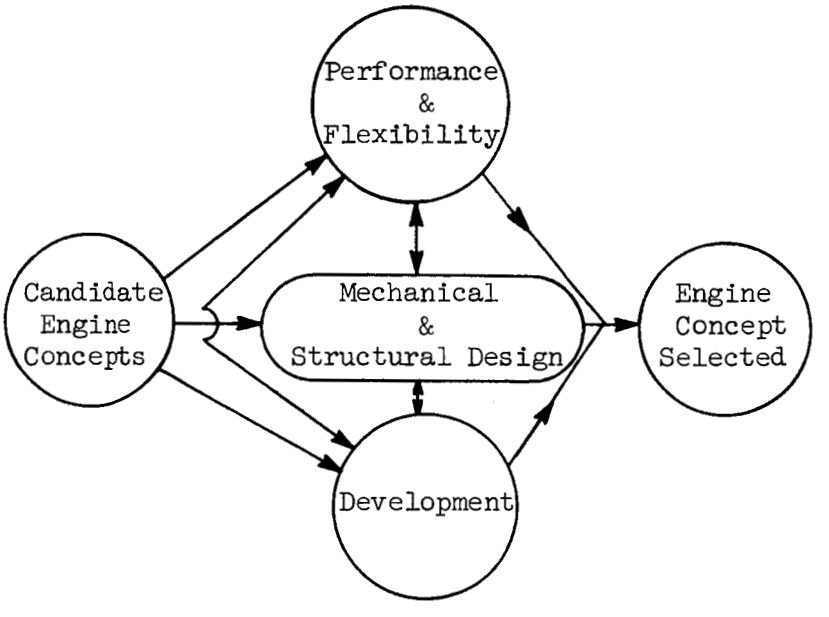

5.0 DEVELOPMENT OF ENGINE CONCEPT

5.1 Baseline Engine Configurations

At the initiation of the hypersonic engine project, a systematic review of the NASA Statement of Work was made to define the requirements of the flight research engine. In interpreting the general guidelines, it was recognized that operational and performance flexibility would be a prime requirement for

the research engine as reflected in the Engine Selection Criteria (Section 4.0). A parallel review was also made of previous Marquardt ramjet, Scramjet, and hypersonic engine studies, analyses, and tests conducted to date for comparison with these requirements.

A major problem early recognized was that of providing adequate engine performance over the required speed range. At low speeds, air flow spillage must be minimized and internal contraction must be small to prevent choking of the inlet and to provide startup. At the high speeds, additional contraction is required to meet the performance requirements. At least two approaches to this dilemma were obvious. The use of variable geometry configurations to match spillage and contraction requirements and the use of thermal compression with low contraction ratio fixed geometry inlets. Configurations employing these concepts were developed and included in the candidate engine concepts definition activity, and only those configurations judged capable of meeting the minimum NASA requirements were then analyzed. The surviving engine concepts are summarized schematically in Figure 3 and are shown individually in Figures 4 through 9. Pertinent features of each engine are summarized as follows:

Configuration A is an axisymmetric, variable geometry engine employing a translating centerbody. Based upon Marquardt's past experience, the meeting of minimum performance goals was insured. However, it was noted that the design and development of actuators and seals for a regeneratively cooled engine would require major effort.

Configuration B is on the opposite end of the development requirement spectrum, and it was chosen as a candidate because of its relatively straightforward design. This configuration is again axisymmetric but it employs a fixed geometry inlet with a conical centerbody spike wherein most of the inlet compression is achieved externally. Although design and development requirements were considerably eased, engine performance was known to be lower, whereas the spillage and external drag were considerably higher.

Configurations A and B produce relatively uniform flow at the throat and entrance to the combustor. By this it is meant that by symmetry, the flow is identical through any plane containing the axis of symmetry. By contrast, the remaining configurations of Figure 3 produce a nonuniform compression flow field for thermal compression purposes. As described in Reference 1, fuel is injected in discrete amounts into small regions of high compression and the compression resulting from the combustion of this fuel is used to raise the pressure of the surrounding air.

Configuration C represents again a circular fixed geometry engine but it employs thermal compression. Centerbodies of low surface area are utilized to provide regions of local high compression. The leading edges of the inlet are swept to promote inlet startup and to reduce the leading edge heating.

Configurations D, E, and F are, by means of contrast to A, B, and C, rectangular in cross section rather than circular. Hypersonic ramjet application studies conducted by Marquardt have shown maximum benefit to applications ranging from small missiles to large boosters and to cruise vehicles

employing the modular building concept using rectangular modules. Configurations D, E, and F all employ thermal compression and swept leading edges. The primary variable with these configurations is the size of the centerbody. In configuration D, one large centerbody is incorporated into an engine of square cross section. In Configuration E, one to three small centerbodies are utilized in an engine with rectangular cross section. Configuration F, modeled after Marquardt's "dual mode" engine being tested under Contract AF 33(615)-2834, contains no centerbodies.

These configurations formed the baseline engine configurations during the engine conceptual design phase. It was recognized that some design variation was possible within each configuration. For example Configuration B was later modified to Configuration B-1, incorporating an isentropic spike rather than a conical centerbody spike. Modifications later incorporated into Configurations D and E are also indicated in Figure 3.

5.1.1 Analyses.

5.1.1.1 Inlet.

5.1.1.1.1 Inlet objectives. Based upon the Statement of Work and Marquardt's interpretation of the guidelines, the aerothermodynamic objectives of the inlet may be summarized as follows:

a. The inlet should provide good performance over the Mach number range of 3 to 8, at altitudes from 50,000 to 122,000 feet, and should be adaptable to subsonic as well as to supersonic combustion modes.

b. The inlet contraction must be low enough to insure startup or restart at any Mach number down to 3.0 and yet provide sufficient contraction at higher speeds to provide adequate thrust performance.

c. Inlet spillage should be minimized at low speeds such that adequate thrust performance can be obtained.

d. Since the viscous losses in hypersonic inlets can be predominant, the inlet design should emphasize minimum wetted area. On the other hand, minimizing the wetted area should not be carried to an extreme because of possible boundary layer separation and inlet performance degradation due to too severe a pressure gradient upon the inlet compression surfaces.

e. Since the engine will be installed beneath the X-15A-2 airplane, the inlet should be relatively insensitive to these flow field effects. Slight changes of pressure recovery and mass flow are permissible. However, a primary concern must be that of maintaining a started inlet condition at the local Mach number and flow deflection at the inlet station.

Other objectives imposed by design, structural, and cooling considerations dictate the use of little, if any, variable geometry. Minimum coolant loads are desired, consistent with minimum inlet wetted area.

5.1.1.1.2 Applicable experience. An examination of the research and development history of ramjet engines discloses that combustors and engines cannot be developed independently of the inlet. The Marquardt Corporation, concerned with the research and development of ramjet engines, has through the years been a leader in the field of inlet technology and has produced several notable "firsts" in inlet development. Configurations developed have included two-dimensional, axisymmetric, and three-dimensional shapes and have operated over the range of Mach numbers from subsonic to Mach 22. A summary of inlet development at Marquardt and at its subsidiary, the General Applied Science Laboratories, is given in Appendix A (in Volume II of this report).

5.1.1.1.3 Inlet parameters. A typical inlet parameter chart, relating the various parameters generally used in describing inlet performance, is presented in Figure 10 for Mach 8. This plot was generated, using real gas properties, on Marquardt IBM equipment. For a given enthalpy ratio or static pressure ratio, the inlet process efficiency (K_D) increases with inlet contraction ratio (A_o/A_2). However, an optimum inlet, when considering realistic inlet efficiencies, must be defined in terms of its matching to the remaining portions of the cycle, that is the combustor and nozzle. This matching, for various combustion processes, i.e., constant area, constant pressure, constant Mach number, etc., was analyzed during the conceptual design stages as discussed in later sections of this report.

5.1.1.1.4 Inlet startup and contraction ratio. An extremely important inlet parameter is that of inlet contraction ratio. Assuming realistic inlet and combustion efficiencies, the inlet contraction ratio $(A_2/A_R)_{eff}$ required to meet the minimum performance requirement of the NASA Statement of Work may be defined as shown by the upper dashed line in Figure 11. The lower dashed line indicates the larger contraction ratio (A_R/A_2) required to meet the performance goals of the Statement of Work. At speeds below Mach 6, this lower dashed line has been broadened to indicate subsonic combustion (i.e., to obtain the performance goals, the momentum losses due to heat addition must be minimized). The effective contraction ratio of a fixed geometry internal contraction inlet that will meet the requirement for startup at Mach 3.0 is shown at the higher speeds to provide insufficient contraction to meet the minimum performance requirements. With conventional fixed geometry systems, additional contraction (to meet the performance requirements) is limited because of the startup requirements. Variable geometry systems, of course, would satisfy both contraction ratio startup and performance requirements. The proposed thermal compression concept also satisfies both startup and performance requirements but does not require translating or moving compression elements. The effective contraction ratio of a thermal compression system is shown for comparison in Figure 11.

The effect of a change in the effective contraction ratio on thrust coefficient implied above is shown in Figure 12. This curve indicates that an increase in thrust coefficient of 0.035 will result from an 0.01 decrease in contraction ratio A_2/A_R (or an 0.01 increase in A_R/A_2) at Mach 5.0. The increase in thrust with increase in contraction ratio A_R/A_2 is associated with higher cycle efficiency of the inlet-combustor combination. As the inlet contraction is increased, the static enthalpy and pressures increase while the Mach number decreases. Within the limits of the amount of fuel that can be added during combustion, combustion efficiency increases and combustor total pressure losses decrease with decreasing combustor Mach number.

The effective contraction ratios at various Mach numbers for the inlet configuration of Figure 3 are summarized in Table V. The effective contraction ratios of Configurations B and B-1 are low due to their external compression design. Configurations C, D, E, and F all employ thermal compression and the effective contraction is that corresponding to the initiation of combustion under the thermal compression process. The inlet produces this contraction only locally to initiate combustion. It will be noted that the contraction ratio A_R/A_2 of variable geometry Configuration A is less than those of the thermal compression designs. Because Configuration A is symmetric, the compression produced by the inlet is symmetrical in any plane containing the axis of symmetry, rather than just locally. The maximum compression is, therefore, reduced for Configuration A based upon Marquardt's experience as to the amount of maximum internal contraction possible with axisymmetric inlets. This subject is further discussed in Appendix A.

In the design of fixed geometry inlets, maximum use of the benefits of leading edge sweep must be made. To achieve the maximum effective contraction, leading edge sweep will permit larger contraction ratios than those indicated by one-dimensional Kantrowitz limits. (This subject is also further discussed in Appendix A.) Similarly leading edge sweep permits reduced maximum lip material temperature for a given leading edge radius.

5.1.1.1.5 Preliminary analyses of viscous, heat transfer, and leading edge blunting effects. The diffusion process is the most sensitive phenomenon of the Scramjet engine in terms of its effect upon ramjet engine performance. In the range from Mach 4 to 8, a one count decrease in inlet kinetic energy efficiency will decrease the thrust coefficient by about 3 counts. Similarly, the ramjet thrust is directly proportional to the air flow through the engine. Analyses of the inlet efficiencies and spillage characteristics of the inlets of the candidate engine configurations were therefore made. The overall inlet efficiency is the result of viscous, heat transfer, leading edge bluntness, and shock losses. Typical losses are described as follows, and then the performance characteristics of the various configurations are compared.

$\frac{\Delta C_T}{\Delta \eta_{KE}} = 3$

5.1.1.1.5.1 Leading edge bluntness. Shock losses for sharp leading edge surfaces are well documented in the literature. However, additional losses are incurred due to leading edge bluntness which is necessary to reduce material temperatures to acceptable levels. Figure 13 presents a parametric study of leading edge bluntness losses for conventional rounded leading edges. The leading edge total pressure loss is seen to decrease as the flight Mach number decreases, as the leading edge sweep increases, or if the leading edge radius is reduced. For the non-swept axisymmetric Configurations A and B, the leading edge bluntness must be increased to achieve allowable material temperatures, with associated larger losses. For these configurations, the leading edge losses may be reduced by proper attention to leading edge shape such that the detached bow wave is more rapidly bent back to approach the angle corresponding to the sharp leading edge value (Reference 3). For the swept configurations, the conventional rounded leading edge losses are negligible except in the corners or notches of these configurations.

5.1.1.1.5.2 Viscous effects. Total pressure losses due to viscous drag upon the inlet compression surfaces can be predominant. In addition, if the Reynolds number is not sufficiently high to provide transition prior to the imposition of an unfavorable pressure gradient due to compression surface contour or shock impingement, flow separation may occur with resultant unsatisfactory inlet operation. Typical boundary layer separation criteria, based upon the data of Reference 2, are shown in Figure 14. These data are extremely meager at the Mach numbers and pressure ratios of interest to this ramjet study. Fortunately both sweep and wall cooling promote early transition. Bluntness, however, delays transition as shown in Reference 4.

For comparative purposes, it has been assumed that early transition to turbulent flow for all inlet configurations has occurred for the low altitude flight path. Viscous drag has thus been estimated from compressible turbulent friction coefficients together with the appropriate wetted areas of each configuration (Table IV). The variation in Reynolds number across the ramjet flight envelope is also shown in Figure 14. The change in inlet performance as a function of Reynolds number and contraction ratio is depicted in Figure 15 for a typical configuration. These effects were determined by equating the viscous friction through the momentum relations into an equivalent drag and total pressure loss. For example at Mach 8 and for an equivalent contraction ratio of $A_2/A_R = 0.05$, the reduction in total pressure recovery (P_{T_2}/P_{T_0}) in transversing from the high q trajectory to the low q trajectory is about 0.035 for inlet Configuration E.

Viscous effects upon effective contraction are shown in Figure 16. The changes in Reynolds number due to altitude, Mach number, and contraction ratio were related to the overall boundary layer and displacement thickness assuming a constant boundary layer form factor. The changes in boundary layer displacement thickness were then related to the change in effective area at the throat by considering the perimeter at the throat station. The effects are, as expected, rather small. The largest change in effective contraction ratio occurs at Mach 8. As an example, an effective contraction ratio of 0.05 would decrease about 4% in going from the minimum altitude to the maximum altitude.

5.1.1.1.5.3 Heat transfer effects. The inlet parametric conversion charts, an example of which was presented in Figure 10, have been prepared for adiabatic as well as for non-adiabatic conditions. Using this material, Figure 17 has been prepared, relating the change in inlet kinetic energy efficiency due to heat extraction from the inlet (by either radiative or regenerative cooling). The curve shown is applicable to a wide range of inlet process efficiencies (K_D) and inlet contraction ratios.

A typical heat removal of 0.5% at Mach 8 therefore results in about a 0.55% reduction in inlet kinetic energy efficiency. The change in inlet process efficiency would depend upon the state process along the wall, considering the mode of heat removal. However, a preliminary analysis indicates approximately a one count reduction in K_D for a one count reduction in total enthalpy.

5.1.1.1.6 Typical inlet loss summary. A typical inlet loss summary for Configuration E is shown over the Mach 3 to 8 range for the low altitude trajectory in Figure 18. The losses shown summarize the (sharp leading edge) shock losses, additional shock losses due to leading edge bluntness, and combined viscous and heat losses. The lower curve then corresponds to the final pressure recovery estimate for the configuration. It is noted that the viscous losses are significant. For this inlet, the effective inlet contraction ratio varies from about 0.15 at Mach 3 to 0.05 at Mach 8.

5.1.1.1.7 Summary of inlet efficiency and spillage characteristics. Analyses of the shock, leading edge bluntness, viscous losses, and heat losses have been conducted for the inlet configurations of Figure 3, culminating in final pressure recovery estimates over the Mach number range shown in Figure 19. In addition, the air flow spillage characteristics have been estimated accounting for the inlet geometries, shock structures, and local contraction ratios. (Viscous effects upon spillage characteristics are believed negligible.) Also, these results are tabulated in Table V along with other component efficiency and geometric data for the various engine configurations.

The pressure recovery of variable geometry Configuration A is about equivalent to that of fixed geometry Configurations D and E. For Configuration A, the conventional shock losses are negligible. However, the viscous losses are quite large due to its large wetted area on the centerbody and internal cowl surfaces (Table IV). Leading edge losses are also quite large due to the fact that the cowl surfaces are normal to the local flow. Full capture mass flow occurs at Mach 6. It will be noted that bleed has been assumed necessary to achieve the performance quoted for Configuration A based upon previous Marquardt experience.

Configuration B, the fixed geometry external contraction inlet designed for full capture at Mach 8, did not meet minimum performance goals due to insufficient contraction and its large spillage at low Mach numbers. Configuration B-1 employing a fixed geometry isentropic contour spike designed for full capture at Mach 6 with a small amount of internal contraction was conceived as a revision. As is shown in later sections of this report, this

configuration satisfies the minimum performance goals. However, Configuration B-1 is a high external drag configuration. The remaining configurations, (C, D, E, and F) employing thermal compression with fixed geometry all showed similar characteristics of pressure recovery and mass flow. The lower pressure recovery of the square Configuration D with a large single centerbody is due to its larger viscous losses. Several revisions to Configuration D (up to D-6) were later evolved to increase its performance and to reduce its weight and heat load.

5.1.1.2 Combustor.

5.1.1.2.1 Combustor objectives. Based upon the Statement of Work and Marquardt's interpretation of the guidelines, the aerothermodynamic objectives of the combustor may be summarized as follows:

a. High combustion efficiency and flexibility of operation over the Mach number range of 3 to 8, at altitudes from 50,000 to 122,000 feet, and adaptable to subsonic as well as supersonic combustion modes. To achieve these objectives attention must be given to inlet-combustor matching, fuel scheduling, and location and design of fuel injectors.

b. Momentum losses due to fuel injection to be minimized consistent with fuel injection required for fuel and air mixing and for high combustion efficiency.

Other considerations imposed by design structural and cooling considerations dictate the use of a desirable structural configuration and the use of minimum length and wetted area.

5.1.1.2.2 Applicable experience. The Marquardt Corporation, since its inception over two decades ago, has been a leader in the fields of fuel injection, mixing, and combustion for ramjet applications. The Marquardt Corporation became a pioneer in the field of supersonic combustion in 1957, supported by what is now the Air Force Aero Propulsion Laboratory. A summary of fuel injection and combustor development at Marquardt and at its subsidiary, the General Applied Science Laboratories, is given in Appendix B. In addition a topical report (Reference 5) has been prepared, which presents analytical methods of analysis of the mixing and reaction of hydrogen and air, comparisons with experimental test data, and application to the design of Scramjet combustors using thermal compression. Also Appendix C correlates mixing data from Marquardt and other sources with the objective of outlining the steps required for the practical design of Scramjet combustors.

5.1.1.2.3 Inlet-combustor interaction. To indicate the inlet-combustor interaction for maximum cycle performance, the total pressure recovery at the inlet and at the combustor exit are shown for a range of effective inlet contraction ratios and for various supersonic combustor modes in Figure 20 for

a free stream Mach number of 8. The upper line represents a typical total pressure recovery that might be obtained with a variable geometry inlet operating at a constant process efficiency K_D of 92%. The lower lines in this figure depict the total pressure at the end of the combustor for various supersonic combustion processes. The vertical distance between the upper and lower lines is thus representative of the total pressure loss across the combustor. As the inlet contraction $(A_R/A_2)_{eff}$ increases, the Mach number into the combustor decreases, and the total pressure recovery across the combustor increases. It is noted that at this Mach 8 condition, a maximum total pressure at the end of the combustor requires an overall inlet contraction ratio $(A_R/A_2)_{eff}$ of about 20 to 25. With fixed geometry systems employing three-dimensional flows, the geometric overall contraction ratio is believed limited to the 5 to 8 range if inlet startup is to be achieved at Mach 3.0. (Note: The reader must remember that inlet spillage further reduces the actual contraction to acceptable values.) However, with thermal compression and distributed heat release, an inlet with local geometric contraction ratios of 6 can be operated to provide an effective contraction ratio A_R/A_2 of about 20. Thus, efficient operation across the speed range required can be obtained without variable geometry.

A similar graph of inlet combustion interaction at Mach 4 is presented in Figure 21. At Mach 4.0, the contraction ratio for maximum cycle performance is considerably reduced and is much closer to the contraction ratio limit for startup at Mach 3.0. The requirement for thermal compression for higher cycle efficiency is therefore considerably reduced. The primary purpose of Figure 21, however, is to show the subsonic combustion mode and its comparison to supersonic combustion. It is assumed in this figure that subsonic combustion is achieved by transversing a terminal shock at or near the inlet minimum flow area. The air behind the terminal shock is allowed to diffuse somewhat before combustion is initiated. The total pressure losses for this combined diffusion and subsonic combustion are shown. The resultant total pressures at the end of combustion are considerably higher at Mach 4 for subsonic combustion, in consonance with the higher cycle efficiencies characteristic of subsonic combustion at this Mach number.

In Figures 20 and 21, several supersonic combustion modes have been depicted for illustration. The line labeled constant A-M indicating that the fuel is burned in a constant area duct until Mach 1.0 is reached (after which the duct is expanded and the remaining fuel is burned at constant Mach number), may be seen in these examples to give the highest pressure at the combustor exit. However, in an actual engine, the combustion mode must consider the physical combustor contours and length, limitations imposed upon the practical number and location of fuel injectors, the Mach number range to be covered, etc. Combustor design thus involves many compromises. Constant pressure combustion has been assumed herein as a design goal. This mode appears most likely to satisfy the requirements for efficient, smooth, steady, diffusion-controlled reaction.

5.1.1.2.4 Thermal compression concept. It is desired that the schedule of inlet compression required over the Mach number range be achieved without the use of variable geometry. At the lower speeds, low compression is needed

to avoid excessive spillage and to promote inlet startup. As the flight speed is increased, the spillage will decrease and a higher compression is desired for cycle efficiency. Accordingly, the fixed geometry inlet must be designed for low compression. Three-dimensional effects are used to provide high pressures locally which will not choke the inlet and which will permit the initiation of combustion. This initial combustion is used to provide additional compression of the main air flow. As the flight speed is increased, more fuel is injected and burned in the high pressure region. By proper distribution of the fuel, the desired compression schedule can be obtained to provide efficient performance over the required speed range.

This concept is illustrated in Figure 22 at Mach 8. An inlet with an average geometric contraction ratio of 6 is represented by the triangle symbol. Locally, in the region of the centerbody, the flow is compressed the equivalent of a contraction ratio of 20. Fuel is injected and burned at this small region of high compression, rather than allowing the flow to mix to a low pressure value before the addition of fuel. The resulting combustion is used to gradually compress the main portion of the air flow to the higher pressure at which additional fuel is injected and burned. The schematic line labeled "thermal compression" in Figure 22 indicates this process. It will be noted that somewhat lower total pressures at the combustor exit will result from thermal compression as compared to results with higher aerodynamic compression (circle symbol) and constant pressure combustion. This difference reflects the somewhat higher efficiency of aerodynamic versus thermal compression. However, the resulting pressure at the combustor exit exceeds considerably that of the low contraction fixed geometry engine with uniform fuel injection.

This process is fully explained in Reference 1, using the techniques and methods of Reference 5. Both References 1 and 5 are submitted as topical reports to the Hypersonic Ramjet Experiment Project.

5.1.1.2.5 Combustor area change requirements. The results of the analyses of combustor area change requirements over the Mach number range from 3 to 8 are shown in Figure 23. For good cycle efficiency, it is desired that the combustor area ratio A_3/A_2 be a minimum, or that the combustor pressure recovery (P_{T3}/P_{T2}) be a maximum. It will be noted in Figure 23 that subsonic combustion at the lower speeds provides the best cycle performance. Thermal choking in the subsonic combustion mode is assumed and has been demonstrated experimentally. The following illustrates the supersonic combustion processes: At free stream Mach 4, the inlet diffuses the air to Mach 1.5. For the line labeled "constant area and constant Mach" combustion is originated at Mach 1.5 in a constant area duct until a local Mach number of 1.11 is reached. The remaining fuel for $\phi = 1$ is burned at constant Mach 1.11, resulting in an overall combustor area ratio of about 5. At Mach 8, the inlet compresses the flow to Mach 3.0 and all of the fuel can be burned in a constant area duct. If the Mach 3.0 stream is burned at constant pressure, the area ratio required across the burner is about 3.0. Below a free stream Mach number of about 5, the flow cannot be completely burned in the constant pressure mode because of thermal choking. Constant Mach combustion requires very large area ratios and was omitted from Figure 23.

The actual area ratios and supersonic combustion modes in an engine must take into account the desired engine Mach number and altitude ranges, the limitations of finite fuel injector locations and number of injectors, and the necessity for continuous wall cooling which may dictate the use of all fuel injectors at all operating points.

5.1.1.2.6 Fuel injection and stationwise fuel distribution. Requirements for minimum engine weight and minimum surface area with high combustion efficiency require that the reaction of the hydrogen with the oxygen of the air be accomplished in the shortest possible length. It has now been generally concluded that the supersonic heat addition process above Mach 5 is controlled primarily by the rate of mixing of the fuel injected into the air stream, since the ignition delay and reaction times for hydrogen are small when compared to the rate of diffusion. Below this Mach number, stagnation temperatures are sufficiently low that positive and active ignition techniques are required to initiate combustion.

Analyses of fuel injection are therefore directed at promoting the fuel and air mixing. These analyses are extremely complex, involving highly turbulent flows of dissimilar gases in which the turbulent transport mechanisms plays a big role. Simplifying assumptions are generally introduced which prevent the results from completely representing the practical cases. This subject is discussed in Appendix C and Reference 5.

For our purposes here, we have drawn upon experimental techniques and results to provide a reasonable description of the mixing process. For engines of small characteristic dimensions (i.e., the height or transverse distance across the combustor), the fuel may be injected from flush injectors parallel to the wall. Short mixing lengths can then be obtained by supplying a sufficient number of injectors around the combustor periphery. However, as the combustor characteristic dimension increases, adequate dispersion of the fuel into the air stream requires that the fuel be injected at an angle into the air stream, or injectors may be placed across the duct channel to promote mixing. For either of these cases, some pressure losses are introduced because of the formation of shocks caused by the impinging fuel jets or by the struts. The total pressure losses as a function of fuel injection angle are shown in Figure 24. The net effect of various types of fuel injector-strut combinations from 8000 fps combustion tests conducted by Marquardt are shown in Figure 25. For this particular combustor, the net specific impulse (a measure of combustion efficiency and therefore mixing) increased with the fuel injection angle and the addition of struts to carry the fuel across the duct, i.e., the losses due to strut and fuel injection angle were more than offset by improved mixing.

With the exception of Configuration F, the engine configurations selected for study utilized centerbodies supported by struts from the outer combustor walls, and the characteristic dimension of the engines are such that parallel injectors provide adequate mixing. As is discussed in the Preliminary Design Report, Reference 8, selected individual fuel injectors will also be extended into the combustor gas stream off the wall in order to promote fuel mixing and reduce wall heat fluxes.

Analyses of the fuel injection must also consider the longitudinal fuel injection. The fuel must be distributed longitudinally to avoid shock formations to reduce peak heat loads to the combustor walls, and to account for the change in area requirement across the combustor with Mach number (Figure 23). Assuming for the moment a combustor wall formed by conical expansion, the fuel may be injected and burned near the entrance to this section at high flight speeds. However, at lower flight speed, this same fuel injection location may choke the combustor. Thus for the later case fuel must be injected into a larger area (i.e., further downstream). Necessary cooling of the combustor walls with the fuel prior to fuel injection is also a factor in stationwise fuel distributions, as shown in the next example.

Typical fuel injector stations and the distribution of fuel per injector station are shown in Figure 26 for a typical engine configuration. The total fuel flow at each Mach number corresponds to $\phi = 1.0$. Fuel injector Station A is at the maximum diameter station of the centerbody and is the primary thermal compression injector. However, at low speed its use is limited to reduce any tendency to unstart. Consequently, injector B, which encompasses the aft section of the centerbody as well as the swept top and bottom wall, is utilized at low speed as the primary thermal compression control. Injector D, along the side walls, is used primarily at low speed. At low speeds, injectors C and D predominate, whereas at high speeds injectors B and C predominate.

The predicted effect of distributed fuel injection (thermal compression) on the contraction ratio of a typical engine configuration is shown in Figure 27.

5.1.1.2.7 Fuel ignition and reaction kinetics. It was stated in paragraph 5.1.1.2.6 that ignition delay and reaction times are small when compared to the rate of diffusion. This statement must now be qualified by the statement that combustion has been initiated. For combustion pressures of one atmosphere, a stoichiometric mixture of hydrogen and air will autoignite with reasonable ignition delay times at about 1700°R. Results of shock-tube ignition characteristics from Reference 6 are presented in Figure 28. For the Mach numbers and pressures expected in the hypersonic ramjet project combustor, an ignition source will be required for engine startups at about Mach 5 or less. Once ignited, ramjet combustion can be sustained at lower Mach numbers (ambient temperatures) if the fuel is heated as in a regenerative chamber. For example combustion has successfully been sustained at one atmosphere pressure with Mach 2 temperatures (Reference 3).

The combustion efficiency of a typical ramjet combustor is a function of the degree of mixing of the fuel into the air and upon the degree of completion of combustion of this mixture in the engine. For a given length combustor, the degree of completeness of combustion is a function of the ignition and reaction times. In order to estimate the combustion efficiencies of the various engine configurations over the Mach range 3 to 8, it was necessary to assume a fuel injector pattern and to estimate the reaction kinetics. Figure 29 is a typical map of combustor inlet conditions for two

values of effective inlet contraction ratio. Using these conditions, the total reaction time for 95% release of total heat was determined using the results of Marquardt's IBM kinetics program. In making the estimates of combustion efficiency for each configuration, allowance was made for the fact that mixing and reaction occur simultaneously, and for the range of conditions investigated, the reaction speeds up the mixing processes.

5.1.1.2.8 Summary of combustion efficiency variations with Mach number. Combustion efficiences for the various engine configurations have been estimated for both high and low q flight boundaries at stoichiometric conditions over the speed range of Mach 3 to 8 (Figure 30). Consideration has been given to the combustor aerothermodynamic environment considering both mixing and reaction efficiencies. The nominal combustor region is approximately 20 inches long, dictated largely by the swept fuel injection pattern.

Efficiencies of at least 95% should be achievable for subsonic combustion based upon the aerothermodynamic environment. The upper value of combustion efficiency is defined primarily by mixing efficiency which is limited by practical considerations of the fuel injector stations and numbers of injectors.

Somewhat higher efficiencies for the low q flight boundary are predicted upon the basis of mixing which is promoted at the low q condition.

5.1.1.3 Nozzle.

5.1.1.3.1 Nozzle objectives. The aerothermodynamic objectives for the nozzle are as follows:

a. To attain high nozzle efficiency over the Mach range 3 to 8 and for the altitude range of the hypersonic ramjet experiment project engine.

b. The provision of efficient matching of nozzle-combustor components over the speed range considering the dual mode objectives imposed upon the design.

c. To provide optimum nozzle area expansion considering the speed range of operation and the installational limitations of paragraph 4.3.1.2 of Statement of Work (L-4947).

Other objectives include the use of desirable structural configurations using fixed geometry components of minimum wetted area and length for minimum cooling requirements consistent with the performance goals.

5.1.1.3.2 Applicable experience. Since 1957, Marquardt has been engaged in a continuing series of programs combining detailed analysis with experimentation to assess the progress of recombination in exhaust nozzle systems and

the resulting effects upon engine performance. Increasing degrees of sophistication have been accomplished, leading to the capability of designing exhaust nozzle systems with a high confidence level that a maximum degree of recombination consistent with practical hardware limitations will be obtained. A summary of this nozzle development is given in Appendix D.

5.1.1.3.3 Inlet-combustor-nozzle interaction. The total pressure through the inlet, combustor, and nozzle are traced as a function of effective inlet contraction ratio in Figure 31 for free stream Mach 8. This plot utilizes the same data as in Figure 20 but it has been expanded using a logarithmic scale to enlarge the ordinates. It will be noted that the optimum inlet contraction, i.e., the inlet contraction $(A_R/A_2)_{eff}$ for which the total pressure recovery across the engine is a maximum, shifts to a somewhat lower value when the nozzle losses are included. Nozzle losses are chargeable to divergence, viscous effects, and nonequilibrium conditions. As the inlet contraction ratio is increased for a given overall engine area ratio, the nozzle losses, paricularly those losses due to nonequilibrium, increase. The sources and mangitude of the nozzle losses are next discussed.

5.1.1.3.4 Nozzle parameters. A typical nozzle parameter chart, relating those parameters used to describe nozzle performance and efficiency, is shown in Figure 32. Charts of this type have been prepared for adiabatic as well as for non-adiabatic conditions and for a range of entrance Mach numbers, temperatures, and pressures characteristics of the Hypersonic Ramjet Experiment Project.

5.1.1.3.5 Nozzle area expansion. The performance of the Hypersonic Ramjet Experiment Engine is quite sensitive to the nozzle area expansion available. The internal thrust coefficient of the engine at a typical operating condition at Mach 8 is shown in Figure 33 as a function of the overall engine area ratio A_4/A_R. Maximum internal thrust is obtained with a fully expanded nozzle ($P_4 = P_\infty$). At the conditions specified in Figure 33, the fully expanded nozzle corresponds to an overall engine area ratio in excess of 5.0. However, the Hypersonic Ramjet Engine is limited to an overall engine area ratio of 2 (paragraph 4.3.1.2). Figure 33 thus indicates the compromise to ramjet engine performance.

5.1.1.3.6 Viscid and inviscid losses.

5.1.1.3.6.1 Nozzle viscous losses. A parametric study of nozzle viscous losses has been conducted for a range of flight conditions, nozzle area ratios, nozzle divergence angles, and for supersonic and subsonic combustion modes for environments characteristic of the Hypersonic Ramjet Research Engine Project. The results in terms of nozzle kinetic energy efficiency are shown in Figure 34.

For a given nozzle area ratio, the resultant nozzle energy efficiency decreases rapidly with decreasing nozzle divergence (increasing nozzle length). The effect of inlet contraction ratio and combustion mode on the viscous losses are small. It can be seen that the viscous losses in the nozzle can be significant for nozzles with large surface area.

5.1.1.3.6.2 Nozzle divergence losses. Nozzle divergence losses, as defined by nozzle kinetic energy efficiency, are shown in Figure 35 for two-dimensional and conical nozzles. These losses are the result of departure from parallel axial flow at the nozzle exit. It is concluded that nozzle divergence losses are small for the range of divergence angles of interest and that increases in nozzle divergence angle to reduce viscous losses may be beneficial to overall cycle performance.

5.1.1.3.6.3 Nozzle losses due to non-adiabatic conditions. In Figure 36, the change in nozzle kinetic energy efficiency due to heat extraction (either by radiation and/or regenerative cooling) or by heat addition (due to heat release of reacting products in the nozzle section) is shown as a function of nozzle entrance Mach number. The curve shown is applicable for a range of nozzle process efficiencies (K_n) or total enthalpy ratios. The change in nozzle process efficiency due to non-adiabatic conditions is a function of the state process along the nozzle wall. Due to partial heat release in the nozzle, the overall effects of heat loss in the nozzle are believed small.

5.1.1.3.6.4 Nozzle losses due to nonequilibrium expansion. Parametric studies of the nozzle kinetic energy efficiency as a function of freezing area ratio in the nozzle were conducted. Typical results for a low q trajectory and for a range of Mach numbers are shown in Figure 37. Charts of this type have been used in conjunction with finite rate chemistry to estimate the nozzle nonequilibrium losses for the various engine configurations previously described over the Mach number and altitude range of interest. For example, the gas composition in a typical nozzle with supersonic combustion at Mach 8 at 120,000 feet is shown in Figure 38. The water and nitrogen constituents (mole fractions) reach equilibrium conditions quite early and are not shown. At this flight condition, it should generally be expected that the gas has reached equilibrium conditions at an area ratio between 2.5 and 3.0. In terms of nozzle process efficiency, a 5% error in nozzle process efficiency would result if equilibrium chemistry were assumed rather than finite rate chemistry at the high altitude condition.

5.1.1.3.7 Typical nozzle loss summary. Divergence, viscous, and nonequilibrium losses in the nozzle of engine Configuration E are summarized as a function of Mach number in Figure 39. For these preliminary studies, it has been assumed that the nozzle flow is adiabatic. The losses in Figure 39 reflect the aerothermodynamic conditions and the lines of Configuration E (Figure 8) and do not reflect a possible reduction in losses by the use of more divergent walls to reduce the viscous effects.

Optimization of the nozzle expansion angle will be of the type indicated in Figure 40. Nozzle friction and divergence loss factors are such that the overall nozzle efficiency may be improved by increasing the nozzle expansion angle from the current 6° for Configuration E to about 10° assuming a nozzle expansion area ratio A_4/A_3 of about 4. The nonequilibrium losses will increase somewhat but the net effect is an improvement in nozzle efficiency.

The estimated nozzle efficiency for Configuration E for both supersonic and subsonic combustion modes are shown in Figure 41. This chart again indicated the possible gain in optimizing the nozzle divergence angle.

5.1.1.3.8 Nozzle performance variation with Mach number. The resultant nozzle efficiencies for the various nozzle configurations considering divergence, friction, and nonequilibrium losses are summarized in Figure 42. The basic trends as evidenced by this chart are primarily associated with the wetted area and viscous friction of the various nozzle configurations with the higher wetted area configurations having the lowest nozzle efficiencies. Pertinent nozzle parameters for the various nozzle configurations are presented for reference in Table VI.

5.1.1.4 Ramjet cycle.

5.1.1.4.1 Ramjet cycle analysis objectives. The objectives of the ramjet cycle analyses are to define the component functional requirements, to establish the engine performance levels with these component efficiencies, and to establish the component area relationships and component integration.

5.1.1.4.2 Component functional requirements. An analysis was conducted to establish the component performances required such that the engine would meet the minimum performance goals of the Statement of Work (L-4947), and the results are shown in Figure 43. A nozzle kinetic energy efficiency of 95% was assumed. The effect of a change in nozzle efficiency from this value may be established with the aid of Figure 44.

The effects of a change in component performance in terms of kinetic energy efficiency on the internal thrust coefficient of the ramjet is presented in Figure 44. The order to their effects upon the engine thrust are the inlet, the nozzle, and the combustor.

The area requirements for the various components were summarized in Figures 11, 23, and 33.

5.1.1.4.3 Typical engine performance with supersonic combustion. The typical thrust coefficients of two conventional (one-dimensional) fixed geometry engine configurations, assuming reasonable component efficiencies

over the Mach number range, are presented in Figure 45. In each configuration, the inlet flow is compressed uniformly and burned at constant pressure. (At the lower speeds for each configuration, a portion of the combustion takes place at constant Mach number to avoid choking.)

It will be noted that the engine configuration having the low value of contraction ($A_2/A_R = 0.15$) will not meet the mimimum performance requirements at the higher Mach numbers. While the high contraction inlet will exceed the minimum performance requirements at high speeds, provision must be made to accomplish the startup requirements of the engine at Mach 3.0 as well as to improve its performance at Mach 4.0.

The dashed line represents the predicted performance of an engine utilizing thermal compression, which provides an effective contraction ratio (A_2/A_R) of 0.05 at high speeds and 0.15 at the lower speeds. At high speed, some performance decrement is expected in comparison to the geometric contraction 0.05 engine. This loss, thought to be conservative, is due to practical limitations of combustor length and area distribution and fixed fuel injector locations.

5.1.1.4.4 Thermal compression processes. The compression resulting from the mixing and combustion of hydrogen injected into the air stream must be accounted for in the design of the engine. In order to avoid the thermal choking of the combustor at low Mach numbers, consideration must be given to the stationwise fuel distribution. At the higher Mach numbers, the energy added by the combustion of the fuel is small in comparison to the kinetic energy of the air stream and thus the stationwise fuel distribution is less influenced by choking considerations. (It may, however, be influenced by combustor wall heat flux considerations.)

The application of thermal compression in the present Hypersonic Ramjet Experiment Project takes advantage of these principles. By distributed heat release, the compression resulting from the mixing and burning of a portion of the injected fuel can be used to raise the pressure (increase the effective contraction ratio) at which the remaining fuel is injected and burned. Thus, an engine inlet of modest geometric contraction ratio and low spillage can be used to satisfy the present Mach range and operational limits required. As the Mach number is increased, additional fuel is injected in the forward injectors to increase the effective contraction ratio of the inlet as required for performance considerations.

The theoretical approach to thermal compression is based upon the analyses of diffusion controlled, equilibrium combustion of hydrogen in air as reported in Reference 5. Also, the application of thermal compression to inlet-combustor design and interaction are given in Reference 1, along with appropriate substantiating data.

5.1.1.4.5 Subsonic combustion with thermal compression. Typical ramjet engine performance employing thermal compression in both supersonic and subsonic combustion modes is shown in Figure 46. With the subsonic combustion case, the fuel is injected and burned in a distributed manner such that a smooth transition to subsonic flow occurs, with a substantial amount of the fuel being burned subsonically. The flow is thermally choked in the nozzle.

This concept for transition to subsonic combustion is based upon jet mixing with combustion studies currently in progress. An example of these studies is shown in Figures 47 and 48 for a flight Mach number of 4 at an altitude of 75,000 feet, showing the results of a two-dimensional mixing analyses with turbulent diffusion and equilibrium combustion. The Mach number at the point of injection is 1.3, and hydrogen is expanded from a stagnation pressure of 200 psi with $\phi = 1.0$. The subsequent mixing and combustion is shown in three stages. In the first, a compression takes place which decelerates the flow gradually to subsonic speed. In the second, subsonic combustion continues at constant pressure. In the third zone, the flow is reaccelerated to supersonic. Tests to verify this process have been conducted. The distributed heat release method of conversion to subsonic combustion has two advantages over the conventional normal shock transition. First, the static pressure and temperature are reduced, and secondly, the necessity for control of the position of the normal shock in a swept duct is eliminated. However, some reduction in performance in the subsonic mode will be incurred. Both the conventional normal shock and thermal compression transitions to subsonic combustion will be studied.

5.1.1.4.6 Summary of supersonic combustion engine performance. Based upon the resultant inlet, combustor, and nozzle efficiencies previously presented, supersonic combustion ramjet cycle performance for the various engine configurations previously described has been determined as shown in Figure 49 for the high q portion of the flight envelope. Performance, in general, has been determined assuming a constant pressure combustion mode.

Configuration B, utilizing a fixed conical centerbody in an axisymmetric configuration, did not meet the minimum performance goals and is not presented. Configuration B-1 shown herein was modified to include an isentropic spike centerbody with full capture at Mach 6 rather than at 8 as was the case for Configuration B. With supersonic combustion, all configurations except Configuration B-1 met the minimum performance goals. (With subsonic combustion at the lower speeds, all configurations met or exceeded the minimum performance goals.) Configurations C, D, E, and F, employing thermal compression, are roughly comparable in performance. Only minor performance differences exist for the low q portion of the flight envelope in comparison to the results presented in Figure 49.

5.1.1.4.7 Summary of subsonic combustion engine performance. Subsonic combustion performance in terms of internal thrust coefficient and fuel specific impulse for the various engine configurations is presented in Figure 50 for the high q trajectory. As indicated, the minimum performance

goals can be met or exceeded with all configurations. The performance shown in this figure is based upon normal shock transition to the subsonic mode. Again only minor differences exist for the high altitude or low q trajectory.

5.1.1.4.8 Summary of component efficiencies and geometric factors. A summary of component efficiencies and geometric factors for the various engine configurations is presented in Table VII. The table includes operation at Mach 4, 6, and 8 in the supersonic mode, at Mach 3, 4, and 6 in the subsonic mode for high and low q flight paths.

5.1.1.5 Structures and cooling. The choice of a primary (cooled) structural concept and the thermal protection system is affected by many factors, ranging from overall system requirements, aircraft/engine interface, fabrication considerations, to component technology. In this engine concept study, preliminary consideration was given to the structural and cooling concepts such that relative evaluation and comparisons could be made. These preliminary studies included examination of the critical cooling conditions for the flight envelope and studies of critical component areas. The following guidelines and objectives which the final structural and cooling concept must satisfy were established as the result of the studies described herein: (1) Compatibility with the aircraft, its operation, and ground support, (2) Aircraft and pilot safety, (3) Weight limitations, (4) Cost, (5) Feasibility of development in the desired time period, (6) Ease of maintenance and refurbishment, (7) Maximum flexibility for the intended use, and (8) Maximum use of existing technology and experience.

5.1.1.5.1 Critical cooling conditions. Cooling requirements vary over the flight envelope of the X-15A-2 aircraft. Required coolant fuel flows (determined for an equivalence ratio of unity), maximum required cooling equivalence ratio, maximum combustor heat flux, and maximum leading edge temperature (radiation cooled) have been correlated with the flight envelope. The flight Mach number and altitude where these various conditions occur are shown in Figure 51.

The minimum absolute fuel flow (unity equivalence ratio) occurs at approximately Mach 6 at maximum altitude, while maximum absolute fuel flow (unity equivalence ratio) occurs slightly above Mach 4 at minimum altitude. The maximum cooling equivalence ratio occurs at Mach 8 and maximum altitude. The maximum combustor heat flux and the maximum leading edge temperature (radiation cooled) occur at Mach 8 and minimum altitude. These points were used to aid in defining the scope of, and the flight condition constraints upon, the Hypersonic Ramjet Engine cooling system.

5.1.1.5.2 Critical components.

5.1.1.5.2.1 Inlet leading edge. Maximum leading edge temperatures have been evaluated at the maximum heat flux flight condition of Mach 8 at 88,000 feet with radiation cooled leading edges. Assuming zero heat conduction in the leading edge (a conservative approximation), a stagnation (or maximum) convective heat flux input (determined by the method introduced by Fay and Riddell in Reference 7) was balanced by a radiation heat flux output from the leading edge and a maximum, equilibrium temperature resulted. Maximum leading edge temperatures were obtained over a range of cylinderical edge and spherical nose radii and leading edge sweep angles. These temperatures are shown in Figure 52.

As the leading edge radius becomes very small, the maximum wall temperature approaches the stagnation temperature of the high velocity air stream, while more significantly, the wall temperature sharply decreases with increasing radius and sweep angle. For a given radius, say 1/16-inch, the spherical tip temperature is approximately 4100°R. The cylindrical edge temperature, at this radius, is about 3900°R with zero sweep and decreases to approximately 3000°R with 60° of sweep. These temperature levels will be somewhat reduced by considering conduction normal to the leading edge and will be reduced still further by the heat sink effect of the inlet's interior surface regenerative cooling system.

A similar parametric study was conducted assuming regeneratively cooled leading edges. The maximum wall temperature for a cylindrical, regeneratively cooled leading edge was determined for the maximum heat flux flight condition of Mach 8 at 88,000 feet. The assumed sweep angle was zero degrees and the hydrogen coolant was assumed to be introduced at 100°R and 275 psia. Maximum temperatures are shown in Figure 53 for the tubes (leading edge cylinder) of 1/16 and 1/8-inch outer radius as a function of hydrogen flow rate. The input convective heat flux was determined using the method introduced by Fay and Riddell (Reference 7). The convective cooling was determined using the analytical methods described by Reference 12. Both methods and a description of the assumptions made are described in Reference 8. Consideration of the maximum wall temperature obtained makes it apparent that either 1/16 or 1/8-inch radius leading edges at zero degrees sweep angle could be regeneratively cooled to acceptable temperature levels with reasonable hydrogen flow rates.

The inlet leading edges may be permanently attached or replaceable. Structural concepts investigated for each of these possibilities were studied. Figure 54 shows the permanent leading edge concepts that were evaluated.

One concept is the use of regeneratively cooled edges which attach to the cooled inlet interior surface structure and which are fabricated from either tubing or formed shell material having the required wall thickness. This system probably requires a separate hydrogen coolant circuit.

In the second concept, a radiation cooled shell of refractory material such as hafnium-tantalum or coated columbium is fabricated and formed into a leading edge which is attached to the inlet structure by welded refractory retaining pins. High temperature protection is primarily accomplished by

the protective oxide formed by the hafnium-tantalum alloy or by the coating on the columbium base metal.

Thirdly, radiation cooled solid refractory sections of bar stock can be machined into leading edge sections and joined by tungsten inert gas (TIG) or electron beam welding (EB) techniques to the inlet structure. The columbium would require a protective coating.

Also a transpiration cooled shell section can be fabricated of porous N-155 sintered wire mesh material (such as Rigimesh) and electron beam welded to the inlet structure. Again a separate hydrogen circuit probably would be used.

Interchange/replacement of the leading edge is a desirable design feature. Leading edges are subjected to high operating temperatures, particle impingement, erosion, oxidation, vibration, and other environments leading to structural decay. Furthermore, leading edge bluntness effects on heat transfer and inlet/engine performance are worthwhile research test objectives. Therefore, the design of removable leading edges was also studied.

The replaceable leading edge concepts illustrated in Figure 55 include a radiation and convectively cooled shell, a radiation and convectively cooled solid, and a transpiration cooled shell. The radiation cooled shell concept features a refractory shell formed into a leading edge structure spring loaded into the inlet cowl structure. This shell can be fabricated in lengths to fit Scramjet leading edge contours. The candidate refractory materials are hafnium-tantalum or coated columbium. Added cooling is provided by the heat sink effect of the hydrogen cooled inlet structure.

The radiation cooled solid concept incorporates spring pin retention of solid refractory leading edge lengths assembled to form the complete edge. The spring pin is kept cool by immersion into the inlet's regenerative coolant circuit.

In the third concept, transpiration cooled leading edge assemblies are installed on tubular studs projecting from the inlet structural cowl. These assemblies would be retained by lock washer design and high temperature sealant. Cooling flow into the transpiration shell section is metered from the inlet hydrogen cooling circuit, thereby eliminating the need for a supplementary circuit.

5.1.1.5.2.2 Engine structure concepts with regenerative cooling. Structural design studies incorporating regenerative cooling were initially predicated on the capability developed by the contractor in the fabrication of flightweight hydrogen cooled combustion chambers and exhaust nozzles using superalloy materials such as Hastelloy-X and Rene' 41. These designs were predicated upon a regenerative cooling system which is an integral part of the structure.

For example, several candidate methods of regeneratively cooled wall construction are shown in Figure 56 and photographs of regenerative structures built and tested at Marquardt are shown in Figure 57. In the concepts of Figure 56, the regenerative system is an integral part of the structure. Several types of this composite structure can be fabricated out of reinforced round tubes, honeycomb panel reinforced tubes, channel reinforced D tubes, rib sheet, or rib panel sections. A combustor weight comparison for three of these configurations is shown in Figure 58.

However, as the Phase I studies progressed, the design criteria and objectives described earlier pointed the way gradually to a new and significantly better structural concept. This concept is shown in Figure 59. The regeneratively cooled walls are not part of the primary load carrying structure. A composite insulative/ablative interlayer between the regenerative cooling system and the primary structure reduces the temperature at which the primary structure must function. Furthermore, this concept has a significant effect upon the aircraft and pilot safety. This structural concept is discussed more fully in paragraph 5.2.2 and also in Reference 8. A photograph and a sketch of a typical corrugated regeneratively cooled panel (Hastelloy-X) for this structural/cooling concept is shown in Figure 60.

5.1.1.5.2.3 Engine exterior surface structural/cooling concepts. The external surface of the Hypersonic Ramjet Engine aft of the leading edge region experiences lower heat fluxes than the interior surface of the engine. Consequently, several structural/cooling concepts can be considered as shown in Figure 61.

1. Regeneratively cooled structure is quite effective but not necessary and will not be used in the development of the preliminary design.

2. Radiation cooled shingle panel structure is attractive in its simplicity. The composite structure shown is composed of radiation cooled Hastelloy-X shingles (to allow thermal expansion) and an insulating substrate on a stiffened (honeycomb) panel.

3. Ablative thermal protection has been selected for the X-15A-2 airplane. Exterior shells or removable panels that enclose the engine structure logically could be similarly coated with this refurbishable ablative material.

In all cases, the exterior surface materials would operate at low stress levels. Figure 62 shows the radiation equilibrium surface temperatures that exist one foot aft of the leading edge (pylon effect not included).

Metal surface temperatures for two of these engine exterior skin concepts have been estimated as shown in Figure 63. The first concept was the radiation cooled, all-metal skin and was evaluated at the maximum heat flux flight condition of Mach 8 at 88,000 feet. The second was the metal structural skin, ablatively cooled externally by an Emerson Electric

ablative material (T-500A) and evaluated over the high q trajectory of the X-15A-2 aircraft. The maximum radiation-cooled metal temperature was 3500°R immediately in front of the engine support pylon leading edge. The estimated thickness of the Emerson Electric T-500A ablative material required to maintain a maximum substrate (metal-ablative bond) temperature of 960°R is also shown in Figure 63.

5.1.1.5.3 Engine heat flux and cooling requirements. The engine internal heat flux along the upper X-15A-2 flight altitude boundary is presented in Figure 64 for one of the candidate engine configurations used during the engine concept selection study of Phase I. The parameter presented is the ratio of the local heat flux to the product of the fuel flow (at unity equivalence ratio) and enthalpy rise of the hydrogen fuel (between 60° and 2000°R). The heat flux values were computed for an assumed wall temperature of 2260°R and an inlet effective contraction ratio (A_2/A_R) of 0.05. In these preliminary studies, a Cornell Laboratory correlation (Reference 9) and the Bartz method (Reference 10) were used to determine the heat flux for the supersonic and subsonic modes, respectively.

At Mach 3, the inlet requires no cooling and subsonic combustion requires more total coolant flow than supersonic combustion. The same is true at Mach 6, except that the inlet now requires cooling, and in addition, the total requirements are higher than at Mach 3. At Mach 8, subsonic combustion is not planned. However, the supersonic combustion coolant requirement (ϕ) is maximum at this condition.

The relative cooling equivalence ratios shown on Figure 65 show the effect on cooling requirements of altitude and combustion mode over the X-15A-2 flight envelope. The interior surface of the engine was assumed 100% regeneratively cooled to a surface temperature of 2260°R over the envelope except at low flight Mach numbers where the air side adiabatic wall temperature over the inlet was below this assumed temperature. Again an inlet effective contraction ratio of 0.05 was assumed. Cooling requirements are higher with subsonic combustion than with supersonic combustion at a given flight Mach number and altitude. Cooling requirements (ϕ) increase with altitude for a given combustion mode and flight Mach number.

During preliminary design studies, influence coefficients are of great value in making trade-off evaluations. One basic parameter used in ramjet studies is the inlet contraction ratio. Variation in this parameter significantly changes the aerothermodynamic properties through the engine. This, in turn, affects engine thrust and heat flux distribution within the engine. The variation in relative cooling equivalence ratio with contraction ratio is shown in Figure 66 for flight conditions of Mach 8 at 122,000 feet with study engine Configuration E.

A 40% increase in effective contraction ratio (A_2/A_r) will result in approximately a 30% reduction in required cooling flow, corresponding with a reduction in engine thrust as shown earlier in Figure 12. These influence coefficients will be considered during engine preliminary design as one way of minimizing cooling flow requirements while maintaining an acceptable level of engine thrust.

5.1.1.5.4 Engine static pressure loading. Static pressure distributions for engine Configuration E are presented in Figure 67 for the supersonic combustion mode of operation. Pressures for M_∞ = 3, 6, and 8 are shown for altitudes corresponding to the lower flight boundary. It is noted that pressures are maximum at M_∞ = 6. Subsonic combustion will result in 10 to 20% higher engine static pressures than for supersonic combustion. The amount of increase will depend upon the effective contraction achieved with the subsonic mode and upon the method of transition to subsonic flow as discussed earlier. Maximum subsonic combustion flight Mach numbers, which will be established during the preliminary design phase, will be determined by consideration of engine weight (internal static pressure) and the pressure available at the fuel injector station.

5.1.1.6 Development Requirements.

5.1.1.6.1 Introduction. As discussed earlier, the six candidate engine concepts were reviewed and analyzed from performance, structural, and development viewpoints. All configurations were judged capable of meeting the minimum performance requirements and each configuration was believed capable of being developed into a reliable structural/cooling arrangement. However, the amount of development required to bring each configuration to fruition varies. The configurations differ in complexity, structural arrangement, operations, thermal loading, cooling requirements, availability of materials, and techniques for critical components, etc. Since the amount of development is reflected in ultimate cost/time, items affecting the development must be considered in the engine selection.

5.1.1.6.2 Method of approach. Several methods of approach to the review and analysis of the development requirements were considered for the preliminary phases of this program. The development of any one of the candidate engine configurations would require sub-scale and full scale component and subsystem development, selection and modification of test facilities and equipment, materials development, fabrication and tooling development, and qualification and acceptance testing of the final product. Thus one method of approach considered was that of outlining and scheduling the development for each configuration. However, it was realized that considerable commonality existed between configurations and that this phase of the effort might be more profitably used if differences in the development requirements were outlined. This latter approach was taken herein, permitting the more salient development items to be composed on a relative basis in Section 5.2 of this report.

5.1.1.6.3 Advanced techniques requirements. A measure of the time required and the difficulty of development is the number of advanced technique requirements incorporated into each of the engine configurations. The items considered by Marquardt as those requiring considerable advancement in the

state of the art are shown in Figure 68. The engine geometry control system, sliding seals, the use of normal leading edges on the inlet, and the use of cooled, long stroke, high response actuators are required with the axisymmetric variable geometry Configuration A. Normal leading edges are listed because of their considerably higher heat fluxes (temperatures). Even with their operational problems (i.e., danger of leading edge denting or cracking), regenerative leading edges would probably be required. Marquardt considers replaceable regenerative leading edges a difficult design problem and recommends against their use.

As noted in Figure 68, thermal compression as incorporated into Configurations C, D, E, and F, is listed as an advanced technique. Although several tests have been successfully conducted with thermal compression, this is a relatively new and unexploited technique to achieve good performance and low heat loads from a low contraction ratio, fixed geometry engine. Furthermore, care must be given to the inlet-combustor matching.

It is clearly evident from Figure 68 that engine Configuration A, due to its variable geometry feature, requires the largest utilization of advanced techniques and, therefore, in Marquardt's opinion would be the most expensive to develop. The remaining configurations are about equal, with Configuration B rated somewhat lower, and Configuration C somewhat higher than the average. The fixed and simplified geometry of Configuration B has one primary problem, the design of the leading edge, which it is believed could be overcome by design. Configuration C is rated somewhat more expensive to develop because a portion of its leading edge is normal to the free stream flow. Also, the aerodynamic development of the inlet compression surfaces would be somewhat more complex.

Advanced technology items not considered in Figure 68 because they are common to all engine configurations include the use of static seals in a hostile environment and the problems associated with fuel metering and fuel distributions. Static seals were originally considered for use as a requirement when incorporating internal load cell instrumentation (for example, Figure 69). However, further studies have indicated that static seals will be required irrespective of the use of load cells inasmuch as fabrication and manufacturing planning have shown the need for fabrication of all engines in sections. In addition, further trade-off studies comparing the advantages and disadvantages of the internal load cell concept have led Marquardt to recommend against their use (Section 5.2.4). Similarly, reviews with various manufacturers of flow metering equipment for the environments, ranges, and sizes required have indicated the need for demonstration of reliable equipment. Minimum instrumentation development is required, consisting almost entirely of flight packing of current state of the art instruments. The fuel distribution system is not regarded as difficult, but practical experience is lacking.

5.1.1.6.4 Development testing. Another item affecting development costs is the differences in the utility and range of operation of available test facilities when considering the differences in shape and configuration of the candidate engine concepts. A review of existing Government full scale

test facilities shows that engine burning times at high Mach number, low altitude conditions will be limited. In particular, the requirement for high Mach number simulation reduces the run time available. Therefore, it is apparent that the free jet nozzle which allows flight simulation should be made as small as possible to minimize free jet spillage. There must be sufficient nozzle exit area around the engine inlet so that the facility nozzle can be started. Also, in the case of the unstarted inlet, neither the amount of flow spillage nor the flow pattern within the inlet should be influenced by the nozzle exit disturbance or the reflection of the spillage shock system. In order to minimize spillage consistent with the above limitations, the facility free jet nozzle may be contoured to the shape and form the the engine inlet. However, as free jet nozzles increase in size, economics play an increasingly bigger role. Round free jet nozzles of large size are considerably less expensive to build, and the testing and development of the round axisymmetric engine is, therefore, minimized. With the other configurations, a penalty in cost will be incurred, either in the form of reduced run time for a given test cell occupancy or in the form of cost of development of contoured nozzles.

5.1.1.6.5 Instrumentation. The development of the instrumentation required for the Hypersonic Ramjet Research Engine is discussed in Section 5.2.4 of this report.

5.1.1.7 X-15A Compatibility and flight safety. Each engine configuration has been evaluated with respect to the X-15A-2 compatibility and flight safety requirements as specified in the Statement of Work. These requirements were included in the Summary of Guidelines and Requirements of Appendix A to the Statement of Work in Tables I and II herein, respectively. The more salient items are summarized herein.

5.1.1.7.1 Mach number-altitude profile. As discussed in paragraph 5.1.1.4, all engine configurations are believed capable of meeting the minimum test performance requirements over the Mach range 4 to 8, with an altitude range capability of at least 15,000 feet from the selected Mach number altitude profile.

5.1.1.7.2 Engine weight and center of gravity. All configurations initially studied employed load cells for internal thrust measurements, a structural spine and removable inlets, combustor-nozzle sections, and outer skin panels (Figure 69). A relative weight comparison is included in Figure 70.

The engine center of gravity was determined to establish possible effects upon the engine jettison system. Although there were variations between configurations, the results did not indicate a significant influence in the engine concept selection. Also, the changes in the X-15A-2

center of gravity due to weight and center of gravity of the various engines varied only slightly with the limitations in possible engine location and installation upon the X-15A-2. Without internal load cells, all configurations met the maximum weight allowance. The recommended configuration taken into the preliminary design phase, Configuration D-6, weighs approximately 700 pounds.

5.1.1.7.3 Dimensional aspects. The allowable ramjet installation envelope for the X-15A-2 is shown in Figure 2 of Appendix A of the Statement of Work. All engine configurations considered comply with these envelope restrictions.

The inlet capture area was selected at the minimum allowable of 1.76 sq ft. This decision was based upon considerations of required engine and cooling fuel flows and engine weight. Consider first the required fuel flow. For $\phi = 1$, the engine fuel flow is proportional to the engine capture areas. If the required cooling flows are small, the maximum engine fuel flow is proportional to the engine capture areas. On the other hand, if the required cooling flows are high, the maximum engine fuel flow is proportional to the engine wetted area. In either high or low cooling cases, the engine fuel flow will be a minimum for the smallest engine. Remembering that the X-15A-2 hydrogen storage is limited to 48 pounds, maximum ramjet test time is provided by the smallest engine capture area. Three weight criteria were considered, namely, engine component weight which is proportional to internal surface area, component weight wherein hoop stress is held constant, and component weights wherein structural deflection was held constant. In all three cases, the lightest engine components (i.e., engine) correspond to the minimum capture area.

The nominal exit nozzle area selected was the maximum allowed, corresponding to an overall engine area ratio of 2.0. The nozzle for the Hypersonic Ramjet is considerably under-expanded as was indicated in Figure 33. Maximum thrust is therefore obtained by expanding the nozzle to as large an area as possible. Some penalty in external drag is incurred by use of the maximum engine area ratio allowable. However, a maximum thrust-minus-drag is achieved with this selection. The actual, as opposed to nominal nozzle exit area, is somewhat less than twice the inlet capture area for all engine configurations as is shown in Table VII. The external skin line at the nozzle exit station is located at its closest proximity to the vehicle. The actual exit nozzle flow area must account for the structural engine depth at the nozzle exit station. The round engine configurations have the smallest nozzle flow area as a result of their shape and the above restrictions.

5.1.1.7.4 Operation and flight safety. A philosophy developed at the initiation of the Phase I studies was that no failure of the research engine or associated structure and subsystems will endanger the normal flight safety of the X-15 or its pilot. Furthermore, operation of the ramjet engine shall require a minimum of pilot attention, with engine operation and control

as automatic as possible. Thrust and drag measurement systems for each engine system were incorporated. Similarly, safety precautions, such as engine jettison under any normal condition within the X-15A-2 flight envelope, purge systems, fire warning lights, and cockpit panels to monitor the engine operation for the pilot, have been assumed for all engine concepts considered. Maximum flight safety will be insured through the use of two types of discrete point fire and overheat detection systems. Although a detailed approach to the operational and safety requirements was not possible for each engine considered in the conceptual design stage, preliminary studies indicated that no significant differences between engines should result. With the engine selected for preliminary design, these studies and analyses have been greatly advanced, and safe and reliable systems have been evolved as discussed in Reference 8.

5.1.1.7.5 Ground equipment. The analysis of support requirements revealed that satisfactory solutions to handling, maintenance, and check-out procedures could be defined for ramjet geometries within the limits specified by "X-15A-2 Ground Clearance" in Figure 2 of Appendix A of the Statement of Work and without the necessity of restrictions on the aerothermodynamic configuration of the ramjet. The time constraints for flight turn-around to impose certain maintainability criteria on the engine design. The structural design must consider accessibility and assembly methods consistent with replacement of components which may be subject to damage due to flight temperature environments or recovery and the replacement of expended components. Also, access to the adjustments for the fuel control must be provided to allow resetting for trajectory considerations and adjustment to a predetermined fuel schedule.

5.1.1.7.6 Thrust and drag measurement. The engine must be installed in its support in a manner that allows measurement of engine thrust and drag during flight. In these conceptual design studies, it was assumed that all but 12 inches of the lower ventral fin would be removed and that the engine would be supported and mounted 12 inches from the lower vehicle skinline on this fin. Within this fin volume would be located the ramjet control package, fuel lines, instrumentation lines, a separation mechanism for ramjet ejection upon malfunction, and a load cell to establish net thrust and drag loads upon the engine. The aft section of the fin was assumed to contain the present speed brake and actuation system.

It is desired that only the axial forces upon the engine be reacted, and that extraneous forces be minimized in design of the engine support interface. Although a detailed design of the load cell and strut support were beyond the scope of the preliminary studies, preliminary layouts indicated no significant differences in the thrust and drag measurement difficulties between the various engine configurations. Existing load cells were believed capable of handling the axial aerodynamic and inertial loads as well as being relatively insensitive to the thermal gradients that might exist within the engine support cavity.

5.2 Comparative Studies

The baseline engine configurations have been described and the results of preliminary analyses of component and ramjet cycle performance, structural and cooling aspects, development requirements, and factors affecting the X-15A compatibility and flight safety for the various engines have been presented. Comparative studies of the various engine concepts are now discussed.

5.2.1 Performance and operational flexibility.

5.2.1.1 Component performance. A summary of component efficiencies and geometric factors for the various engine configurations is presented in Table VII. The table includes operation at Mach 4, 6, and 8 in the supersonic mode and Mach 3, 4, and 6 in the subsonic mode for both the low and high altitude flight boundaries. The component interrelationships discussed under the component analyses section of this report are evident in this table.

5.2.1.2 Engine performance. The thrust and impulse performance for each engine concept has been estimated utilizing the appropriate component efficiencies. Conditions examined have included supersonic and subsonic combustion modes over the Mach range and at the high and low altitude extremes of the X-15A-2 flight envelope. Realizing that some design variation is possible within each configuration, all configurations were judged capable of meeting the minimum performance requirements and to be equally capable as to range of speed and altitude of operation and adaptability to variations in combustion mode. The performance of the thermal compression configurations are about equal, each exceeding the performance of the variable geometry configuration. The higher viscous losses and the inability to achieve higher effective contraction ratios with the axisymmetric configuration contributed to its smaller performance potential. As expected, the lowest performance was achieved with the fixed geometry, axisymmetric configuration.

5.2.2 Structures and cooling.

5.2.2.1 Comparison of cooling requirements of candidate engine configurations. Cooling requirement studies conducted during the engine concept selection study of Phase I were primarily directed toward obtaining the relative cooling requirements of the engine configurations represented schematically in Figure 3. Heat flux profiles were obtained for these engine configurations assuming that the engine internal engine surfaces were regeneratively cooled and maintained at a constant wall temperature of 2260°R. The maximum cooling equivalence ratio occurs at the upper right-hand corner of the proposed flight corridor, at Mach 8, 80,000 feet altitude. Therefore, this condition was selected for the comparison. The cumulative surface areas as a function

of axial length are shown in Figure 71 for each engine configuration. (Configurations A, B, and D which have large centerbodies, have considerably larger wetted areas.) Heat flux distributions for the various engine configurations studied are given in Figure 72. The analyses are based upon the Cornell correlation (Reference 9). An integration of these heat flux profiles over the engine surface was made to determine the cooling requirements as presented in Figure 73. The relative cooling equivalence ratios and various geometric data are compared. The most important parameter is the regenerative system cooling requirements, or the relative cooling equivalence ratio, evaluated at Mach 8 at 122,000 feet. This cooling parameter variation follows closely the wetted area variations of the engine and the high heat flux combustor area. Because of the high heat flux on the leading edges, replaceable leading edges are believed feasible only with Configurations D, E, and F.

The results of detailed design in reducing the cooling requirement for a given system are shown in Figure 74 for the selected engine Configuration D. The centerbody was reduced considerably in size, resulting in reduction in wetted area. The fuel injection system was tailored to the inlet-combustor geometry, resulting in shorter combustor sections exposed to the maximum heat flux. Similar improvements resulting from refinements in the design would be expected for the other engine configurations. The initial point for Configuration E is shown for comparison in Figure 74. In particular, the interstaging and sweep of fuel injectors for the thermal compression systems can result in short, reasonable maximum flux level, high performance systems. On the other hand, less can be done to reduce the combustor heat flux in the axisymmetric uniform flow Configurations A and B, wherein the fuel injectors have been assumed arranged in rows normal to the entering flow (See paragraph 5.2.6).

The results of the cooling study were integrated with the performance analysis results and other studies conducted during the engine concept selection activity of Phase I. From this, the selected engine Configuration D-6 (shown in Figure 84) to be used for the preliminary design study evolved.

5.2.2.2 Basis for the selected structural/cooling design approach. The structural and cooling concepts studied during the early part of the Phase I studies were evaluated with respect to the selected engine configuration and compared on the basis of several important considerations related to the overall system requirements and to existing fabrication and component technology. Specifically, the selected structural/cooling concept must satisfy the following criteria:

1. Aircraft and pilot safety
2. Feasibility of development in the desired time period
3. Maximum flexibility for intended use
4. Compatibility with the aircraft, its operation and ground support

5. Weight limitations

6. Cost

7. Maintenance and refurbishment requirements

8. Maximum use of existing technology and experience

As the Phase I studies progressed, these criteria coupled with the results of system and configuration evaluations pointed the way gradually to the structural and cooling concepts reflected in the selected engine. Along the way many techniques, materials, and methods successfully applied in earlier technology programs were evaluated, modified, and, in some cases, rejected because of incompatibility with the stated objectives. The concept finally chosen meets the above criteria and, in Marquardt's opinion, fully satisfies the technical objectives delineated by NASA.

Figure 59 schematically shows the selected structural and cooling concepts. The following are the major features and the reasons for their selection:

1. Separation of the primary structure and regeneratively cooled interior walls so that the regeneratively cooled walls are not part of the primary load carrying structure. These walls serve truly as a thermal protection for the engine structure and satisfy a minimum of extraneous mechanical requirements, i.e., they contain hydrogen fuel under pressure and transmit the internal engine pressures to the primary structure. This approach allowed great flexibility in the choice of designs for these surfaces and many simplifications from a development and fabrication point of view. It also led to a concept which greatly contributes to the safety aspects of the engine, as described below.

2. Use of a composite insulative/ablative interlayer between the regeneratively cooled surface and the primary structure. This feature satisfies several requirements, but has a most significant effect on aircraft and pilot safety, design, weight, and cost of the primary structure. In case of a failure in the regenerative cooling function leading to a loss of the cooling panel,(the engine component subjected to the most hostile environmental stress), the ablative interlayer, which is capable of withstanding direct contact with the combustion gas, will provide a valuable time interval between failure of the regenerative panel and heating of the primary structure to the point of local failure. Under normal operation, the interlayer acts solely as an insulator.

The combination of insulator and ablator will keep the primary structure at a low temperature under the most severe mission conditions. The insulator will limit the temperature at the ablative interface to 500°F maximum, preventing it from ablating under normal (nonemergency) operating conditions. This avoids a requirement for refurbishment in normal operational usage.

Other benefits of this technique are the ability to use easily worked steels for the primary structure, easing of critical tolerances on the regenerative wall-to-structure interface, and full contact pressure load transmission from the walls to the primary structure.

3. Modified monocoque primary structure. This well established aircraft type structure provides the best weight-to-strength ratio next to honeycomb structures and it is ideally suited for the complex shapes of these engines. The low volumetric structural fraction of such a structure allows room for the many components (instrumentation transducers, fuel injectors and manifolds, plumbing and harnesses) and together with a removable outer skin, permits ready access to the equipment. Being a redundant structure, it is capable of sustaining local damage without catastrophic failure (i.e., failsafe by aircraft standards).

4. Uncomplicated cooling system. The favorable heat flux conditions of the overall engine concept and the flexibility provided by the separation of the cooling system from the primary structure allows the application of relatively simple regenerative surface designs. The regeneratively cooled panel design shown in Figure 60 provides the necessary flexibility to satisfy heat transfer requirements, is relatively easy to fabricate with existing technology ,and minimizes potential leakage paths. The cooling circuitry arrived at is the result of careful evaluation of cooling needs, natural mechanical interfaces, and assembly and check-out considerations. For example, the choice of separate cooling circuits for the leading edge areas provides an interface with the main engine portions which is compatible with the needs of design, fabrication, and assembly. The analytical studies showed that the use of constant height panels and the use of blockage in the corrugated flow passages for control of coolant flow and heat transfer will satisfy the overall cooling needs of the engine. Fabrication problems and cost are reduced in comparison with contoured flow passage approaches.

5. Thermal stress and development aspects. Thermal stress problems, which are inherent in many cases, such as the regeneratively cooled walls and leading edges, are substantially eased by the separation of primary load carrying structure and cooling elements. By virtue of the insulative interlayer concept, the primary structure will see only limited temperature variations which a redundant structure can easily accommodate. The high thermal stress elements, not being subject to the restraints imposed by primary load carrying needs, can be designed to their own specific needs. Typically, regeneratively cooled panels can grow and deform in a manner which enhances their functional effectiveness and takes full advantage of the containment offered by the primary structure. The essential independence of structure and cooling system elements allows parallel development of these very important components all through the program. This procedure will result in early evaluation of these critical elements long before a complete engine could be made available.

6. Materials and manufacturing processes. The chosen engine concept reduces materials and fabrication problems in the primary structures to a well known and established level of technology. Materials considerations for the high temperature elements are reported in Appendix F. The combined effects of the features discussed above result in substantial simplifications in this area too. The materials, fabrication, and joining techniques needed in the execution of this design are either readily available today or sufficiently far along to be available when needed. Some of the technology work performed at Marquardt in the area of hypersonic propulsion called for considerably more sophisticated techniques than this engine will require.

5.2.2.3 Basis for the selected critical component designs.

5.2.2.2.1 Leading edge. The maximum leading edge temperatures of the Scramjet engine on the X-15A-2 aircraft will occur at the Mach 8 flight condition at 88,000 feet altitude. These maximum leading edge temperatures were initially evaluated at this condition assuming only radiation cooling of the leading edge and no conduction into the leading edge material. As presented in Figure 52, spherical and cylindrical leading edges of various sweep angles were evaluated to determine the maximum wall temperature as a function of leading edge radius. The spherical and cylindrical leading edges with small sweep angles would require materials such as beryllium, columbium, and hafnium alloys, all of which require a coating for oxidation protection.

Regeneratively cooled leading edge configurations were initially evaluated assuming leading edge sweep angles of zero degrees. Figure 53 shows the maximum wall temperature as a function of hydrogen coolant flow rate to a 1/16 and 1/8-inch radius leading edge tube. Figure 53 is somewhat conservative because it does not consider radiation from the leading edge surface nor conduction laterally along the leading edge tube. Also, the leading edge sweep angle is larger than zero degrees over most of the leading edge surface. However, the cooling adequacy could be seriously affected by tube denting, reducing the coolant flow rate with a resultant increase in metal temperature. Because of these operational as well as development difficulty problems, regeneratively cooled leading edges are not recommended.

Permanent and replaceable leading edge structural design concepts were evaluated to obtain the best compromise between durability, use of state of the art techniques, and replaceability. The selected leading edge cowl configuration is shown in Figure 75. This configuration uses a state of the art material (Hastelloy-X), it is replaceable by the use of pinned joints, and it is significantly more durable than the thin wall leading edge tubes shown in Figure 54. The results of the analyses show that with temperatures no greater than 1200° on the back surface of a leading edge maintained by a coolant circuit, the maximum wall temperature of the leading edge will be maintained at a reasonable temperature.

As shown in Figure 52, the spike tip, or spherical leading edge, of the Scramjet centerbody will operate at a higher temperature level than the cylindrical leading edge of the cowl. Accessibility to the Scramjet centerbody during fabrication and for field serviceability was an important consideration in the spike tip design selection. Consequently, the spike tip will be fabricated from a high temperature capability refractory material for use on Mach 8 flights and need not be cooled on the back surface.

5.2.2.3.2 Radiation cooled centerbody forward section. The forward section of the centerbody will be uncooled and will be fabricated as a detachable section of the main centerbody. Figure 76 shows the surface temperature of this section as a function of axial station. This radiation cooled surface will extend 18 inches aft of the spike tip where the temperature level is within the ability of available refractory metals. The wall temperatures shown in Figure 76 are those of the vertical centerline of the centerbody where the heating rates are maximum. These results include the effect of the decrease in radiation view factor with increased axial location.

5.2.2.3.3 Engine interior surface regenerative cooling. The selected engine configuration has a coolant requirement which is compatible with the fuel schedule of the engine. The heat flux distributions for the selected engine are given in Figure 77 for the Mach 8, 88,000 feet altitude condition. The three-dimensionality of the engine internal flow and the use of swept internal contours require that the engine cooling system have a high degree of versatility. Several coolant passage designs (depicted in Figure 56) were evaluated. Some of the designs shown are representative of those developed by Marquardt for use on previous and existing Air Force programs. The most suitable coolant panel configuration for this application is shown in Figure 60. This type of panel represents a low cost, easily manufacturable, and versatile system, and it is especially valuable as a system to which continual refinements may be applied without seriously affecting schedules or costs. This design is described in Reference 8.

5.2.2.3.4 Engine exterior surface structure/cooling. The candidate methods considered for protecting the external surface of the engine have been presented in Figure 61 and were described in an earlier section. Compatibility with the X-15A-2 aircraft, reliability, and ease of refurbishment have all been important considerations in selecting the external surface structure. Based upon these considerations, the external engine surface will be thermally protected by the ablative selected by NASA for protection of the external surface of the X-15A-2 aircraft. This ablative will be applied in various thicknesses over the engine external surface as dictated by the variation in heating rates to the external surface. Special consideration will be given to the region of the external surface exposed to the shock system generated by the vehicle/engine pylon. Figure 63 shows the ablative thickness requirements in the vicinity of this shock system and also shows that a 1/8-inch thickness of ablative will maintain the temperatures of the

remainder of the external engine surface at satisfactory levels. This figure shows the results assuming Emerson T-500 as a possible ablative.

5.2.3 Development. The relative development difficulties for each of the study engine configurations are compared in Figure 78. The following design or development items were considered: Inlet design, inlet development, sliding seals, static seals, combustor design and development, fuel flow control, fuel distribution control, coolant distribution control, engine geometry control, engine geometry actuation and control systems, regenerative cooling systems, leading edges for low sweep angles, replaceable leading edges, thrust load cell installation, internal load cell installation, replaceable centerbodies, and test facility utilizations for development testing. Each design or development item was assigned a weighting factor and the relative development difficulty for each item was judged. Summation of this matrix indicated that Configuration A would be the most difficult to develop. As expected, Configuration B-1 would be the most straightforward to develop. Configurations C, D-6, E, and F are all judged about equal in development difficulty. In the initial studies, the development difficulty of Configuration D was rated somewhat higher because of its heat load and difficulties in internal load cell installation. Continuing studies dispelled the high heat load factor of Configuration D (i.e., Configuration D-6 in Figure 74). Also, internal load cell arrangement was abandoned because of mechanical, structural, safety, and reliability aspects as discussed in paragraph 5.2.4. Relative cost of developments, ease of structural design, ease of coolant system design, interchangeability, and weight are shown in Figure 70.

Engine life is believed inversely related to the difficulty of engine development, i.e., engine life decreases as the engine development difficulty increases. However, it is believed that the required engine life as specified in Section 4.1 of Appendix A of the Statement of Work can be satisfied with any of the study configuration engines. Maintenance, refurbishment, and turn-around time of course favor the less complex engines.

The number of engines required for adequate ground and flight tests programs is difficult to estimate without going through a complete development plan for each engine. The problem is related to the probability of a catastrophic failure, such as the burnout of the regenerative cooling system, and its effect upon the engine. If such a failure occurs and the engine structure is not protected for sufficient time to turn off the fuel flow and abandon the test condition, the number of engines required for testing is at least proportional to the number of advance techniques and high risk items incorporated in the engine design. If the engine structure is reasonably protected, as it should be to maximize X-15A-2 and pilot safety, the number of engines required is not greatly different and is not, therefore, a major factor in engine concept selection.

5.2.4 Instrumentation. A preliminary report on ground and flight test instrumentation requirements (Reference 11) was published at the time of the mid-term oral review. In fulfilling the Statement of Work and the Addendum of April 26, 1965, it was recognized that internal load cells, reacting the forces on the inlet and combustor-nozzle, would provide redundancy in determination of the internal ramjet thrust, and also would aid in determination of the effeciency of these internal components without the use of probes and survey rakes inserted into the gas stream. These studies were conducted contemporaneously with the engine concept studies, and the ability to include internal load cells into the mechanical/structural design of the engine was rated along with other selection criteria. Figure 69 for example, shows the internal load cell arrangement with engine Configuration E.

As the studies continued, however, it became evident that the development of the internal load cell arrangement would be extremely difficult, even for the axisymmetric engine where the split between inlet and combustor could be located at a planar section. Alignment, cooling, the mechanical design, sliding seals, etc., presented added complexities. In particular, the internal load cell arrangements forced undesired compromises to the reliability and safety of the design, inasmuch as the regeneratively cooled panels were of necessity load carrying members. Also, weight became a factor because each internal load cell weighed approximately 5 pounds.

Concurrent with these studies, the problem of defining the internal ramjet thrust from the basic net force load cell and conventional internal instrumentation was continuing. It was reasoned that carefully designed models, simulating the external engine lines and contoured internally such that only friction drag would result, could yield accurate drag measurements. (The base drag can be easily determined.) The cold flow engine model similarly could be used to determine external drag from the net force load cell with a specially contoured internal configuration. Knowing the external engine drag, the net force load cell measurements could then be used to determine the internal thrust. Similarly, the flight engine measurements with fuel-off as opposed to fuel-on would need only a correction for cold flow internal drag which can be reasonably estimated. With this reasoning, the internal load cell configuration was dismissed, and the engine concepts were re-examined to see if this conclusion would change the engine concept selection. The result of this re-examination was to reduce the development difficulty of the thermal compression configurations with respect to the axisymmetric configurations, i.e., it had been considerably more difficult to physically separate the inlet from the combustor-nozzle in order to locate the load cells along the swept planes characteristic of the fuel injector patterns for the thermal compression configurations.

The two other significant instrumentation effects on engine configuration were the availability of volume for the necessary engine pressure and temperature instrumentation and the accessibility of this volume. These are necessary to facilitate higher measurement accuracy through close coupling of measurement point, sensors, and signal conditioning and to allow convenient installation, refurbishment, and calibration of instrumentation.

The relative volume available for instrumentation for the various engine configurations is presented in Table VIII.

5.2.5 Research applicability. There are not a large variety of engines and engine concepts that could be developed, using the available technology, which would satisfy the primary objectives of speed, altitude, performance, weight, safety, etc. of the present study effort. Also, it was recognized that the engine, in addition to meeting minimum performance and operational requirements, must serve as a research tool to advance the technology of hypersonic airbreathing propulsion systems.

A measure of the research applicability to the problems of aerothermodynamics, combustion, and performance is the number of engine variables affecting these items. For the candidate engine concepts studied, the following lists the more salient items: (1) Spike position or ability to vary contraction ratio and engine air flow, (2) Fuel flow, (3) Fuel distribution, (4) Interchangeable centerbodies to change contraction ratio or spillage or to vary the combustor inlet profile, (5) Interchangeable and replaceable inlet leading edges, to determine effects upon engine performance, basic research upon the effects of boundary layer transition, separation, and heat transfer, (6) The capability of subsonic as well as supersonic combustion to better define the optimum transition for mission studies, and (7) The advancement and exploration of the potentials of the thermal compression process. Figure 79 lists these items and a relative comparison of this measure of research flexibility is shown. On this basis, it may be seen that Configurations D and E offer the highest levels of research flexibility.

A similar measure of research flexibility is the applicability of the research test data to the problems of future engine design. For this comparison, three broad areas of applicable technology were established, namely, basic aerodynamics, combustor design, and system interaction. A further breakdown and the results of these studies are summarized in Figure 80 wherein each engine configuration is rated yes or no as to its applicability. Again, on this basis, Configurations D and E have the greatest application. The simplest engine(Configurations B or B-1) provides relatively little practical design information. The application of research test data to the problems of future engine design must also consider the test results to be obtained in light of the configuration arrangements arising from preliminary design and mission studies for future manned and unmanned vehicles. Representative studies are the Scramjet Surface to Air Missiles and AICBM's and the Manned Hypersonic Test Vehicles (MHTV). Extensive application studies by Marquardt, airframe contractors, and NASA show that rectangular/modular engines have maximum potential application (Figures 81 and 82). Similarly, large booster vehicles may utilize the hypersonic ramjet engine located around the periphery of the vehicle. These engines typically would be developed as separate modules.

5.2.6 Inlet Mach number design specification change. In response to the Statement of Work (L-4947, paragraph 5.1.2, Item (7)), The Marquardt Corporation has assessed the relative advantages and disadvantages, for each configuration, of reducing the maximum inlet entrance Mach number from 8 to 7. Total enthalpy would, however, remain constant at the $M_\infty = 8$ value.

Nine comparison items were assumed subject to change as shown in Figure 83. A maximum point value of five was assigned to each item. No point value indicates no change. Summation of this matrix leads to these conclusions:

1. There are no disadvantages incurred by such a specification change.

2. Configuration B profits the most from the specification change. Configuration B has the least performance flexibility by virtue of its simple design. Therefore, reducing the Mach number span over which it must operate (within specified levels) considerably eases its design and development.

3. Configurations A, C, D, E, and F equally profit from such a change but to a lesser extent than Configuration B.

4. The confidence level for all engines is raised by such a change because full scale ground testing can be accomplished over a larger portion of the flight envelope.

5.2.7 Fuel injection and distribution. Axial distribution of fuel injection must be accomplished in all engine configurations considered to provide reasonable performance, to reduce the heat flux to the combustor walls, and to provide sufficient combustion expansion area (to prevent thermal choking). The axial distribution of fuel for the axisymmetric Configurations A and B utilizing staged rows of injectors normal to the direction of the air stream is in general a more difficult job to accomplish than for the engine designed for thermal compression. For such configurations, the compressions resulting from the mixing and combustion of each individual fuel injector will tend to coalesce and form strong shock systems, resulting in lower efficiency and concentrated heat loads on the combustor wall. The amount of fuel injected at a given station, or the total fuel flow, may be restricted to prevent thermal choking. This implies that more axial injector stations may be required, and correspondingly, there would be greater variation in the scheduling of fuel injection for the Mach number and altitude range desired. The axial spreading out of fuel injectors also implies additional combustor length, wetted area, and hence heat load. This, in turn, indicates larger cooling flow rates and reduced operational capability. In summary, for this application, it is evident that the thermal compression configurations have a distinct advantage in fuel distribution, scheduling or injection rates, and cooling equivalence ratio.

5.2.8 Comparative studies - total comparison. Engine study Configurations A through F have been compared considering all major factors affecting engine selection.

Based upon this comparison, the thermal compression configurations clearly emerge as superior research engines. Engine Configuration E, based upon this comparison, was initially selected as the engine to be taken into the preliminary design phase and it was so recommended at the Mid-Term Oral Review in September, 1965. This recommendation was shortly revised in favor of the simpler geometry of the single centerbody Configuration D. Recognizing that high engine performance with fixed geometry low contraction ratio inlets can only be accomplished by exploiting unconventional inlet designs and by careful attention to fuel distribution, it has been reasoned that performance prediction analysis and correlation of both ground and flight test data of these rather complex phenomena initially would be easier to accomplish for the purposes of this program with a less complex engine geometry, i.e., Configuration D-6 rather than Configuration E. To aid the reader, a configuration history of the final engine Configuration D-6 taken into preliminary design and development planning activities is shown schematically in Figure 84. The engine to be developed for the NASA Hypersonic Ramjet Research Engine Project has been designated as the MA-165 Hypersonic Ramjet Engine.

6.0 CONCLUSIONS AND RECOMMENDATIONS

A rectangular engine employing fixed geometry components has been derived. This configuration (Configuration D-6, shown in Figure 85) is believed uniquely suited to the requirements of the Hypersonic Ramjet Experiment Project.

The engine concept utilizes to advantage the thermal compression process. At low speeds, the inlet spillage and contraction ratio are low such that adequate performance may be obtained and such that the inlet will readily swallow the terminal shock during the startup transient. At higher speeds, controlled axial fuel distribution is used to provide the higher effective inlet contraction ratios necessary for adequate performance. Performance exceeding the minimum performance goals over the Mach number range 4 to 8 is achieved without the use of variable geometry components. The engine is capable of operation and produces useful thrust at speeds to Mach 3.0.

The inlet-combustor combination is closely integrated, resulting in nominal inlet and combustor efficiency requirements. The combustor length and heat flux are minimized consistent with the performance requirements. The stationwise distribution of fuel is uniquely suited to the inlet-combustor matching required to utilize the thermal compression process.

The close integration of the inlet-combustor and the design of the inlet permit the attainment of cooling equivalence ratios of less than 1.0. The inlet leading edges are highly swept to promote inlet startup and to reduce the leading edge heat loads. The initial section of the inlet centerbody and the cowl leading edges are radiation cooled.

Internal pressures are nominal. A salient feature of the design is the provision for a cold insulated structure, resulting in light weight, flight safety, reliability, and easy access to fuel injector and instrumentation compartments for maintenance, repair, or ground changes.

The engine provides a maximum of research flexibility. Subsonic as well as supersonic combustion modes are available. The engine is designed to operate over the entire flight envelope of the X-15A-2, and it will provide research test data to guide future hypersonic engine design in the basic areas of aerodynamics, combustion, and system interaction. Interchangeable radiation cooled leading edges on the inlet cowl and centerbody tip will add to the research flexibility of the engine.

Engine development cost and time is certainly minimized by the avoidance of variable geometry. A variable geometry system would require the development of long stroke, high response actuators and control systems in a hostile temperature environment. Sliding seals also would be required.

The selected engine is compatible with the X-15A-2 installation. Automatic control systems (with pilot overrides) are envisioned to minimize required pilot attention. X-15 and pilot safety are fundamental requirements as reflected in the final engine structure/cooling concept. Control display panels for the pilot are envisioned to aid in monitoring the flight tests and to take corrective measures if required. The engine can be jettisoned if required.

7.0 REFERENCES

1. General Applied Sciences Laboratory Report TR598, "Design and Analysis of the NASA Experimental Hypersonic Ramjet Inlet", February 1966. CONFIDENTIAL REPORT.

2. Sterrett, J. R. and J. C. Emery, "Experimental Separation Studies for Two-Dimensional Wedges and Curved Surfaces at Mach Numbers of 4.8 and 6.2," NASA TN D-1014. UNLCASSIFIED REPORT.

3. The Marquardt Corporation Report MP-1358, "Hypersonic Ramjet Experiment Project -- Initial Oral Review." CONFIDENTIAL REPORT.

4. Deem, R. E. and J. S. Murphy, "Flat Plate Boundary Layer Transition at Hypersonic Speeds," AIAA Paper 65-128. UNCLASSIFIED REPORT.

5. General Applied Sciences Laboratory Report TR 569, "Diffusion Controlled Combustion for Scramjet Application." UNCLASSIFIED REPORT.

6. Monsanto Corporation Report AFAPL TR 65-93 U.S. Air Force, "Shock Tube Studies of Fuel-Air Ignition Characteristics." UNCLASSIFIED REPORT.

7. Fay, J. A. and F. R. Riddell, "Theory of Stagnation Point Heat Transfer In Dissociated Air," Journal of Aeronautical Sciences, Vol. 25, No. 2, February 1958, UNCLASSIFIED REPORT.

8. The Marquardt Corporation Report 6102, "Ramjet Preliminary Design Report -- Hypersonic Ramjet Experiment Project," 28 February 1966. CONFIDENTIAL REPORT.

9. Burke, A. F. "Turbulent Boundary Layers on Highly Cooled Surfaces at High Mach Numbers," Cornell Aeronautical Laboratory Report 118, November 1961. UNCLASSIFIED REPORT.

10. Bartz, D. R., "A Simple Equation for Rapid Estimation of Rocket Nozzle Convective Heat Transfer Coefficients," Jet Propulsion, January 1957, pp 49-51. UNCLASSIFIED.

11. The Marquardt Corporation Report 6097, "Preliminary Instrumentation Requirements Report for the NASA Hypersonic Ramjet Experiment Project," 20 September 1965. CONFIDENTIAL REPORT.

12. Eckert, E. R. G., "Engineering Relations for Friction Heat Transfer to Surfaces in High Velocity Flow," Journal of Aeronautical Sciences, Vol. 22, No. 8, August 1955, pp 585-587. UNCLASSIFIED REPORT.

28 February 1966
THE MARQUARDT CORPORATION
Van Nuys, California

LIST OF SYMBOLS

Symbol	Description
A	Area
$C_{T,i}$	Internal thrust coefficient
h	Static enthalpy
h_T, H	Total enthalpy
H_2	Hydrogen
$I_{s,i}$, I_{SF}	Fuel specific impulse
K_D	Inlet process efficiency $(h_2 - h_o')/(h_2 - h_o)$
K_N	Nozzle process efficiency $(h_o - h_4)/(h_3 - h_3')$
M	Mach number
p, P	Static pressure
P_T	Total pressure
q	Dynamic pressure
$\dot{q}$	Heat flux
Re	Reynolds number
R_o, R_N	Inlet leading edge radius
T	Temperature
T_T	Total temperature
T_W	Wall temperature
$\dot{W}_f$	Fuel flow rate
X	Station
Y	Inlet width or characteristic dimension
ϵ_s	Radiation emissivity

LIST OF SYMBOLS (Continued)

Symbol	Description
η_c	Combustion efficiency
η_{KE}	Inlet kinetic energy efficiency $(h_{T,2} - h'_o)/(h_{T,o} - h_o)$
η_N	Nozzle kinetic energy efficiency $(h_{T,4} - h_4)/(h_{T,3} - h'_3)$
θ_j	Fuel injection angle
ϕ	Ratio of coolant or fuel flow to stiochiometric fuel flow
Λ	Inlet leading edge sweep angle

Subscripts

i	Internal
T	Total
f	Fuel
c	Coolant
W	wall
j	Jet
eff	Effective
F	Viscous
D	Divergence
NE	Nonequilibrium
FZ	Freeze
W, S	Surface

Station Notation

∞	Free stream
o	Immediately ahead of inlet
2	Combustor inlet

LIST OF SYMBOLS (Continued)

Symbol	Description
3	Nozzle inlet
4	Nozzle exit
r, R	Reference area, 1.76 sq ft
$0'_3$	Isentropic expansion from state 3 to pressure at state 0
$3'_4$	Isentropic expansion from state 3 to pressure at state 4

TABLE I

SUMMARY OF RESPONSE TO GUIDELINES
FOR HYPERSONIC RAMJET RESEARCH ENGINE PROJECT

Guideline Requirement	Marquardt Response
ENGINE MACH NUMBER AND ALTITUDE CAPABILITIES	
Design flow field	Free stream, Line B-B
Mach number range	As specified
Operational altitude range	X-15A-2 flight envelope
ENGINE PERFORMANCE REQUIREMENTS	
Definitions	η_c - See Preliminary Design Report No. 6102
Performance (Mach 4 to 8)	Free stream; C_{ti}, I_{si}, Figure 2
Performance; X-15A-2 flow field	Not greatly compromised. See Preliminary Design Report No. 6102
Discontinuities	As specified
External drag	Function of installation on X-15A-2
Equivalence ratio (burning)	Selected configuration, D-6, will operate at $\phi \leq 1$ at $M_\infty \geq 4$
ENGINE DESIGN FEATURES	
Engine Size and Overall Configuration	
Capture area	1.76 sq ft
Engine length	82 inches (Configuration D-6)
Nozzle exit area	Twice the inlet capture area
Flight instrumentation	See Preliminary Design Report No. 6102

TABLE I (Continued)

Guideline Requirement	Marquardt Response
Combustor Operating Modes	M_∞ = 3 to 8, supersonic combustion M_∞ = 3 to 6, subsonic combustion
Variable Geometry	None
Structures and Cooling	Thermal protection required
Structural integrity	Maintained at all times. See Preliminary Design Report No. 6102
Cooling	As specified
Fuel	
Fuel for ingition	Hydrogen capacity = 48 lbs See Preliminary Design Report No. 6102
Engines Required and Engine Life	
Number of engines required	3.0 plus 100% spares
Engine life	200 cycles for all components
Engine Starting and Restarting	
Starting and restarting	Configuration selected inherently restartable with fuel flow reduction. Ignition system supplied.
Unstarts	As specified
Purging	As specified
Refurbishment and maintenance	As specified

TABLE II

X-15A AIRPLANE REQUIREMENTS & INFORMATION RELATED TO THE HYPERSONIC RAMJET RESEARCH ENGINE PROJECT

Requirement	Remarks
ENGINE INSTALLATION	
Flight Safety	Safety of X-15 and pilot not to be endangered
Engine jettison	To be incorporated in design of attachment
Purging system	To be incorporated in research engine
Fire warning device	Required for pilot attention
Structural design criteria	Angle of attack = -5°, + 0, + 30° Yaw = ± 7 . Dynamic pressure to 2500 psf Inertia Longitudinal +4.5 g -3.0 Transverse ±1.0 g Normal +6.8 -1.0 g Factor of safety = 1.5 based on ultimate strength
Attachment	
Ground clearance	See Figure 2 of Appendix A to the Statement of Work
Engine removal and replacement	Design for easy removal and replacement
Thrust and drag measurements	Thrust and drag measured in flight
Engine weight	Not to exceed 800 lbs

TABLE II (Continued)

Requirement	Remarks
OPERATION OF ENGINE	
Pilot Control	Minimum pilot attention
Pressurization and Purging	Helium system NASA CR-53481, (Report 6020)
Available Fuel	48 lbs liquid hydrogen.
Available Electrical Power	3-Phase, 115 volts, 400 cycles a-c 28 volts d-c. 10 amps a-c or d-c (To be shared with X-15 instrumentation) 1.5 KVA prelaunch heating power available from B-52. Ramjet electrical system to be fail-safe.
Power and Signal Grounds	Single point grounding by NASA aircraft wiring
Cooling	Compatible with X-15A-2 safety Nonburning cooling phase may use helium system of X-15A-2
Vibration	Environment of 0.06-in. double amplitude at 10 to 55 cps and 3 g vibration from 55 to 2000 cps. Engine and mount designed to avoid vibration inputs at less than 5 cps, between 10 and 15 cps, and between 90 and 100 cps.
Ambient Environment	Low speed ambient environment of B-52 at 45,000 ft. for 75 minutes prior to launch
FLIGHT TEST ASPECTS	
General	Program to consist of 25 flights by NASA at Edwards FRC over present X-15 test range

TABLE II (Continued)

Requirement	Remarks
Early Flight Engine Experiments	Cold flow (Nonburning)
Flight Research with Engine Combustion	At higher speeds in steps to gradually increase severity of environment
Flight Test Times	20 seconds at $M_\infty = 7.8$ 45 seconds at $M_\infty = 7.0$
Landing	Rodgers Dry Lake bed; other dry lake beds in emergency. Engine to accept fine dust associated with current X-15A-2 systems.

TABLE III

ENGINE CONCEPT SELECTION CRITERIA

Performance and Flexibility
Engine performance (Minimum goals)
Component performance (Interrelationships, area requirements, etc.)
Operation flexibility (Altitude, Mach number)
Research potential (Combustor mode, Mach number, altitude, scalability)
Growth potential
External drag
Mechanical/Structural Design
X-15 Compatibility
Size
Shape
Fuel injection and distribution, equivalence ratio
Cooling--Type, sensitivity to design, coolant load
Fuel--Handling, control, purging
Pilot control and monitoring required
Structural concepts
Material requirements
Instrumentation requirements and installation
Degree of variable geometry required
Growth potential
Development
Difficulty
Number of engines required
State of the art
Costs
Testability
Engine life
Weight
Manufacturing and tooling requirements
Reliability

TABLE IV

INLET GEOMETRIC DATA

Configuration	Primary Compression	Characteristic Length (Ins.)	$\frac{A_{wet}}{A_{ref}}$
A	(Isentropic spike)	98.0	16.50
B	15° Cone half angle	32.5	2.47
B-1	(Isentropic spike)	46.0	3.00
C	10° Wedge; 3 1/2° internal cone	28.0	4.00
D	10° Cone half angle	31.0	3.26
D-6	10° Cone half angle	26.0	2.73
E	6° 2-D Isentropic spike	20.3	2.02
F	8° 2-D Isentropic spike	20.3	2.50

TABLE V

SUMMARY OF INLET GEOMETRIC AND PERFORMANCE FACTORS

Configuration	K_D	P_{T_2}/P_{T_o}	η_{KE}	A_o/A_R	$(A_2/A_r)_{eff}$
$M_\infty = 4$					
A	0.910	0.690	0.944	0.87	0.170
B	0.965	0.888	0.989	0.58	0.249
C	0.965	0.770	0.976	0.85	0.140
D	0.955	0.705	0.967	0.85	0.140
D-6	0.970	0.830	0.980	0.95	0.140
E	0.951	0.690	0.965	0.88	0.140
F	0.970	0.820	0.982	0.88	0.140
$M_\infty = 6$					
A	0.900	0.545	0.972	0.92	0.090
B	0.895	0.685	0.984	0.74	0.245
C	0.970	0.620	0.980	0.98	0.050
D	0.950	0.520	0.972	0.98	0.050
D-6	0.965	0.690	0.984	0.98	0.050
E	0.950	0.530	0.972	1.00	0.050
F	0.960	0.633	0.980	1.00	0.050
$M_\infty = 8$					
A	0.920	0.505	0.984	0.93	0.065
B	0.815	0.415	0.979	1.00	0.250
C	0.925	0.400	0.977	1.00	0.050
D	0.930	0.410	0.977	1.00	0.050
D-6	0.935	0.460	0.981	0.98	0.050
E	0.930	0.450	0.980	1.00	0.050
F	0.940	0.490	0.983	1.00	0.050

TABLE VI

NOZZLE GEOMETRIC DATA

Configuration	L"	A_4/A_3	Equivalent Expansion	A_{wet}/A_R	A_4/A_R
A	30.7	3.45	9° conical	8.5	1.88
B	45.7	3.38	8° conical	10.63	1.88
C	27.8	2.93	9° conical	7	1.88
D	38	2.89	4° 2-D	10.28*	2
E	38	2.81	6° 2-D	6.2	1.8
F	38	2.98	6 1/4° 2-D	6.2	1.8

* Includes wetted area of centerbody support struts.

TABLE VII

SUMMARY OF COMPONENT EFFICIENCIES AND GEOMETRY FACTORS FOR ALL CONFIGURATIONS

SUPERSONIC COMBUSTION																		
Parameter	M_o = 4.0						M_o = 6.0						M_o = 8.0					
	Configuration						Configuration						Configuration					
	A	B	C	D	E	F	A	B	C	D	E	F	A	B	C	D	E	F
	HIGH q																	
K_D	0.91	0.965	0.965	0.955	0.951	0.97	0.90	0.895	0.97	0.95	0.95	0.96	0.92	0.815	0.925	0.93	0.93	0.94
P_{T_2}/P_{T_o}	0.69	0.888	0.77	0.705	0.69	0.82	0.545	0.685	0.62	0.520	0.53	0.633	0.505	0.415	0.40	0.410	0.45	0.49
η_{KE}	0.965	0.989	0.976	0.967	0.965	0.982	0.972	0.984	0.98	0.972	0.972	0.98	0.984	0.977	0.977	0.977	0.98	0.983
η_c	0.94	0.94	0.91	0.91	0.91	0.90	0.92	0.89	0.925	0.925	0.925	0.920	0.95	0.87	0.91	0.91	0.91	0.90
ϕ	1.0	1.0	1.0	1.0	1.0	1.0	1.0	1.0	1.0	1.0	1.0	1.0	1.0	1.0	1.0	1.0	1.0	1.0
A_o/A_c	0.87	0.58	0.85	0.853	0.88	0.88	0.92	0.738	0.98	0.985	1.0	1.0	0.935	1.0	1.0	1.0	1.0	1.0
η_M	0.97	0.967	0.974	0.967	0.978	0.976	0.954	0.948	0.962	0.941	0.964	0.963	0.948	0.942	0.957	0.935	0.958	0.957
$(A_2/A_R)_{EFF}$	0.170	0.249	0.14	0.14	0.14	0.14	0.0905	0.245	0.05	0.05	0.05	0.05	0.065	0.25	0.05	0.05	0.05	0.05
A_4/A_R	1.88	1.88	1.88	0.2	1.8	1.8	1.88	1.88	1.88	0.2	1.8	1.8	1.88	1.88	1.88	0.2	1.8	1.8
	LOW q																	
K_D	0.90	0.960	0.960	0.948	0.946	0.965	0.895	0.885	0.96	0.945	0.946	0.955	0.892	0.810	0.920	0.93	0.926	0.935
P_{T_2}/P_{T_o}	0.652	0.872	0.734	0.671	0.675	0.794	0.465	0.665	0.547	0.450	0.499	0.580	0.397	0.395	0.364	0.375	0.424	0.464
η_{KE}	0.959	0.988	0.971	0.962	0.963	0.978	0.966	0.982	0.974	0.964	0.968	0.976	0.95	0.976	0 974	0.975	0.978	0.981
η_c	0.94	0.94	0.94	0.94	0.94	0.935	0.95	0.945	0.95	0.950	0.950	0.945	0.95	0.945	0.935	0.935	0.935	0.930
ϕ	1.0	1.0	1.0	1.0	1.0	1.0	1.0	1.0	1.0	1.0	1.0	1.0	1.0	1.0	1.0	1.0	1.0	1.0
A_o/A_c	0.87	0.58	0.85	0.853	0.88	0.88	0.92	0.738	0.98	0.985	1.0	1.0	0.935	1.0	1.0	1.0	1.0	1.0
η_M	0.942	0.959	0.967	0.959	0.97	0.970	0.943	0.946	0.953	0.928	0.952	0.952	0.934	0.927	0.944	0.916	0.942	0.943
$(A_2/A_R)_{EFF}$	0.169	0.247	0.133	0.133	0.137	0.135	0.090	0.242	0.0448	0.045	0.048	0.046	0.061	0.248	0.047	0.049	0.048	0.048
A_4/A_R	1.88	1.88	1.88	0.2	1.8	1.8	1.88	1.88	1.88	0.2	1.8	1.8	1.88	1.88	1.88	0.2	1.8	1.8

TABLE VII (Continued)

SUBSONIC COMBUSTION																		
Parameter	M_o = 3.0						M_o = 4.0						M_o = 6.0					
	Configuration						Configuration						Configuration					
	A	B	C	D	E	F	A	B	C	D	E	F	A	B	C	D	E	F
	HIGH q																	
K_D	—	—	—	—	—	—	—	—	—	—	—	—	—	—	—	—	—	—
P_{T_2}/P_{T_o}	0.754	0.571	0.854	0.804	0.794	0.903	0.497	0.286	0.764	0.700	0.685	0.813	0.179	0.095	0.433	0.363	0.37	0.441
η_{KE}	0.956	0.904	0.984	0.964	0.962	0.9835	0.931	0.866	0.975	0.966	0.964	0.980	0.911	0.924	0.962	0.953	0.954	0.963
η_c	0.95	0.95	0.95	0.95	0.95	0.95	0.95	0.95	0.95	0.95	0.95	0.95	0.95	0.95	0.95	0.95	0.95	0.95
ϕ	1.0	1.0	1.0	1.0	1.0	1.0	1.0	1.0	1.0	1.0	1.0	1.0	1.0	1.0	1.0	1.0	1.0	1.0
A_o/A_c	0.73	0.53	0.68	0.68	0.51	0.6	0.87	0.58	0.85	0.853	0.88	0.88	0.92	0.738	0.98	0.985	1.0	1.0
η_M	0.976	0.975	0.979	0.971	0.984	0.984	0.967	0.964	0.973	0.949	0.976	0.975	0.950	0.943	0.960	0.905	0.960	0.959
$(A_2/A_R)_{EFF}$	0.442	0.25	0.15	0.15	0.15	0.15	0.257	0.249	0.14	0.14	0.14	0.14	0.137	0.244	0.05	0.05	0.05	0.05
A_4/A_R	1.88	1.88	1.88	0.2	1.8	1.8	1.88	1.88	1.88	0.2	1.8	1.8	1.88	1.88	1.88	0.2	1.8	1.8
	LOW q																	
K_D	—	—	—	—	—	—	—	—	—	—	—	—	—	—	—	—	—	—
P_{T_2}/P_{T_o}	0.749	0.560	0.850	0.800	0.790	0.898	0.470	0.281	0.729	0.666	0.670	0.787	0.153	0.0923	0.382	0.314	0.348	0.404
P_{KE}	0.955	0.900	0.973	0.963	0.961	0.9825	0.925	0.864	0.970	0.961	0.962	0.976	0.90	0.922	0.956	0.945	0.951	0.959
η_c	0.95	0.95	0.95	0.95	0.95	0.95	0.95	0.95	0.95	0.95	0.95	0.95	0.95	0.95	0.95	0.95	0.95	0.95
ϕ	1.0	1.0	1.0	1.0	1.0	1.0	1.0	1.0	1.0	1.0	1.0	1.0	1.0	1.0	1.0	1.0	1.0	1.0
A_o/A_c	0.73	0.53	0.68	0.68	0.51	0.6	0.87	0.58	0.85	0.853	0.88	0.88	0.92	0.738	0.98	0.985	1.0	1.0
η_M	0.950	0.960	0.972	0.955	0.975	0.976	0.937	0.956	0.968	0.936	0.967	0.969	0.940	0.943	0.967	0.885	0.947	0.947
$(A_2/A_R)_{EFF}$	0.437	0.397	0.144	0.144	0.144	0.144	0.250	4.05	0.133	0.133	0.137	0.137	0.127	4.14	0.0448	0.045	0.0478	0.0478
A_4/A_R	1.88	1.88	1.88	2.0	1.8	1.8	1.88	1.88	1.88	2.0	1.8	1.8	1.88	1.88	1.88	2.0	1.8	1.8

TABLE VIII

ENGINE CONCEPT SELECTION

ENGINE GEOMETRY COMPARISON

Configuration	Inlet Capture Area (sq ft)	Exit Nozzle Flow Area (sq ft)	Engine Length (ft)	External Surface Area (sq ft)	Internal Surface Area (sq ft)	Internal Volume (No Struts) (cu ft)
A	1.76	3.28	10.1	38.3	53.0	9.7
B	1.76	3.28	8.6	37.6	44.3	10.0
C	1.76	3.28	6.3	34.1	31.3	6.5
D	1.76	3.52	7.3	41.6	52.2	8.4
E	1.76	3.52	6.5	37.4	29.6	8.0
F	1.76	3.52	6.5	37.4	26.0	8.2

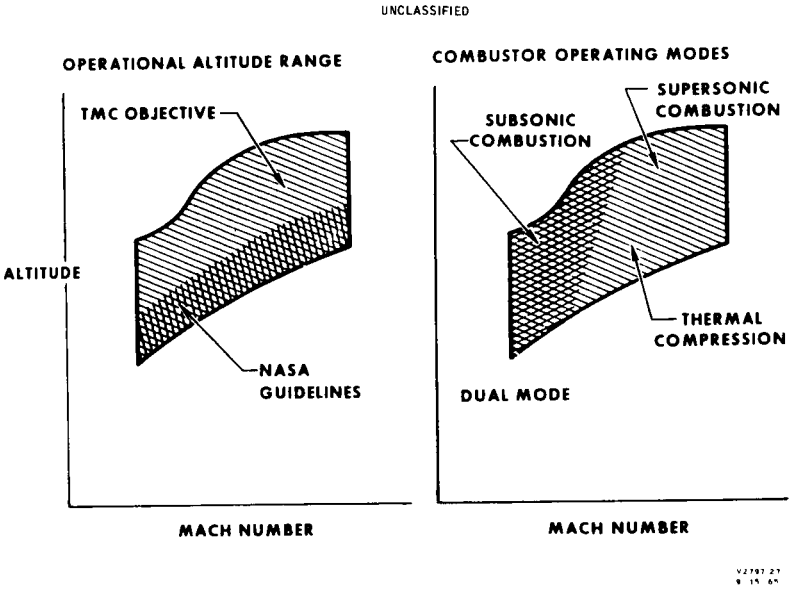

FIGURE 1. Research Flexibility

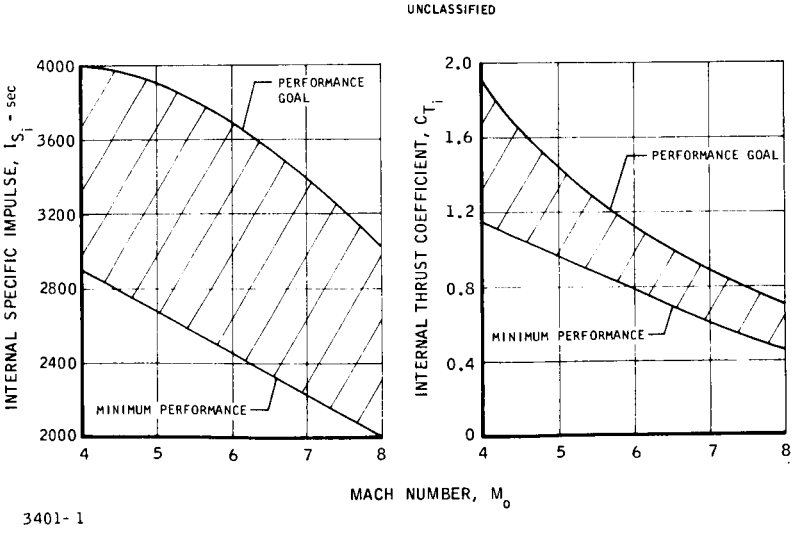

FIGURE 2. Performance Requirements
(Free Stream Conditions)

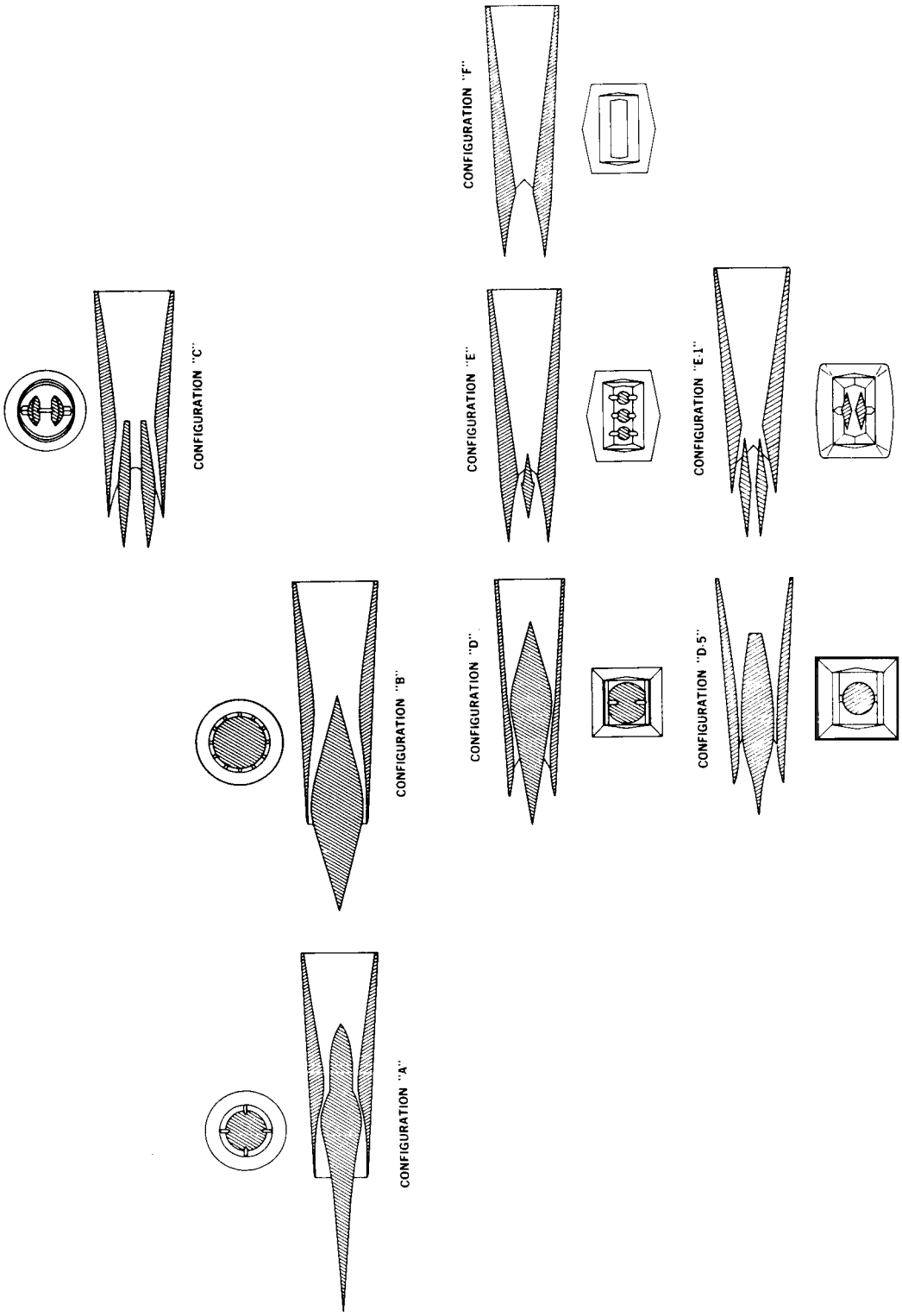

FIGURE 3. Candidate Engine Concepts

3401-19

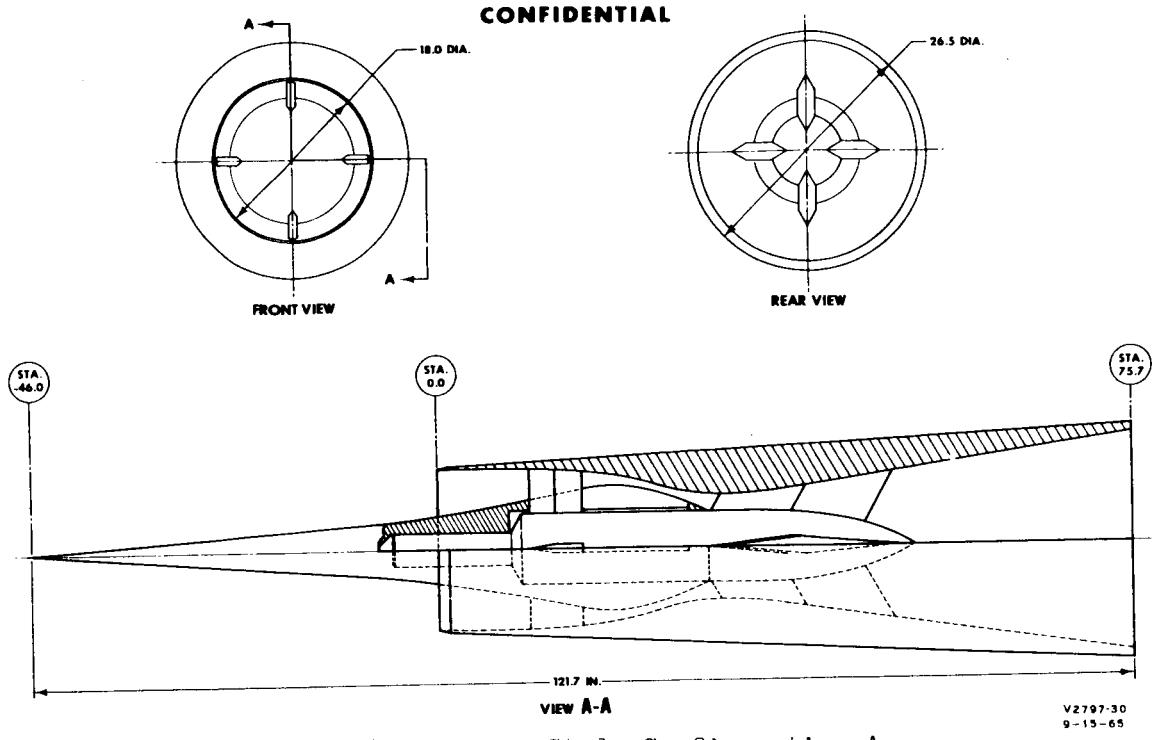

FIGURE 4. Engine Study Configuration A

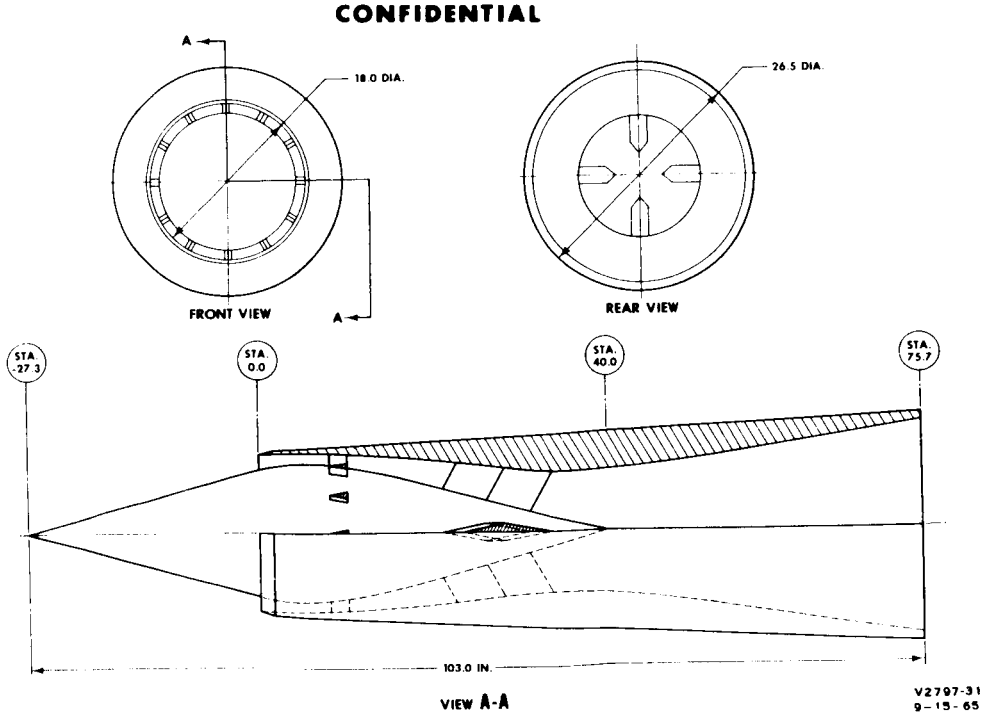

FIGURE 5. Engine Study Configuration B

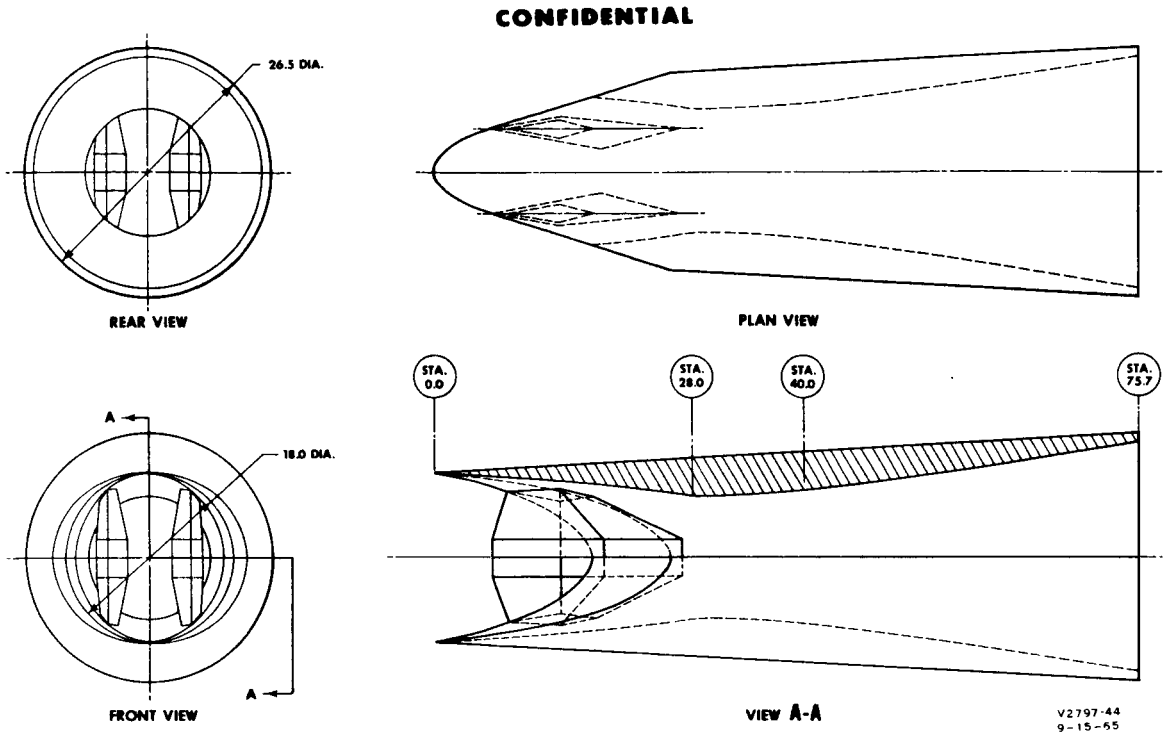

FIGURE 6. Engine Study Configuration C

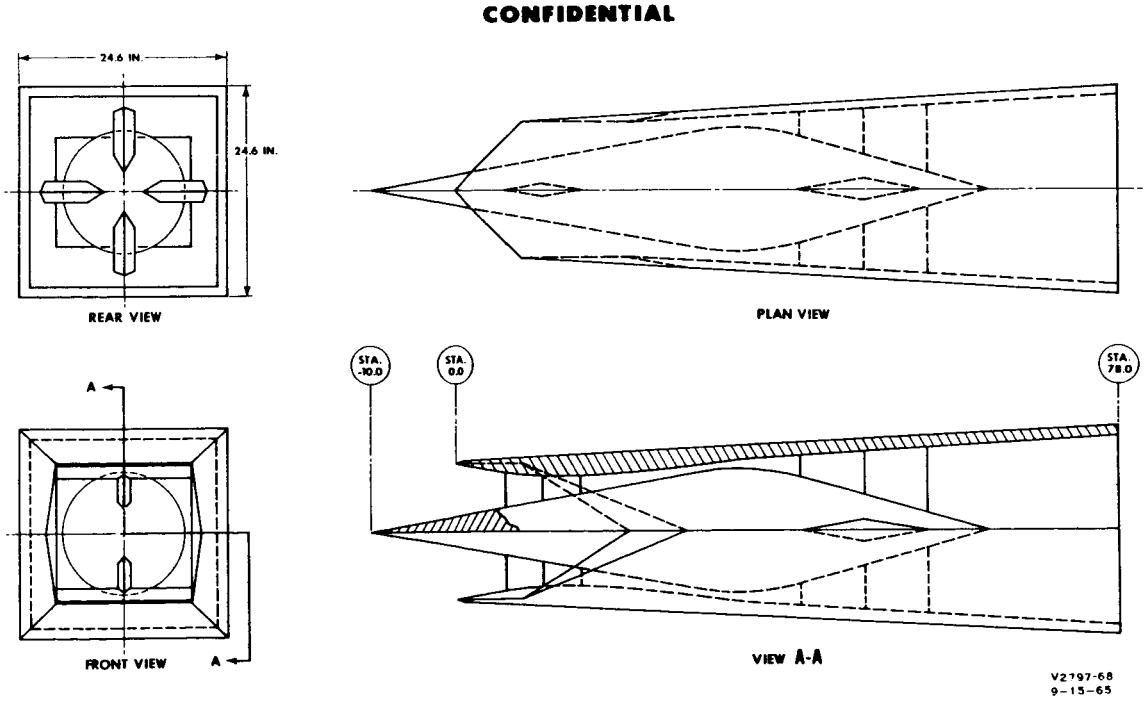

FIGURE 7. Engine Study Configuration D

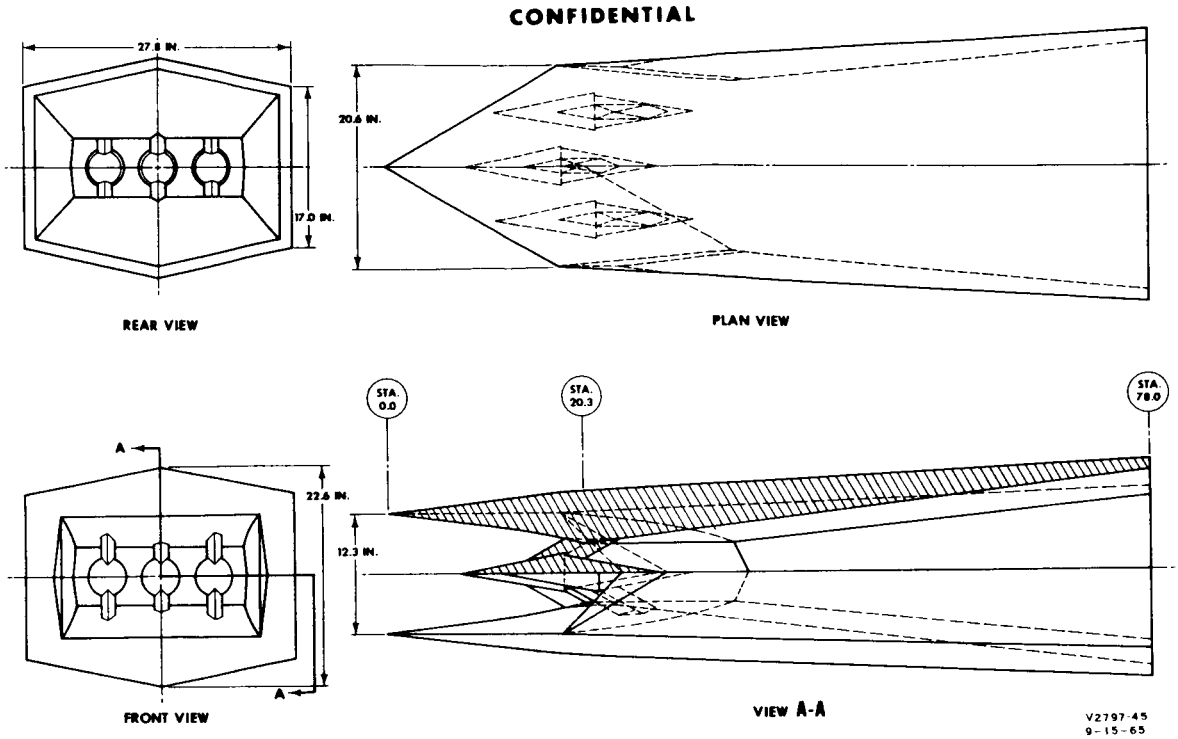

FIGURE 8. Engine Study Configuration E

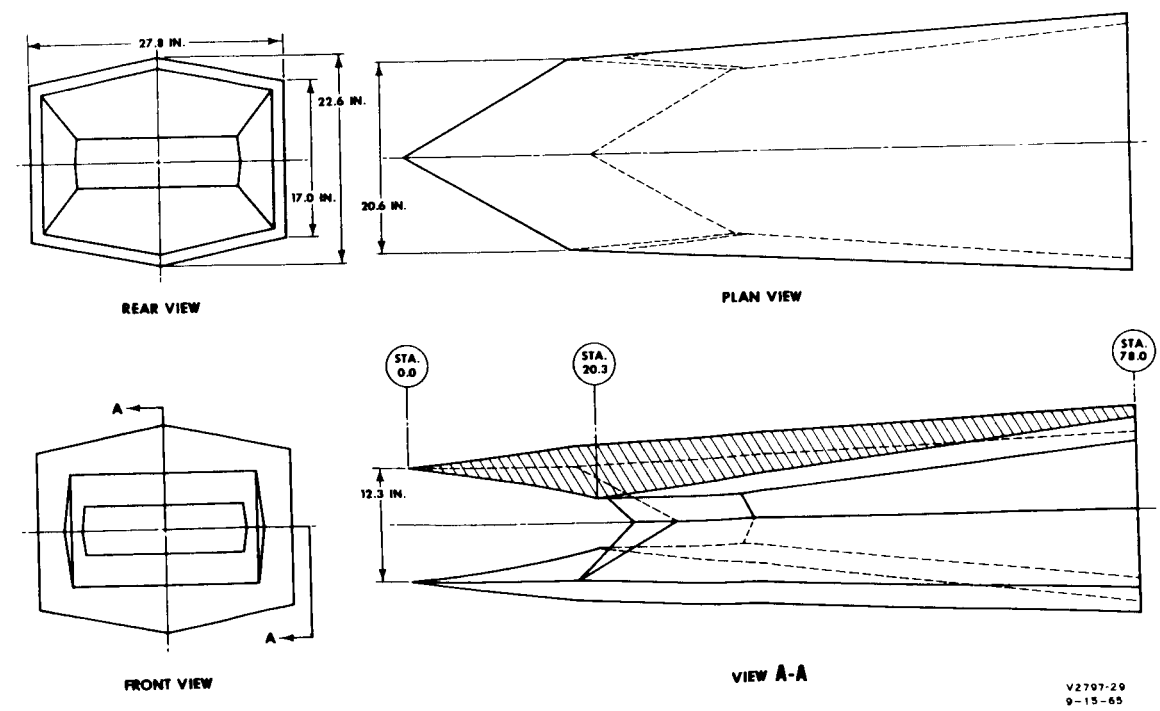

FIGURE 9. Engine Study Configuration F

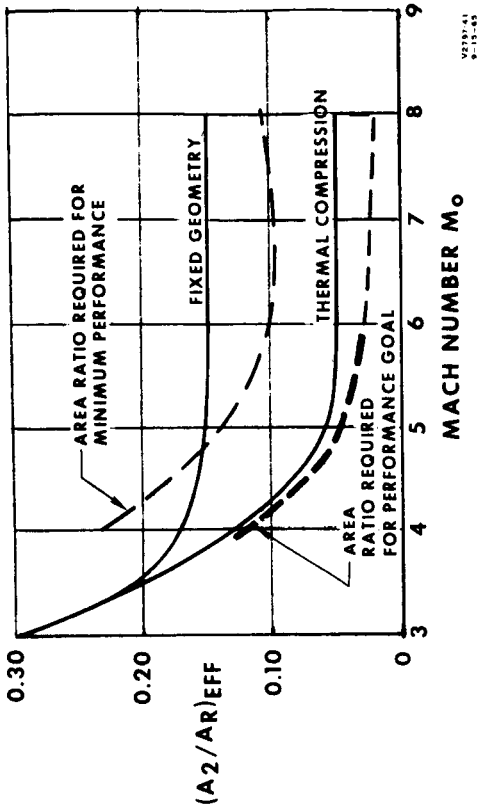

FIGURE 11. Required Inlet Contraction Ratio

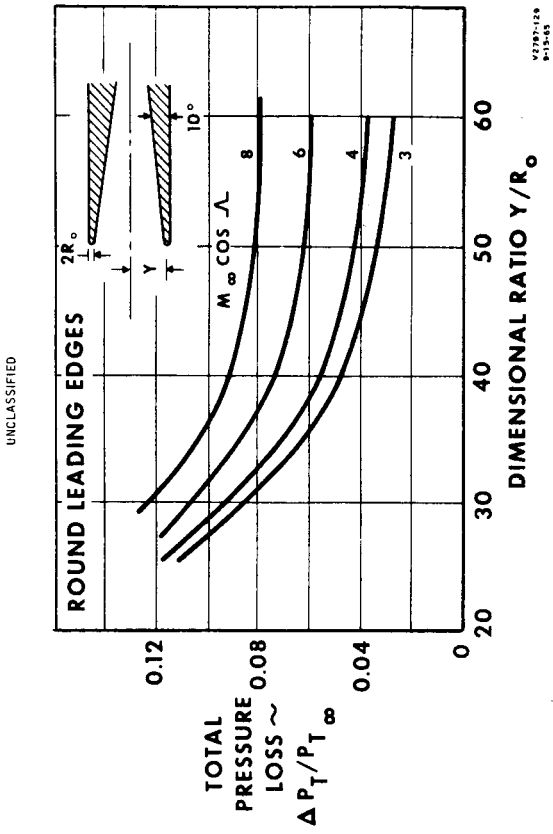

FIGURE 13. Total Pressure Loss Due to Leading Edge Bluntness

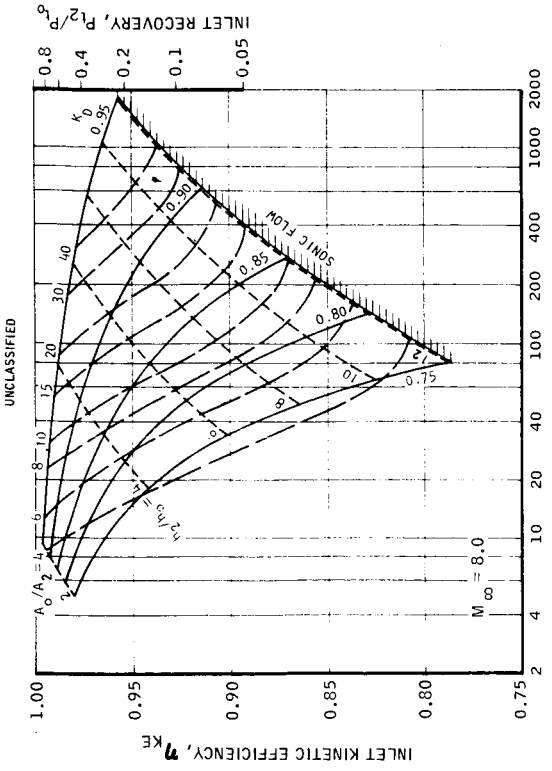

FIGURE 10. Typical Inlet Parameter Chart

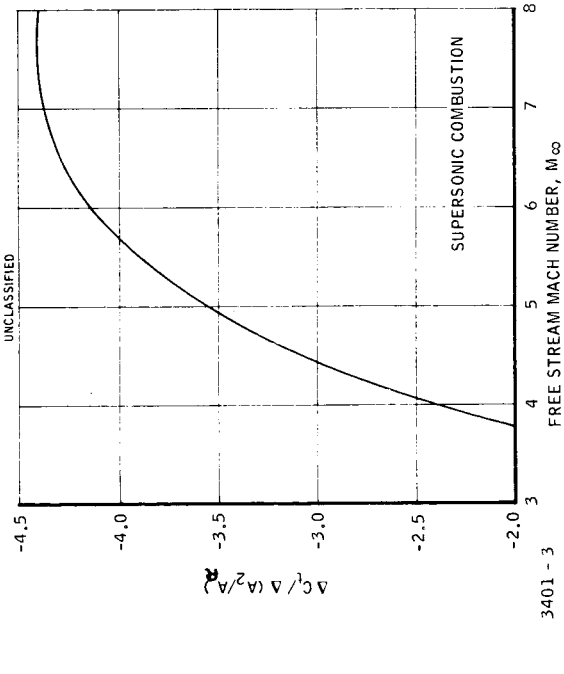

FIGURE 12. Effect of Inlet Effective Contraction Ratio on Thrust Coefficient

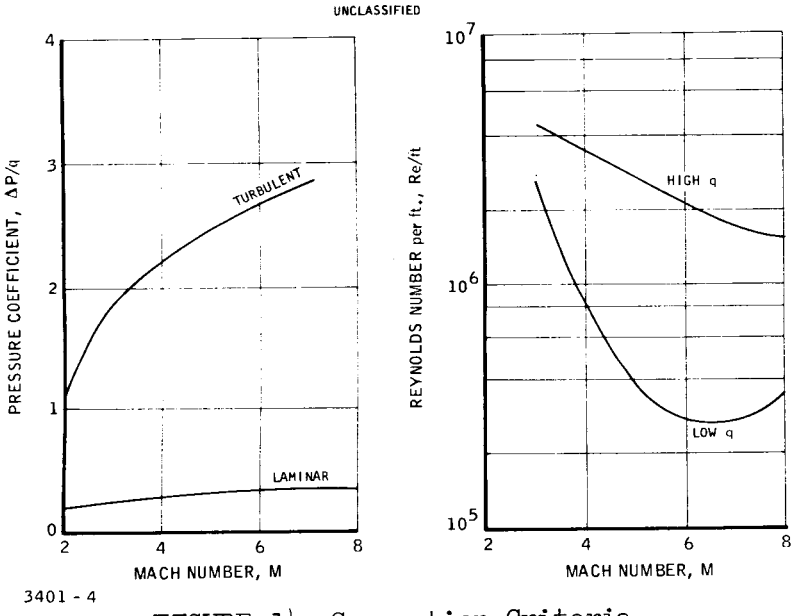

FIGURE 14. Separation Criteria

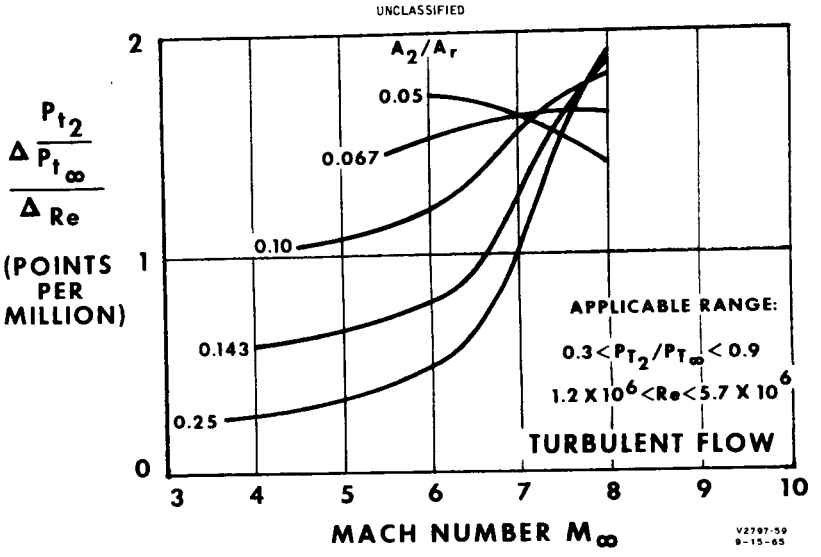

FIGURE 15. Inlet Total Pressure Recovery Friction Drag Influence Coefficients

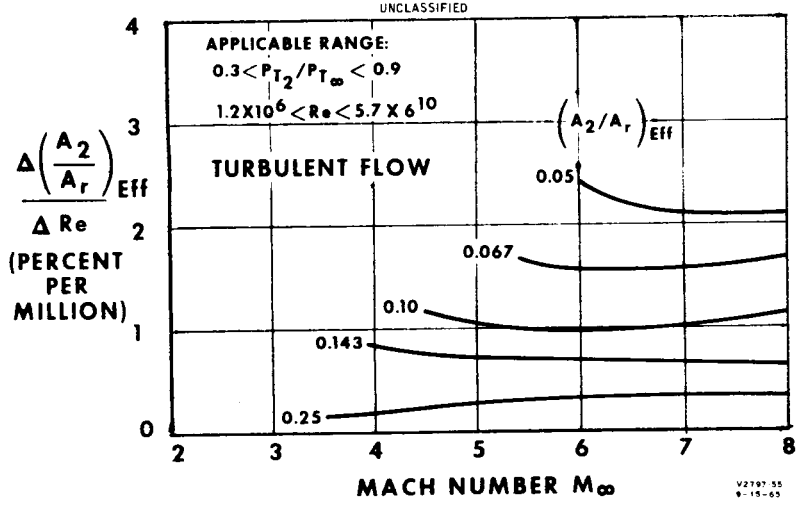

FIGURE 16. Inlet Effective Contraction Ratio Friction Drag Influence Coefficients

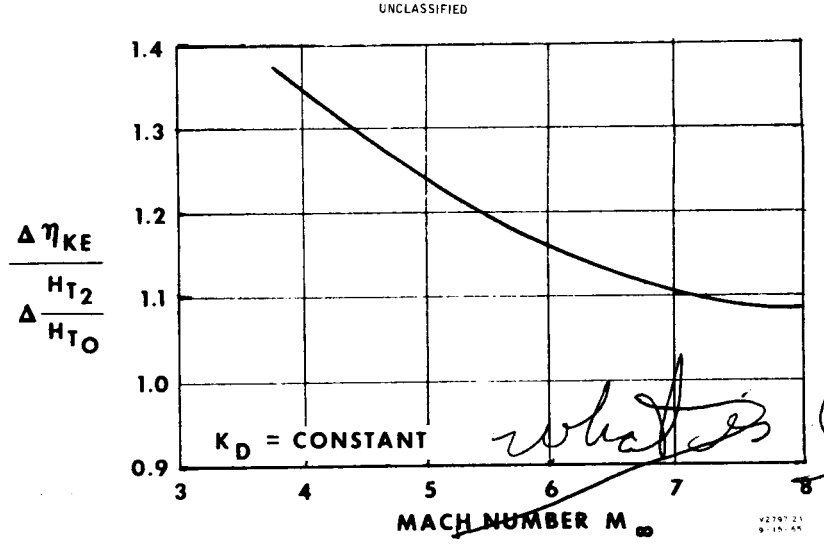

FIGURE 17. Effect of Energy Loss Upon Inlet Efficiency

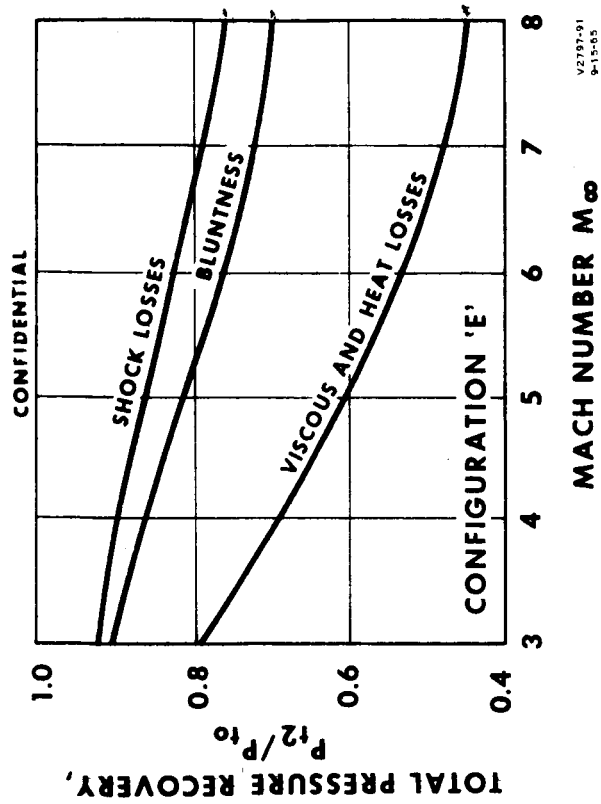

FIGURE 18. Typical Inlet Loss Summary

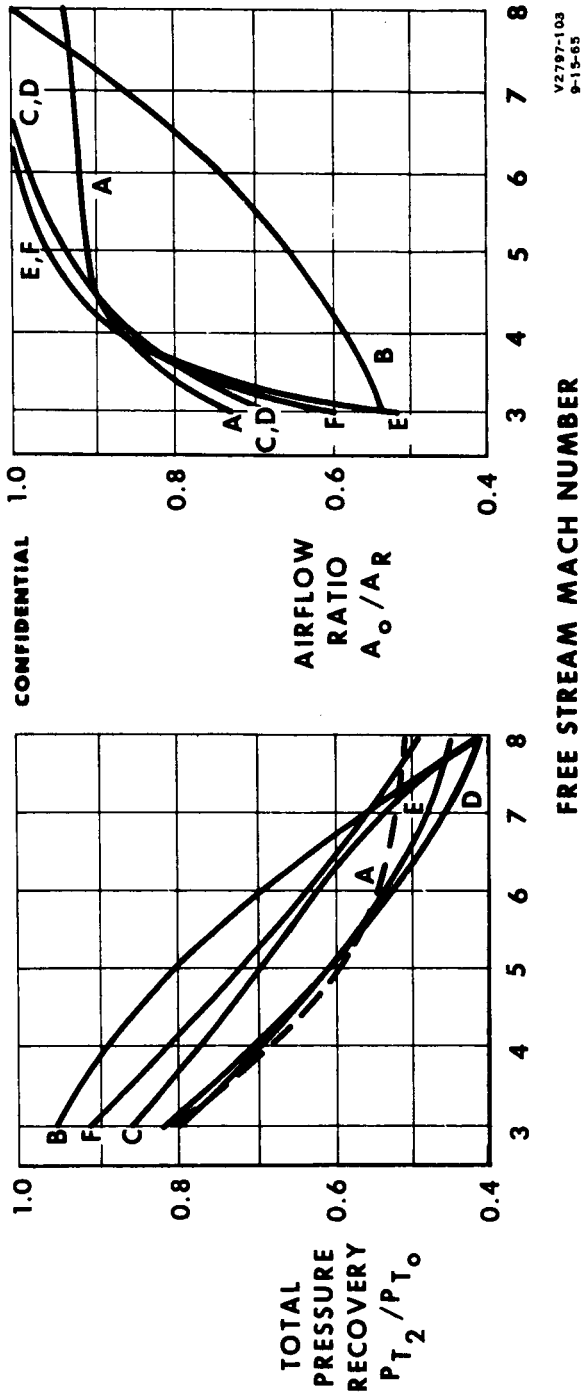

FIGURE 19. Pressure Recovery and Mass Flow, Low Altitude Trajectory

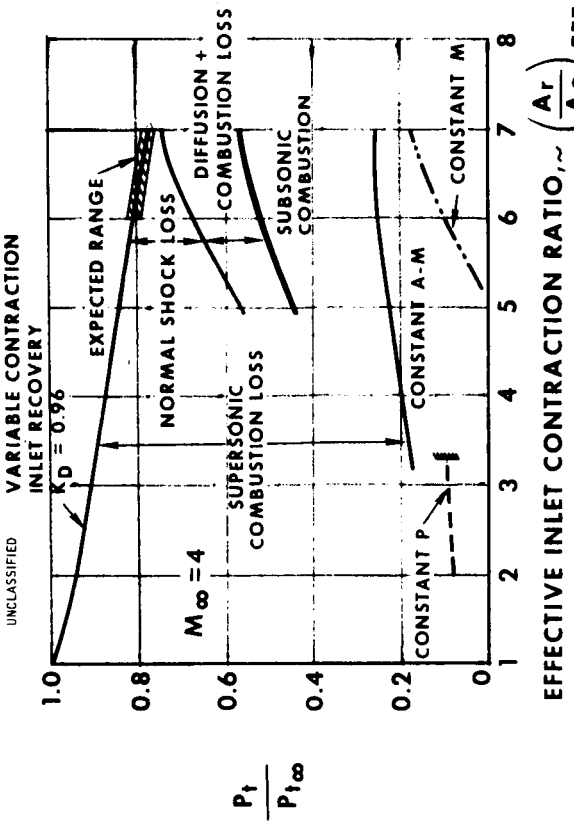

FIGURE 21. Inlet-Combustor Interaction, M_∞ = 4

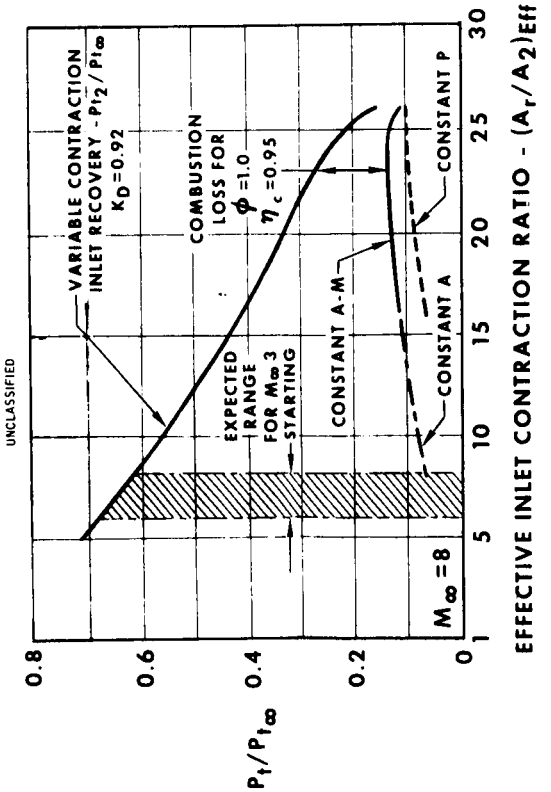

FIGURE 20. Inlet-Combustor Interaction, M_∞ = 8

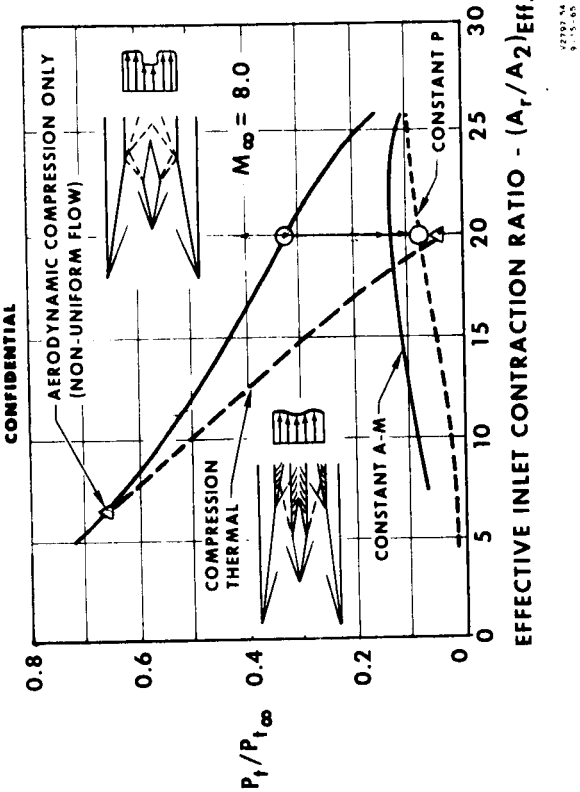

FIGURE 22. Thermal Compression Concept, M_∞ = 8

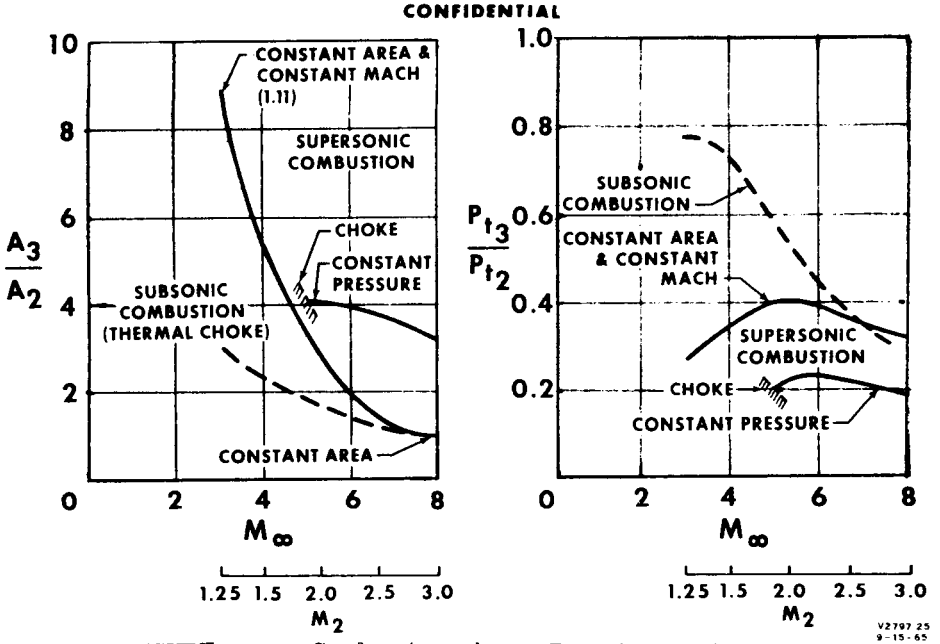

FIGURE 23. Combustor Area Requirements

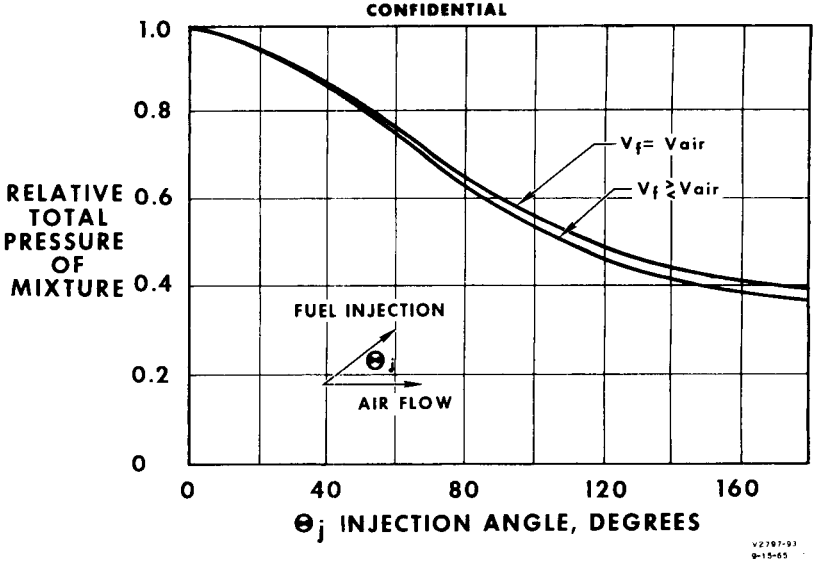

FIGURE 24. Variation of Total Pressure Recovery with Fuel Injection Angle

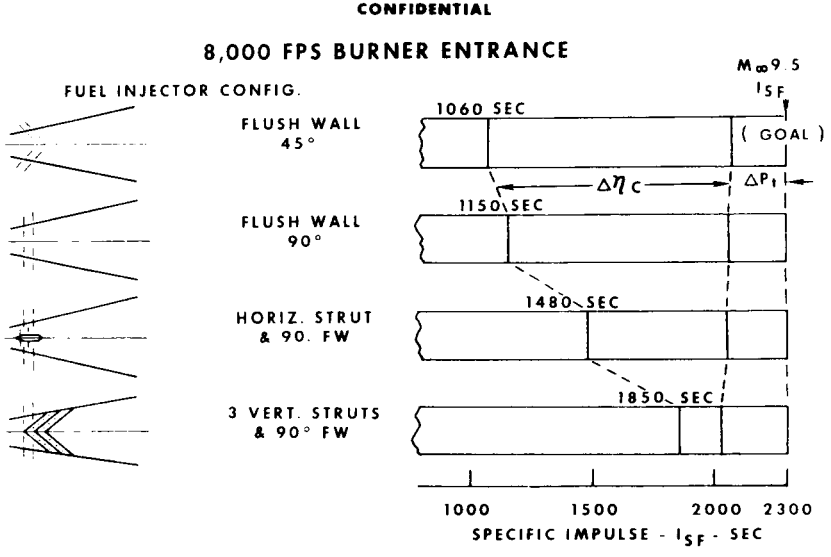

FIGURE 25. Effect of Injection Loss and Combustion Inefficiency on Engine Performance

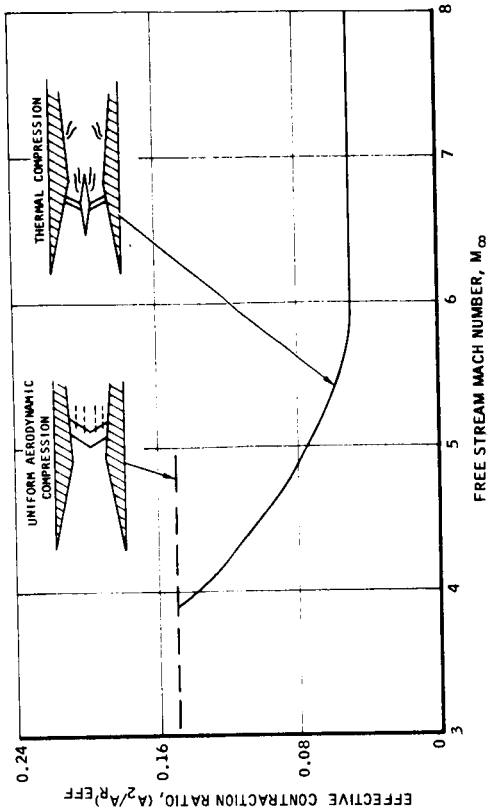

FIGURE 27. Effective Burner Inlet Area

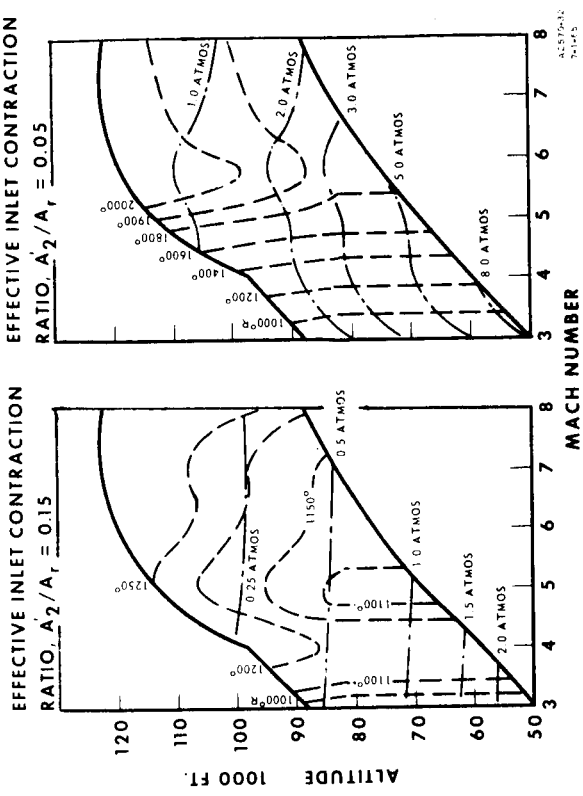

FIGURE 29. Typical Combustor Inlet Conditions

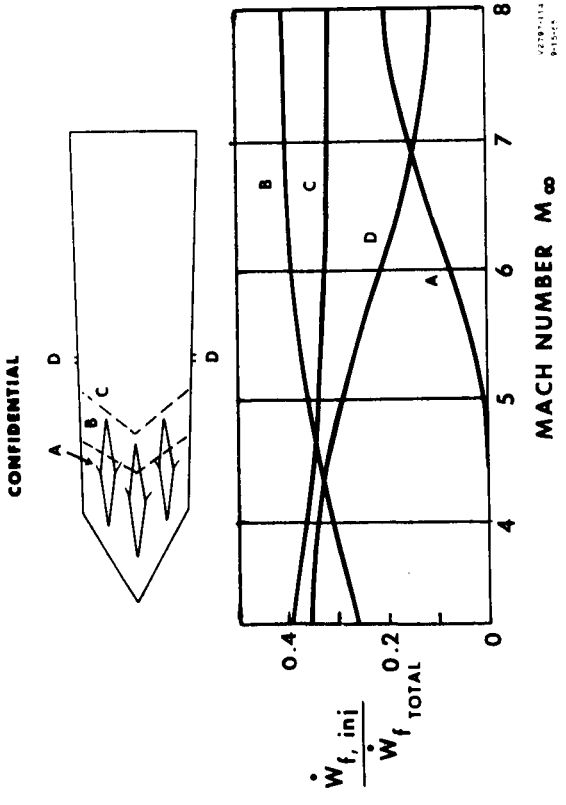

FIGURE 26. Typical Fuel Injector Locations and Fuel Distributions

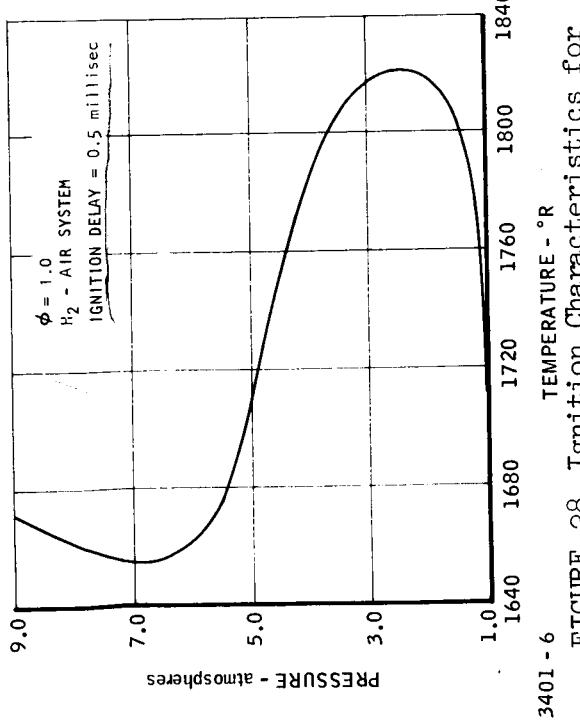

FIGURE 28. Ignition Characteristics for Hydrogen-Air Mixtures

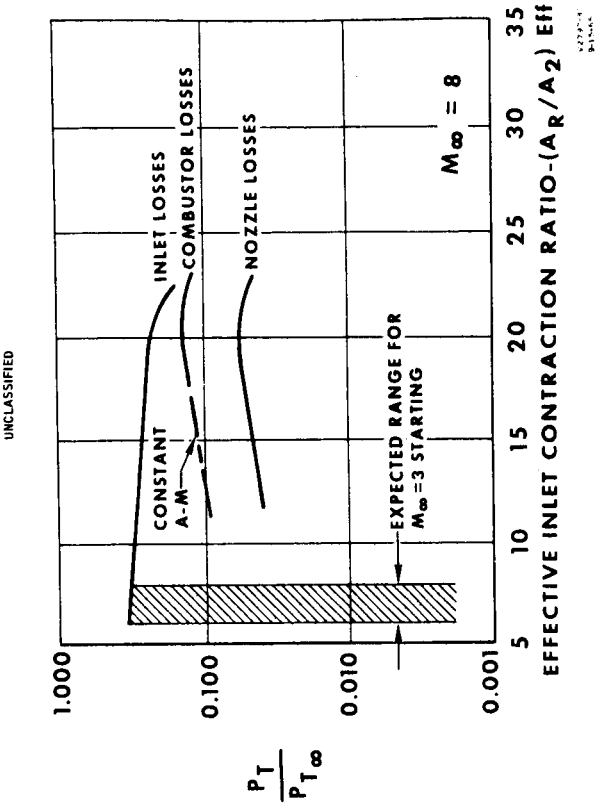

FIGURE 31. Inlet-Combustor-Nozzle Interaction

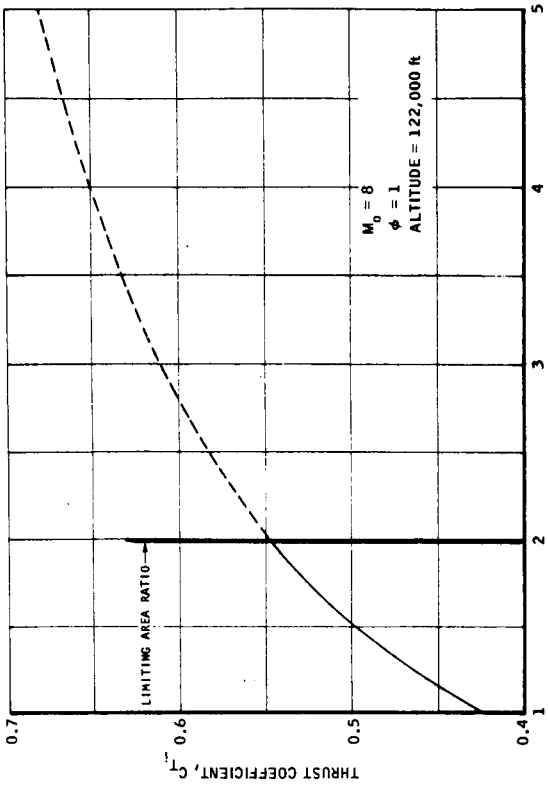

FIGURE 33. Effect of Nozzle Area Ratio

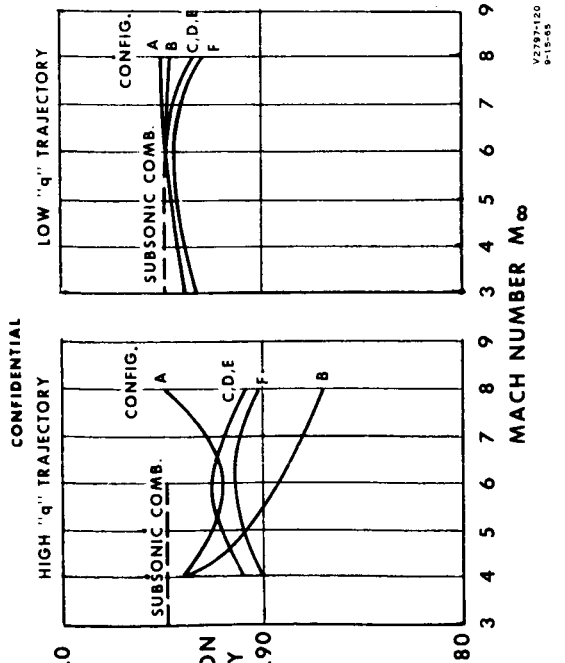

FIGURE 30. Summary of Estimated Combustion Efficiencies

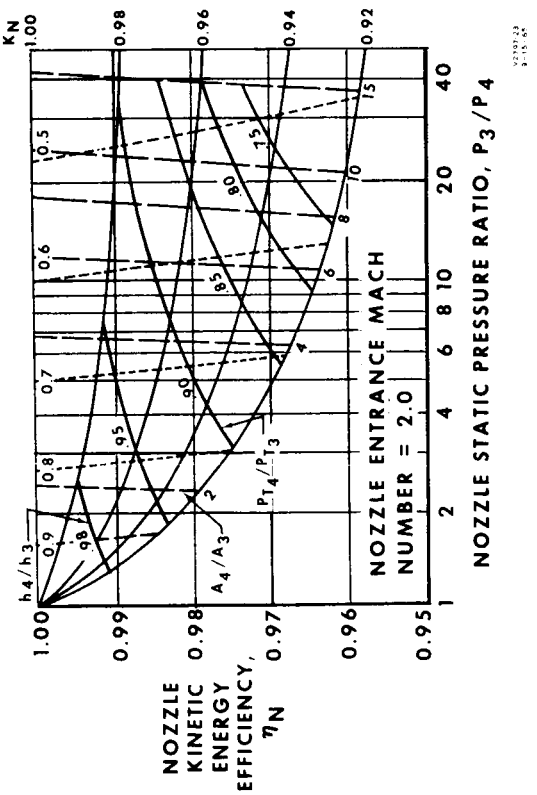

FIGURE 32. Typical Nozzle Parameter Chart

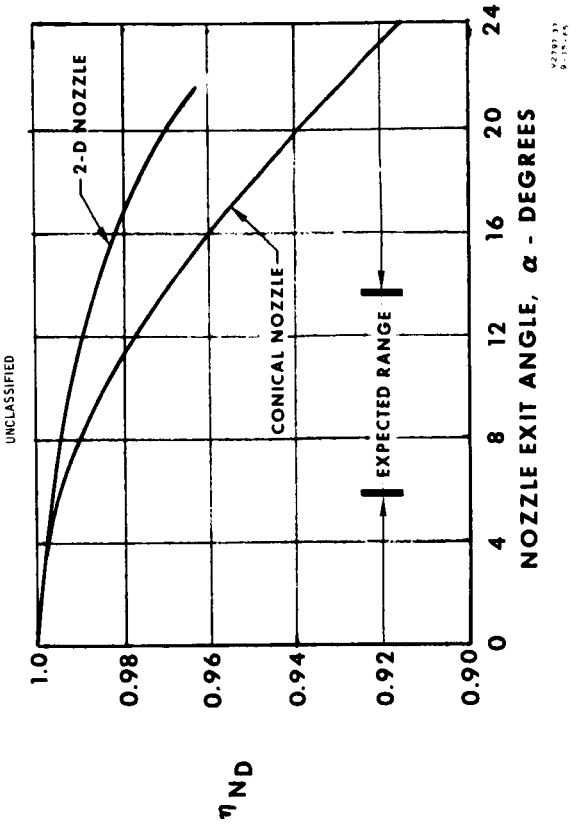

FIGURE 35. Nozzle Divergence Losses

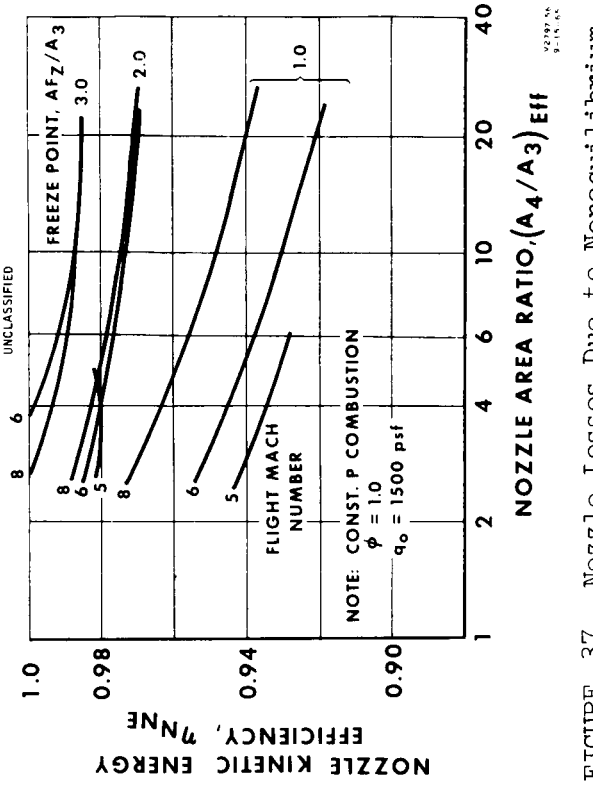

FIGURE 37. Nozzle Losses Due to Nonequilibrium Expansion

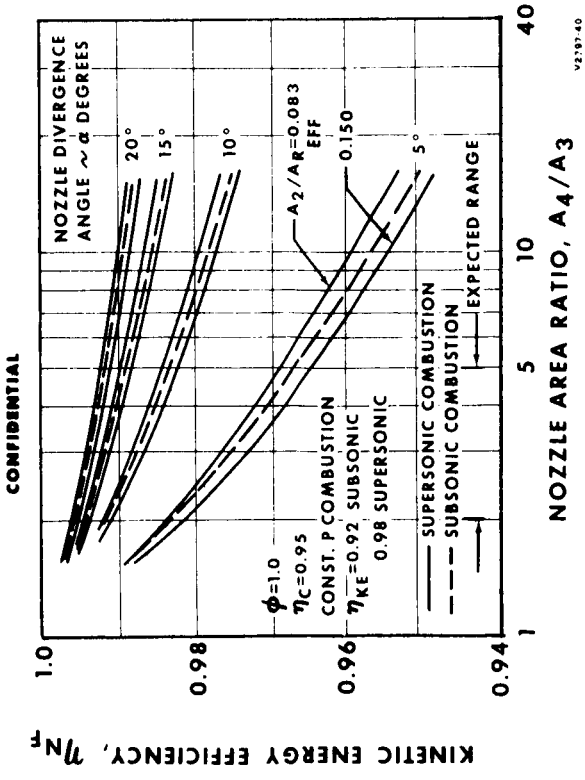

FIGURE 34. Nozzle Viscous Losses

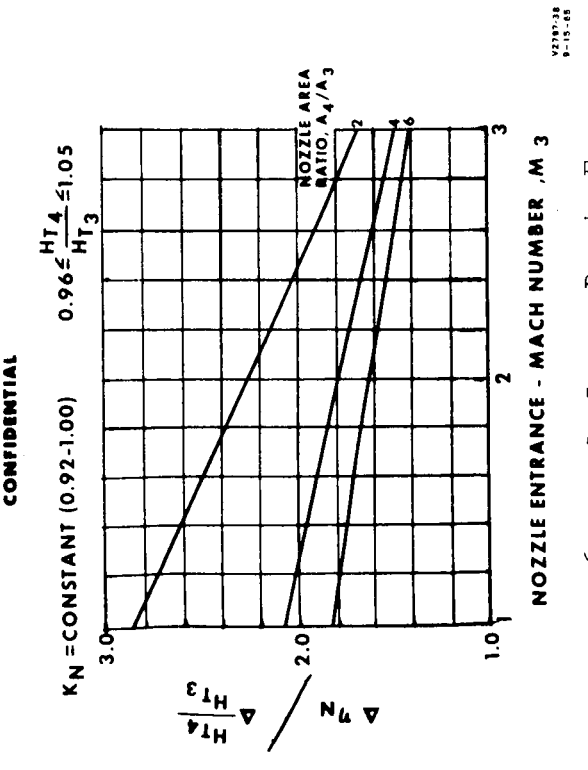

FIGURE 36. Nozzle Losses Due to Energy Extraction

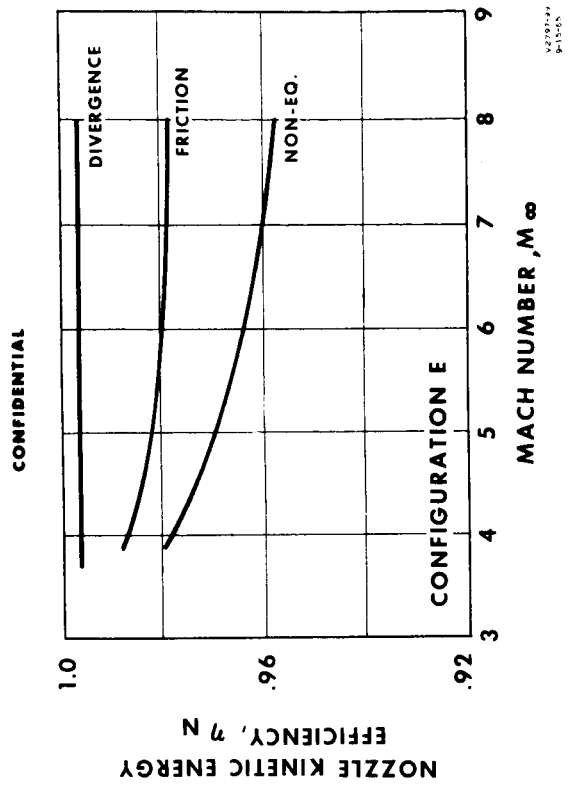

FIGURE 39. Typical Nozzle Loss Summary

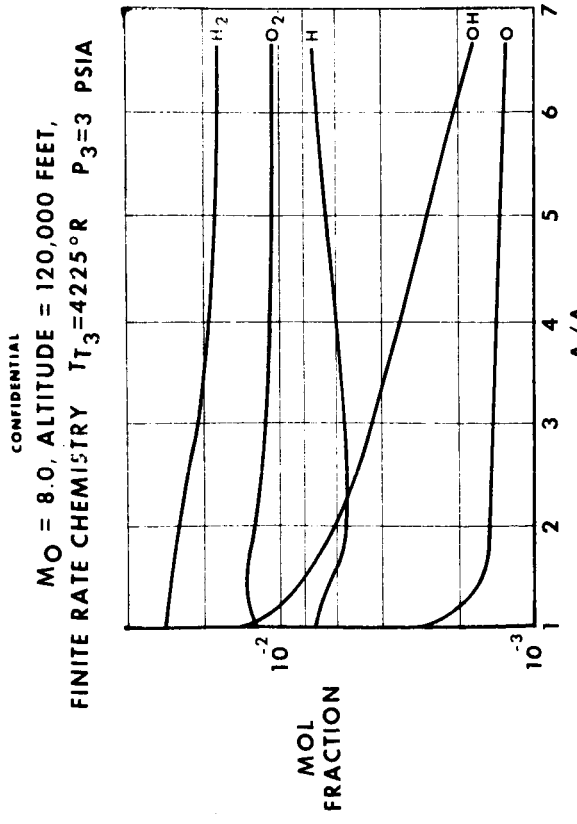

FIGURE 38. Gas Composition in Engine Nozzle

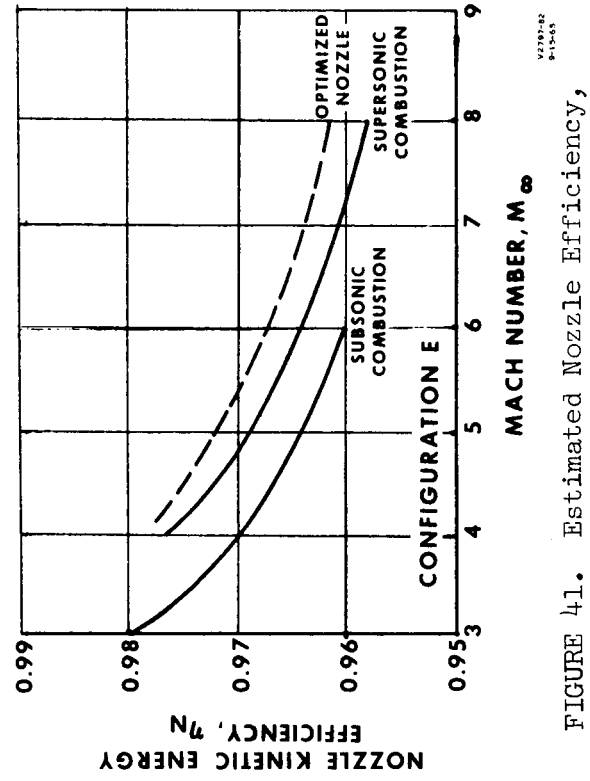

FIGURE 41. Estimated Nozzle Efficiency, Configuration E

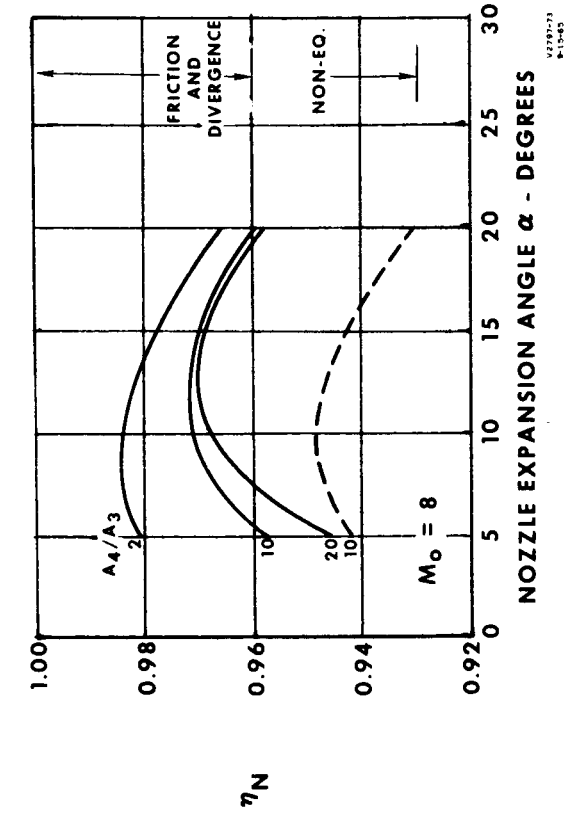

FIGURE 40. Optimization of Nozzle Expansion Angle

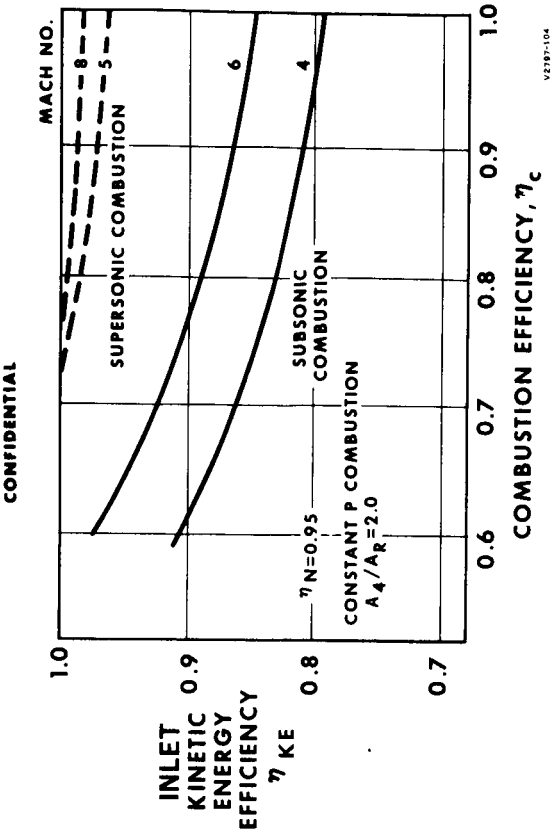

FIGURE 43. Component Functional Relationships for Minimum Performance

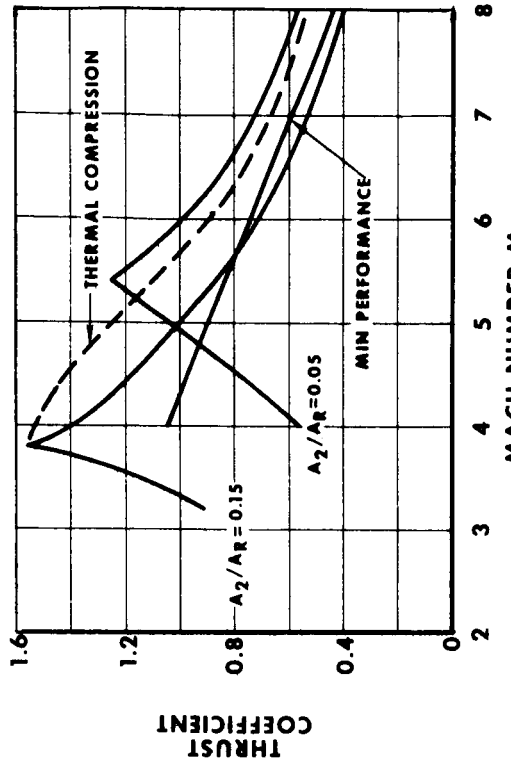

FIGURE 45. Typical Engine Performance with Supersonic Combustion

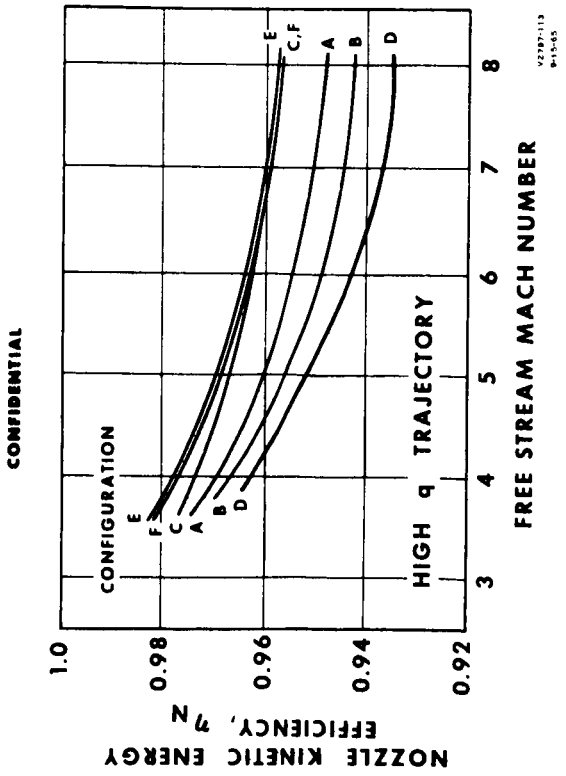

FIGURE 42. Summary of Nozzle Efficiencies

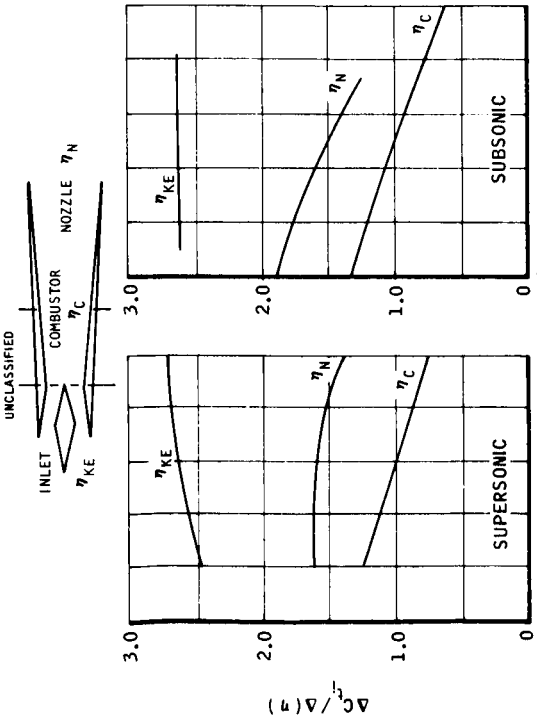

FIGURE 44. Component Functional Requirements - Influence Coefficients

3401-8

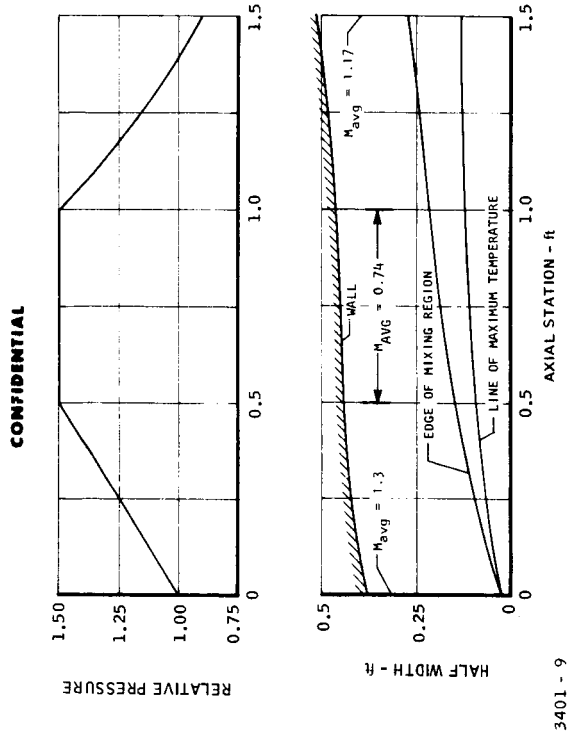

FIGURE 47. Subsonic Combustion Mode Through Thermal Compression

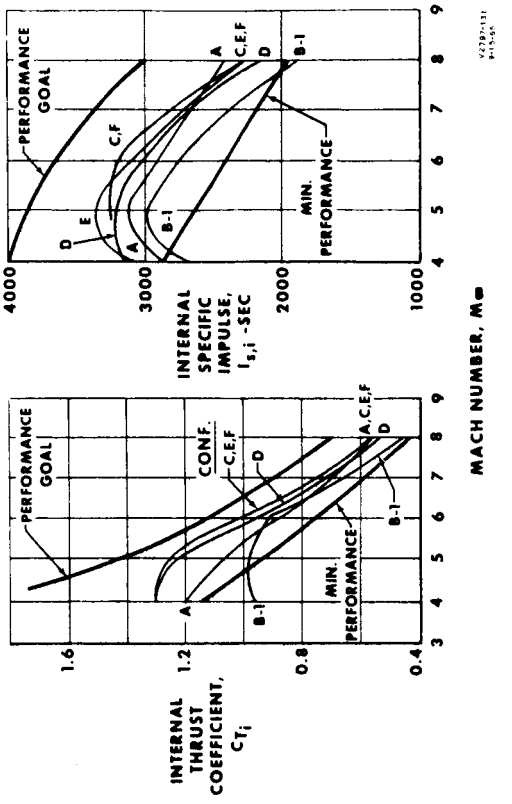

FIGURE 49. Thrust and Impulse Summary - Supersonic Combustion, High q Trajectory

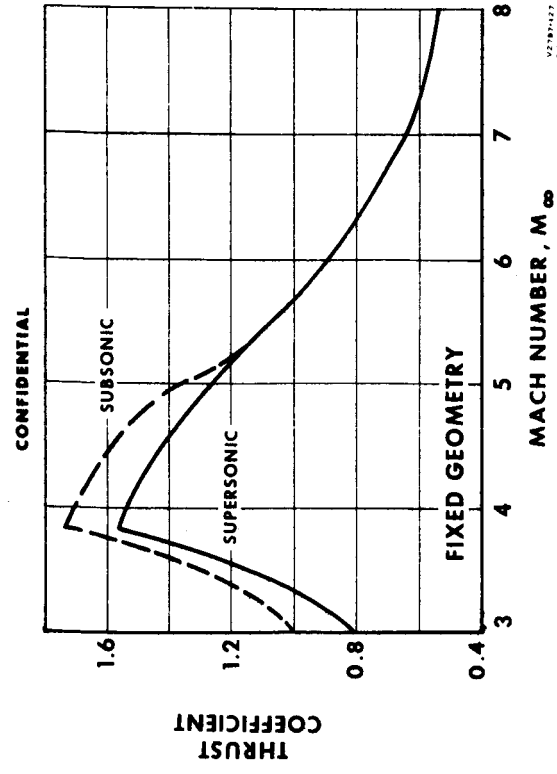

FIGURE 46. Typical Engine Performance with Thermal Compression

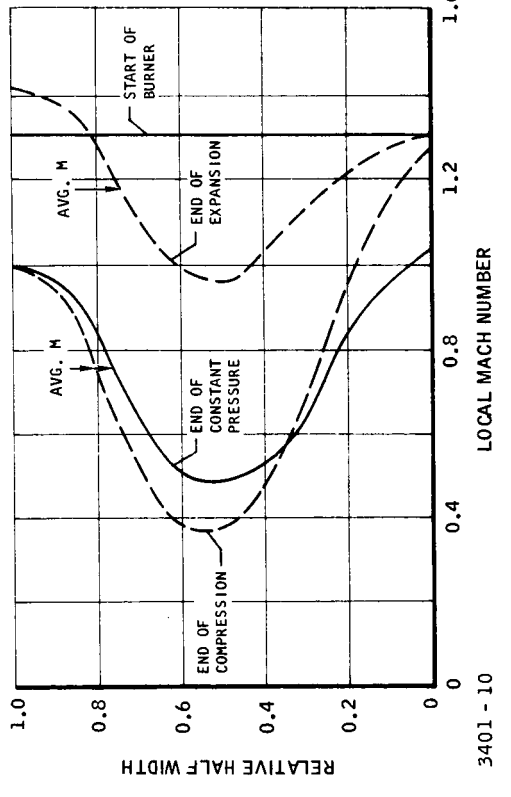

FIGURE 48. Mach Profiles - Subsonic Combustion Through Thermal Compression

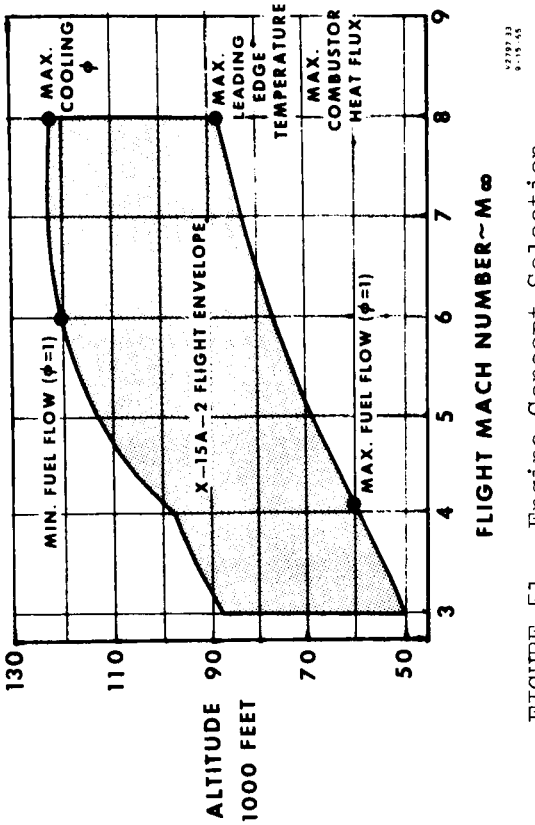

FIGURE 51. Engine Concept Selection - Critical Cooling Conditions

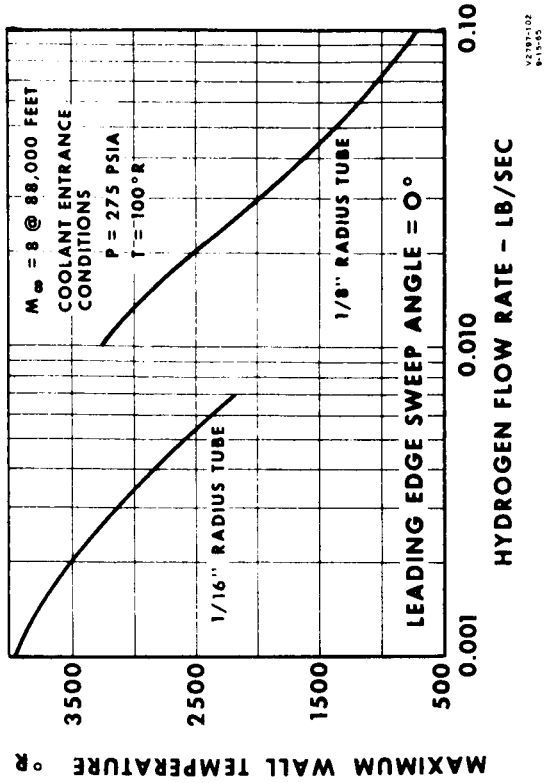

FIGURE 53. Regeneratively Cooled Leading Edge

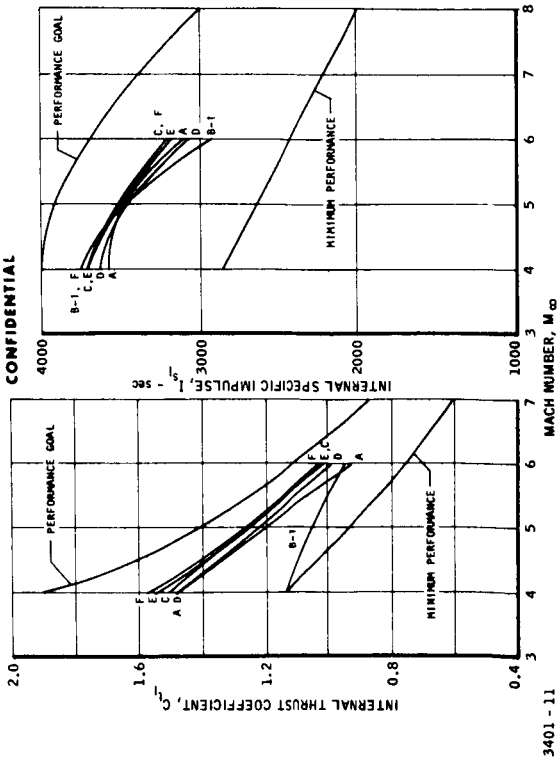

FIGURE 50. Thrust and Impulse Summary - Subsonic Combustion, High q Trajectory

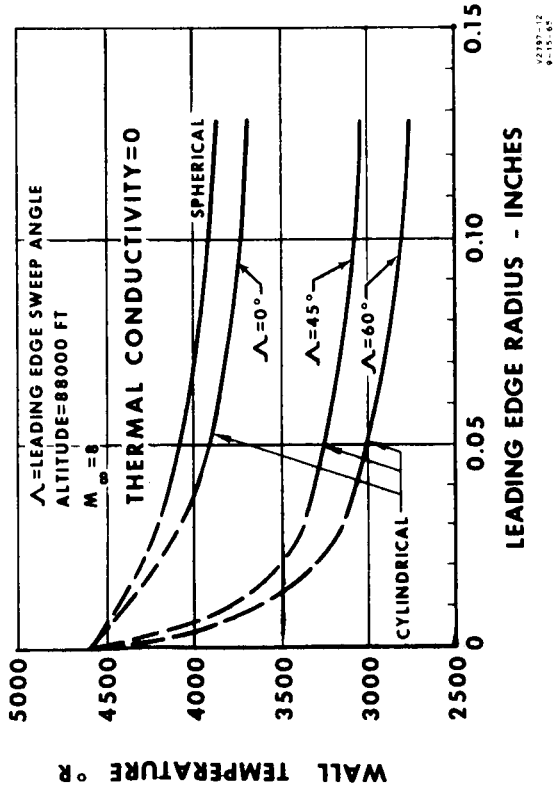

FIGURE 52. Radiation Cooled Leading Edge

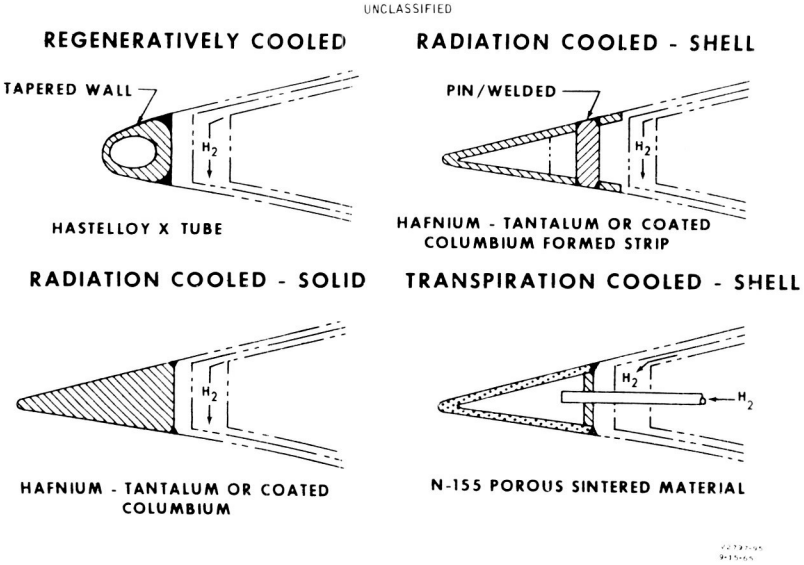

FIGURE 54. Permanent Leading Edge Structural Concepts

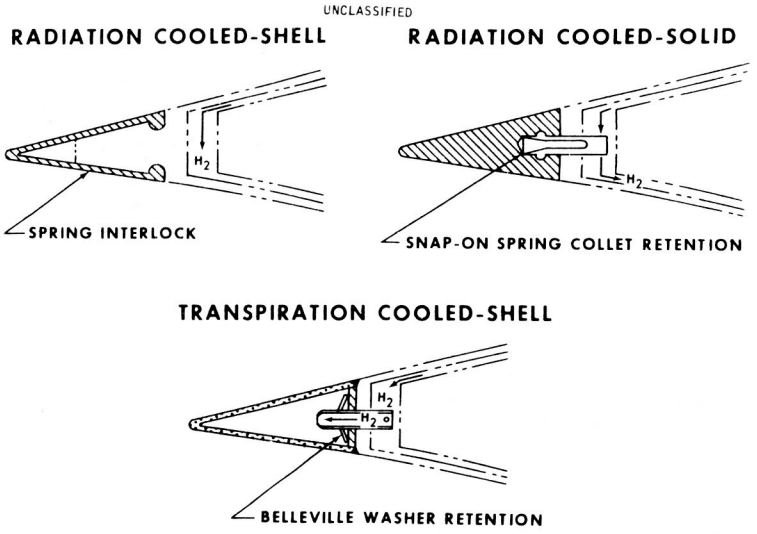

FIGURE 55. Replaceable Leading Edge Structural Concepts

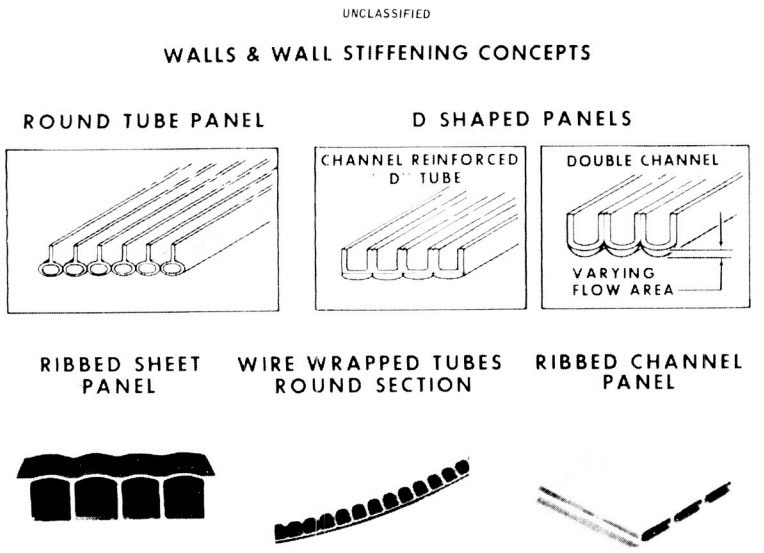

FIGURE 56. Engine Interior Surface Regenerative Cooling

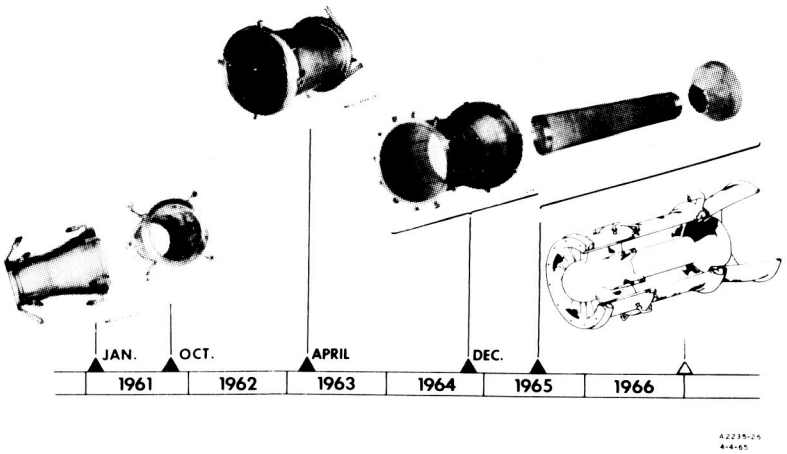

FIGURE 57. Typical Regeneratively Cooled Combustion Chambers

CONFIDENTIAL

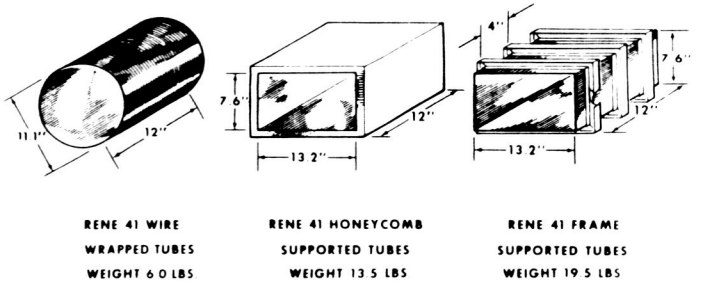

FIGURE 58. Combustor Weight Comparison

CONFIDENTIAL

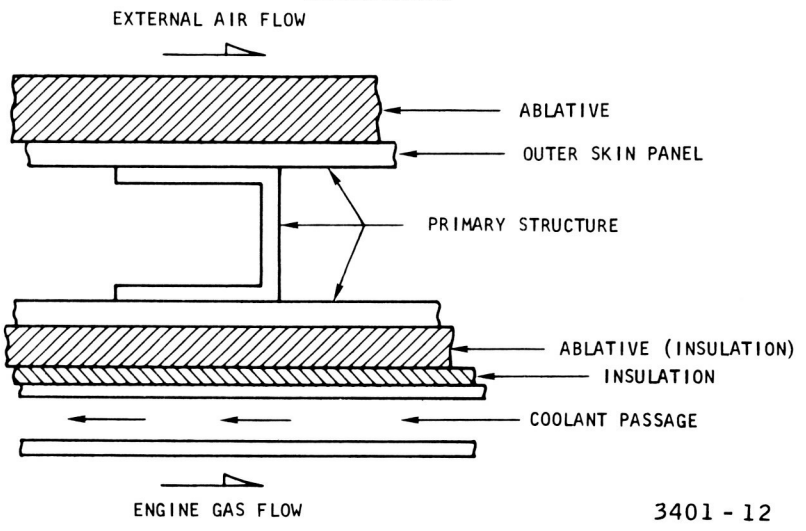

FIGURE 59. Schematic of Insulated Engine Structure/Cooling Systems

UNCLASSIFIED

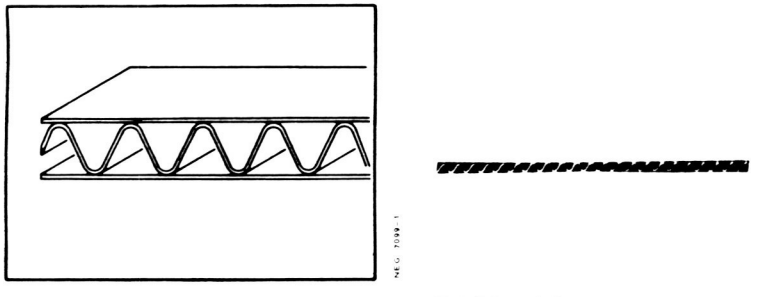

FIGURE 60. Corrugated Regeneratively Cooled Panel

UNCLASSIFIED

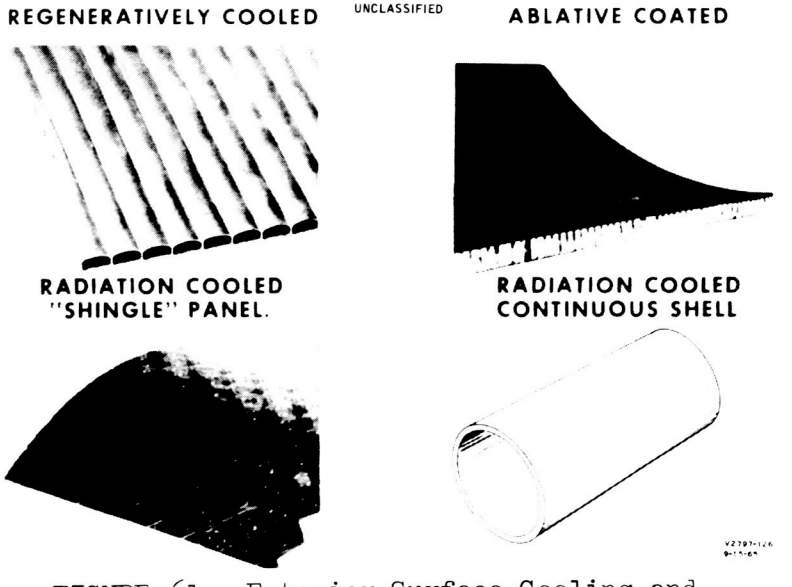

FIGURE 61. Exterior Surface Cooling and Structural Concepts

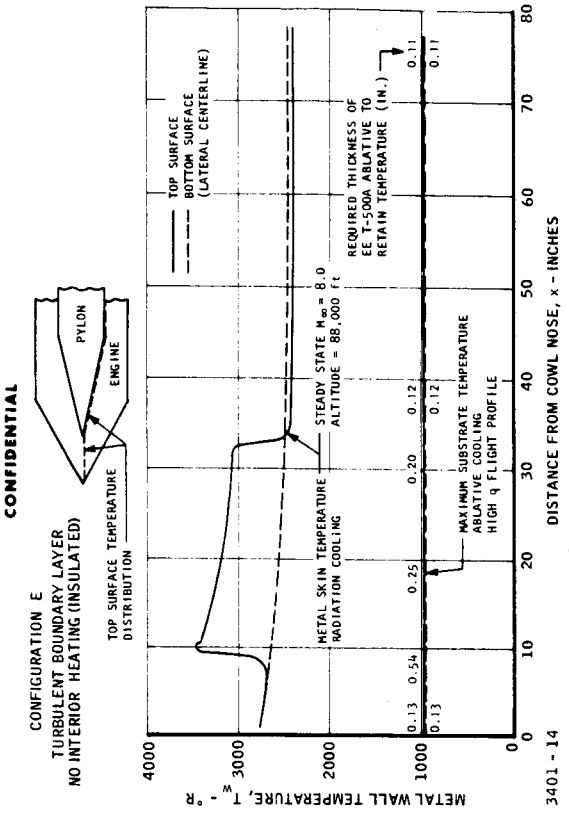

FIGURE 63. Engine Exterior Surface Metal Temperatures

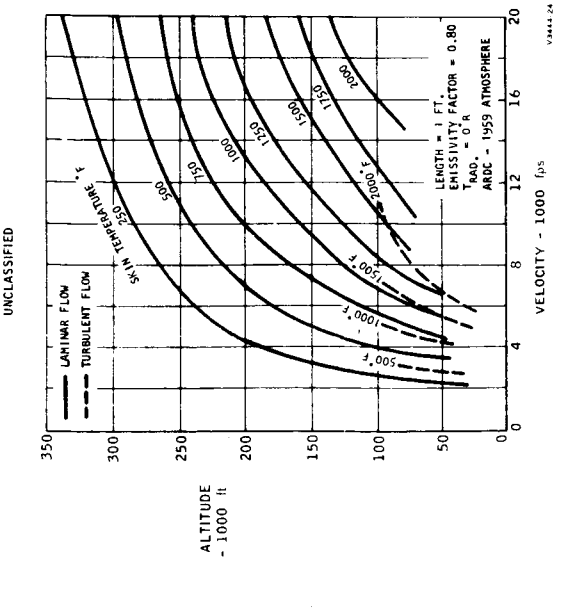

FIGURE 62. Radiation Equilibrium Surface Temperatures

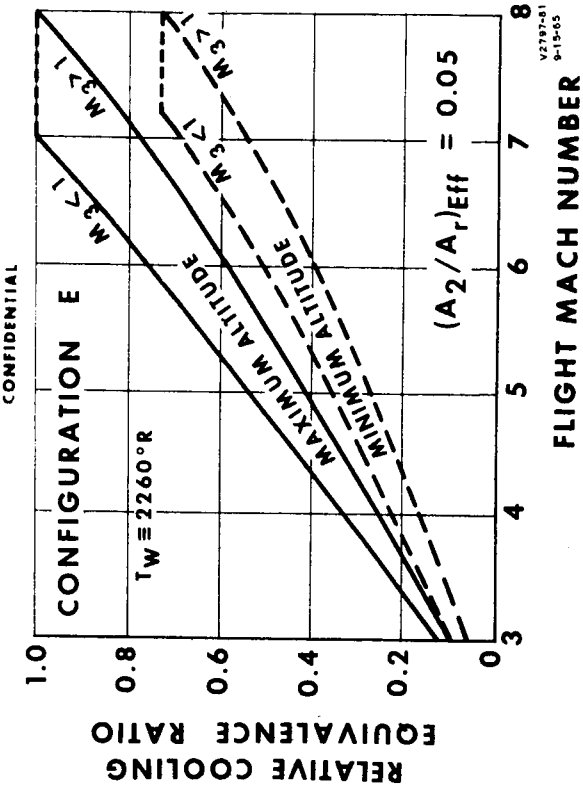

FIGURE 65. Relative Cooling Equivalence Ratios

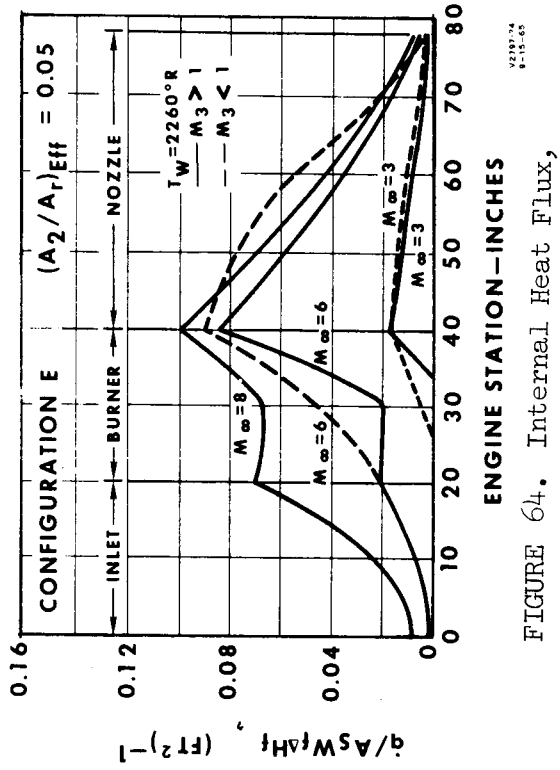

FIGURE 64. Internal Heat Flux, X-15A-2 Upper Boundary

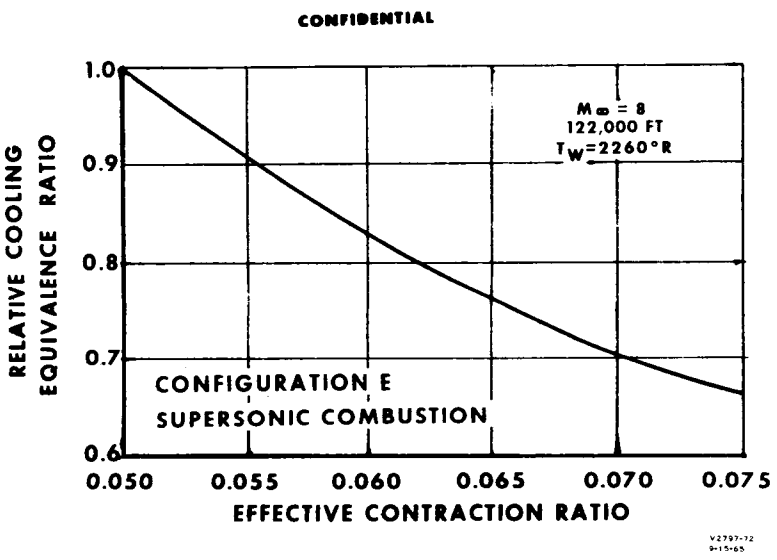

FIGURE 66. Engine Cooling Requirement Sensitivity

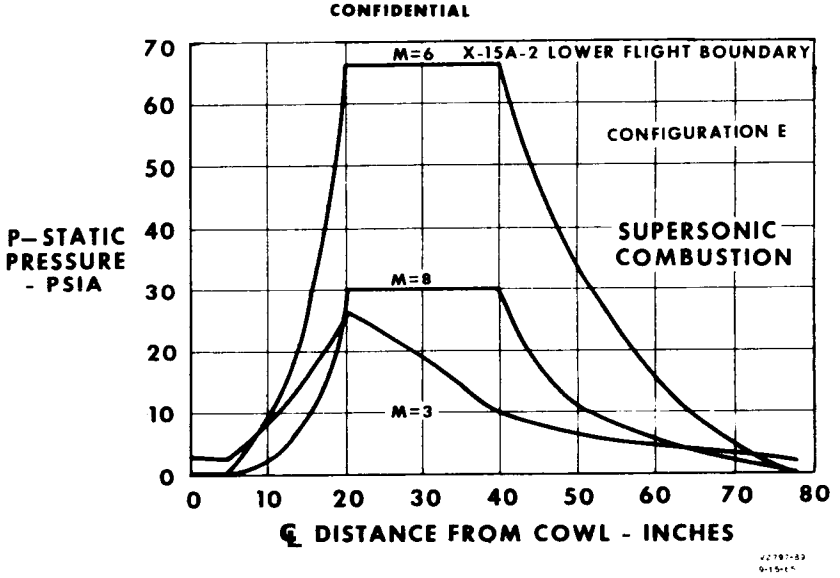

FIGURE 67. Engine Static Pressure Loading

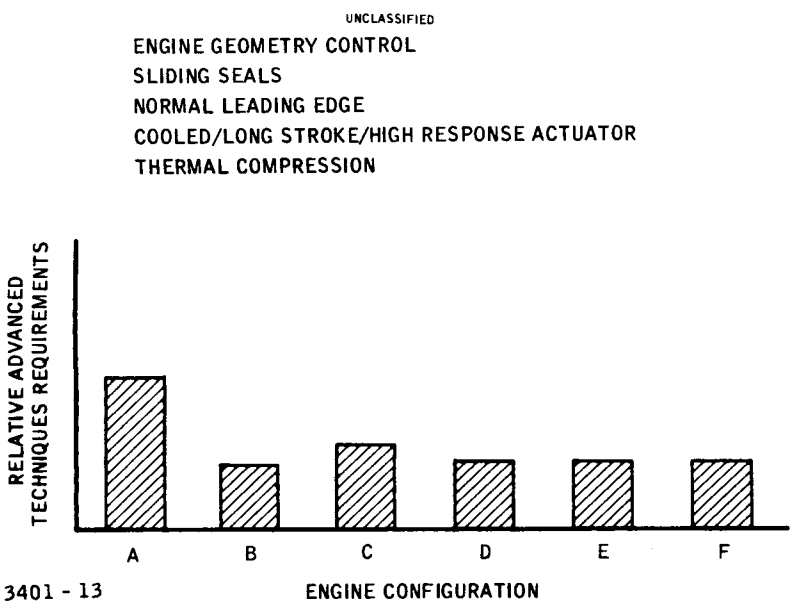

FIGURE 68. Advanced Technique Requirements

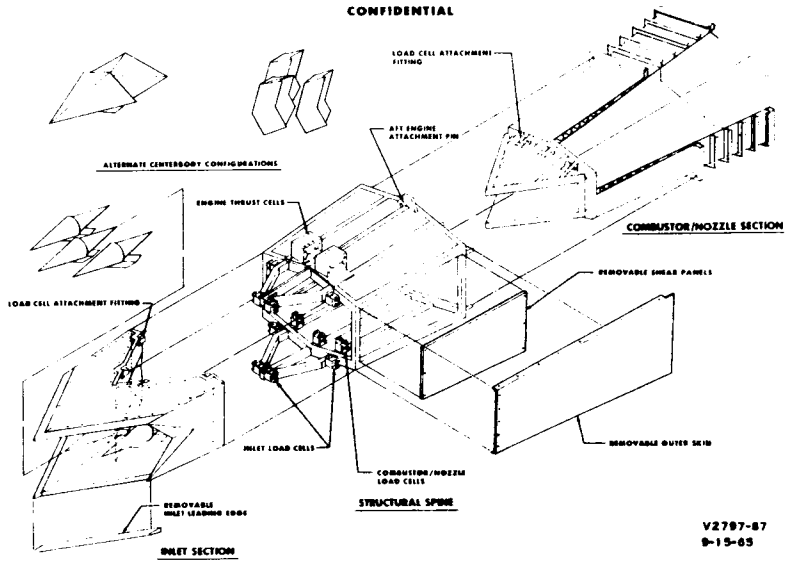

FIGURE 69. Conceptual Engine Structural Arrangement Showing Component Assembly and Interchangeability

UNCLASSIFIED

CONFIGURATION	EASE OF STRUCTURAL DESIGN	EASE OF COOLANT SYSTEM DESIGN	INTERCHANGEABILITY/ REPLACABILITY	RELATIVE WEIGHT	MFG. COST
A	Fair	Fair	Moderate	0.95	High
B - 1	Excellent	Good	Good	0.53	Medium
C	Good	Good	Excellent	0.58	Low
D - 6	Moderate	Moderate	Moderate	1.0	High
E	Fair	Moderate	Moderate	1.0	High
F	Fair	Good	Moderate	0.95	Medium

3401 - 15

FIGURE 70. Relative Engine Weight Comparison

CONFIDENTIAL

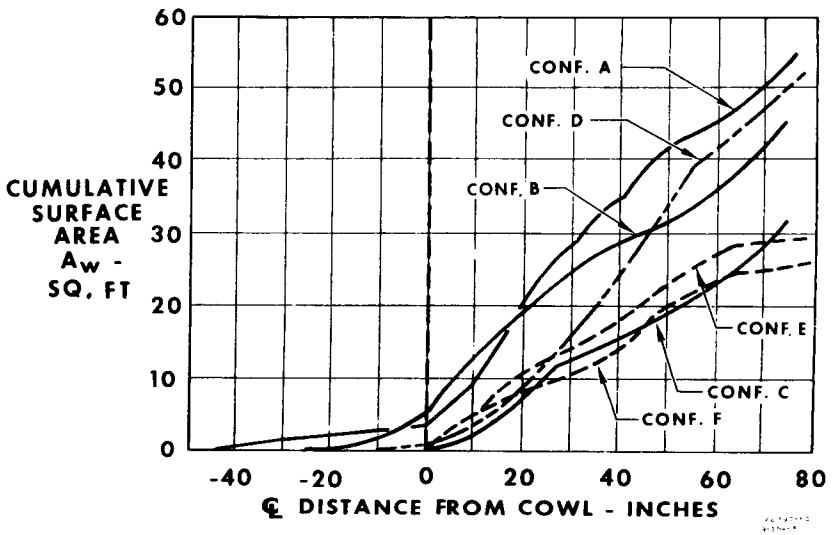

FIGURE 71. Comparative Studies - Engine Interior Surface Wetted Area Distribution

CONFIDENTIAL

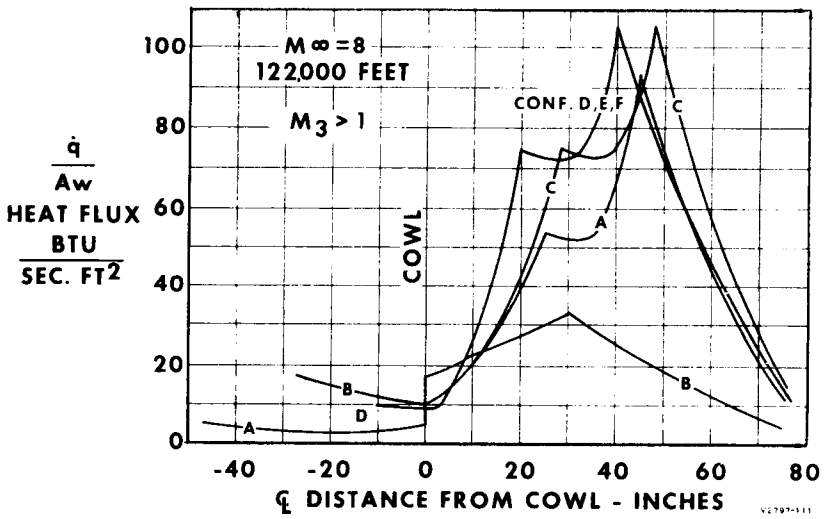

FIGURE 72. Comparative Studies - Engine Interior Surface Heat Flux Distribution

CONFIDENTIAL

CONFIG.	RELATIVE ϕ_c^*	A_{WE} SQ. FT.	A_{WC} SQ. FT.	LEADING EDGE LENGTH INCHES	LEADING EDGE LENGTH $\Lambda < 20°$ INCHES	COOLED SLIDING SEAL
A	1.12	53	12.8	57	57	YES
B	0.46	44	13.3	57	57	NO
C	0.88	31	6.3	92	5	NO
D	1.75	52	16.5	107	~ 0	NO
E	1.00	30	8.8	117	~ 0	NO
F	.88	26	7.6	117	~ 0	NO

* M_∞ = 8.0 @ 122,000 FEET

A_{WE} = ENGINE INTERIOR SURFACE AREA

A_{WC} = COMBUSTOR INTERIOR SURFACE AREA

FIGURE 73. Configuration Cooling Comparison

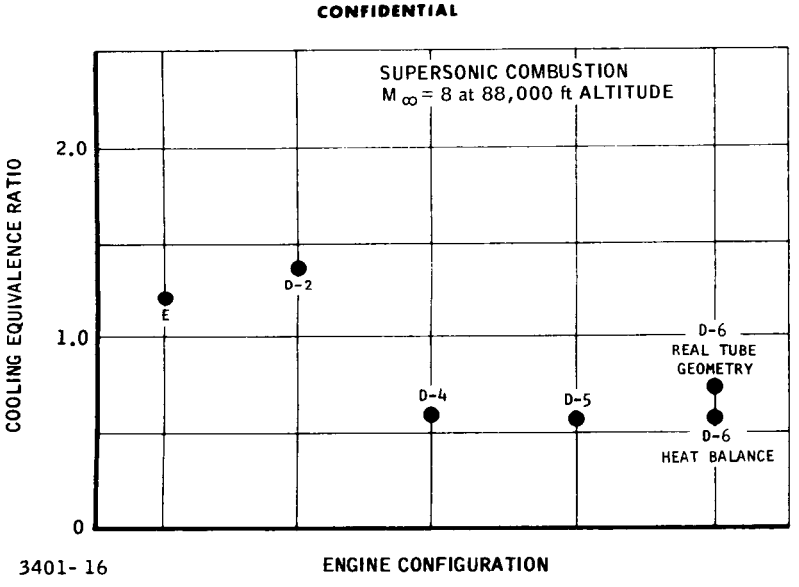

FIGURE 74. Cooling Reduction With Detailed Design

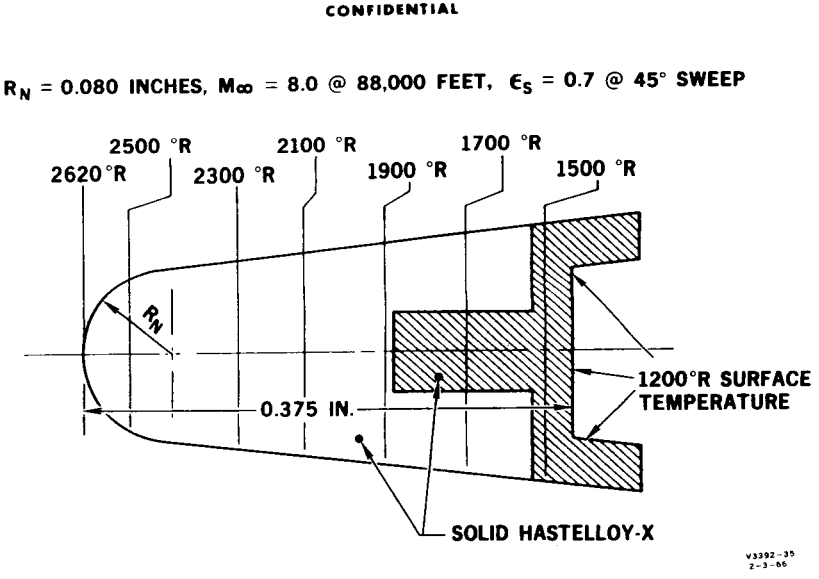

FIGURE 75. Leading Edge Temperature Distribution

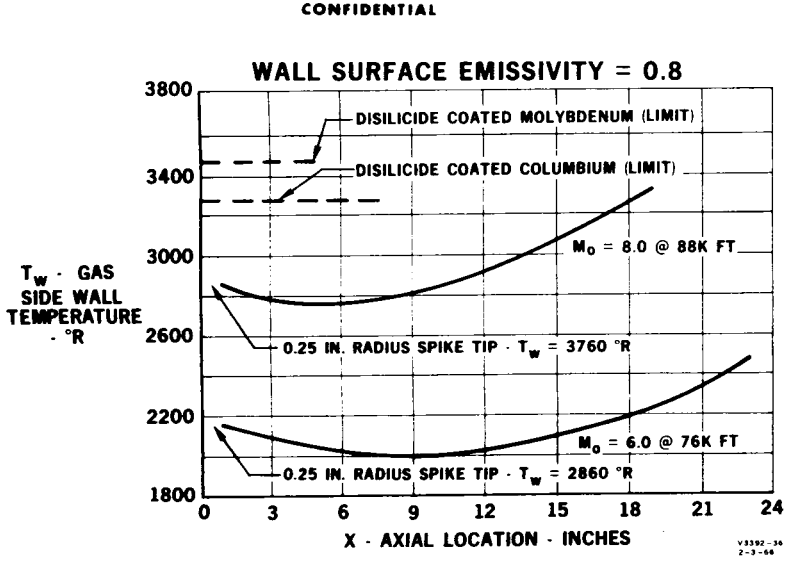

FIGURE 76. Center Body Temperature Distribution, Radiation Cooled Forward Section

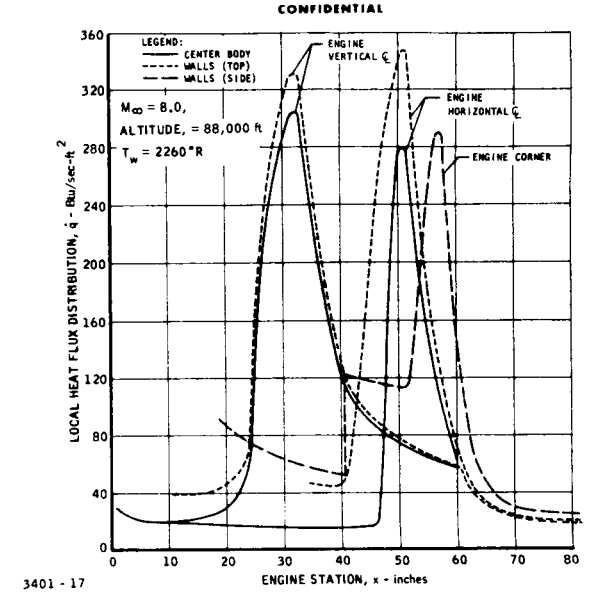

FIGURE 77. Internal Axial Heat Flux Distribution

UNCLASSIFIED

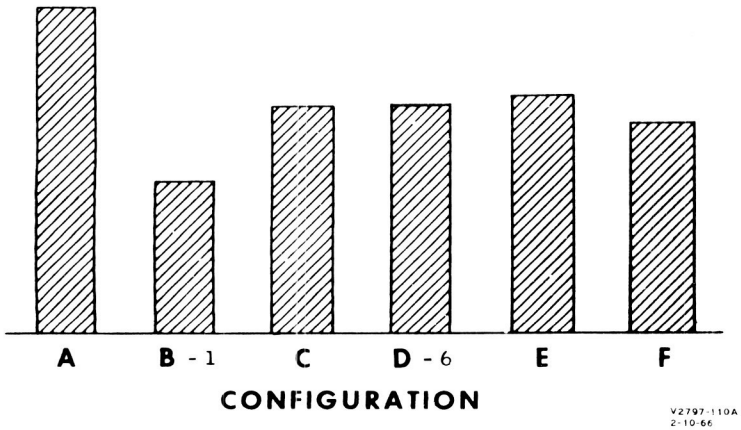

FIGURE 78. Relative Development Difficulty

UNCLASSIFIED

TYPE OF RESEARCH	SUITABILITY					
CONFIGURATION	A	B	C	D	E	F
■ BASIC AERO DYNAMICS						
■ 2-DIMENSIONAL FLOW				X	X	X
■ 3-DIMENSIONAL FLOW			X	X	X	X
■ AXI-SYMMETRIC FLOW	X	X	X			
■ EFFECT OF REYNOLDS NO.	X	X	X	X	X	X
■ EFFECT OF LEADING EDGE BLUNTNESS				X	X	X
■ COMBUSTOR DESIGN						
■ FUEL DISTRIBUTION AND FLOW (ON η_c)	X	X	X	X	X	X
■ FUEL MIXING, DIFFUSION, PENETRATION	X	X	X	X	X	X
■ REACTION KINETICS	X	X	X	X	X	X
■ SYSTEM INTERACTION						
■ ANGLE OF ATTACK	X	X	X	X	X	X
■ ENGINE GEOMETRY	X		X	X	X	
■ INLET RESTART TECHNIQUES (UNSTART CHARACTERISTICS)	X		X	X	X	X
■ CONTROL PARAMETERS	X		X	X	X	X
■ CONTROL DYNAMICS	X		X	X	X	X
■ INSTRUMENTATION	X	X	X	X	X	X
TOTAL	11	7	12	13	13	12

FIGURE 80. Applicability to Problems of Engine Design

CONFIDENTIAL

ENGINE VARIABLES

1. SPIKE POSITION
2. FUEL FLOW
3. FUEL DISTRIBUTION
4. REPLACEABLE CENTERBODY
5. REPLACABLE LEADING EDGE
6. DUAL MODE COMBUSTION
7. THERMAL COMPRESSION

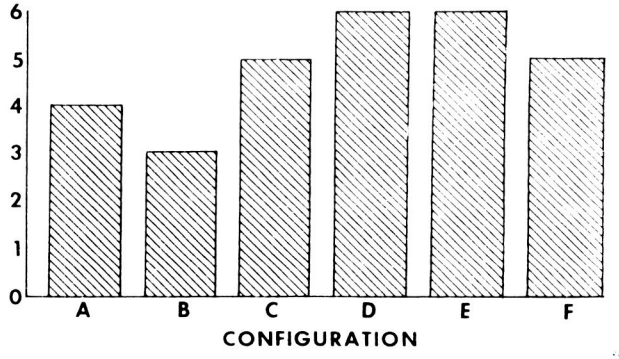

FIGURE 79. Relative Flexibility of Configurations

UNCLASSIFIED

RELATION OF RESEARCH DATA TO POTENTIAL APPLICATIONS

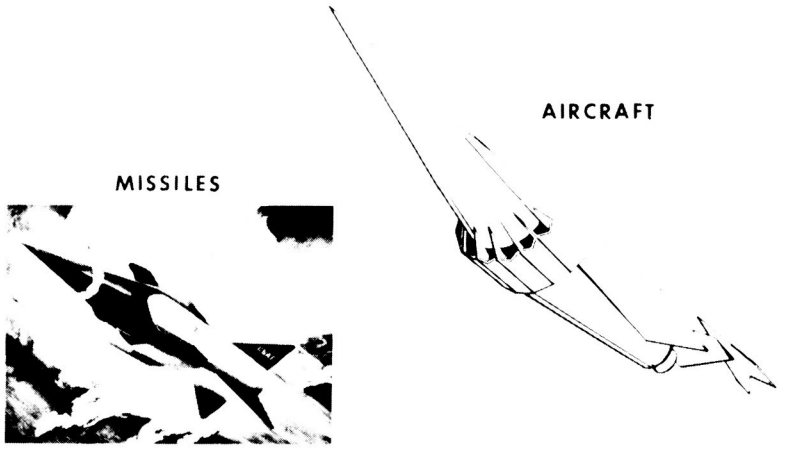

RECTANGULAR ENGINES/MODULES HAVE MAXIMUM APPLICABILITY

FIGURE 81. Potential Applicability

UNCLASSIFIED

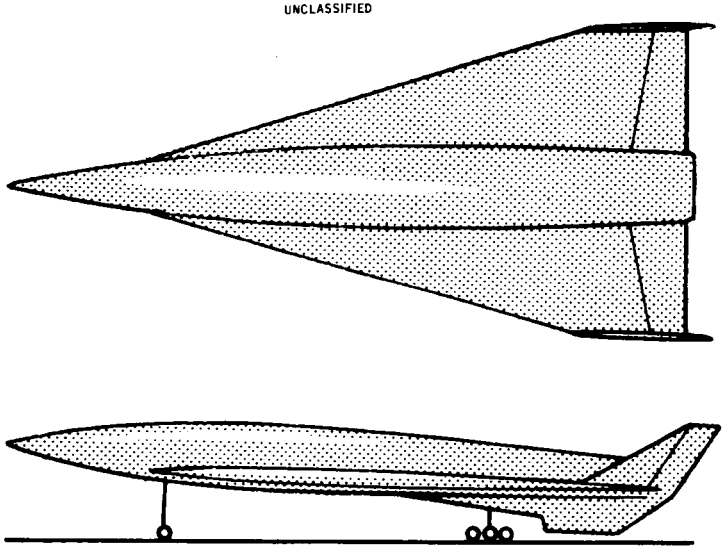

FIGURE 82. Engine Integration with Hypersonic Vehicle

UNCLASSIFIED

RELATIVE ADVANTAGES AND DISADVANTAGES

CONSIDERATION	CONFIGURATION A	B	C	D	E	F
RESEARCH POTENTIAL						
ENGINE COOLING						
DEVELOPMENT COST						
A) ANALYSIS AND TEST	+3	+5	+3	+3	+3	+3
B) FABRICATION						
C) TEST	+1	+2	+1	+1	+1	+1
PERFORMANCE	+3	+5	+3	+3	+3	+3
ENGINE LIFE						
ENGINE WEIGHT						
CONFIDENCE LEVEL	+3	+3	+3	+3	+3	+3
OPERATIONAL FLEXIBILITY						
X-15A-2 COMPATIBILITY						
+ ADVANTAGE Σ	+10	+15	+10	+10	+10	+10
– DISAVANTAGE						

NO DISADVANTAGES INCURRED BY SPECIFICATION CHANGE

V2707-119
9-15-65

FIGURE 83. Inlet Mach Number Design Specification Change Comparison

CONFIDENTIAL

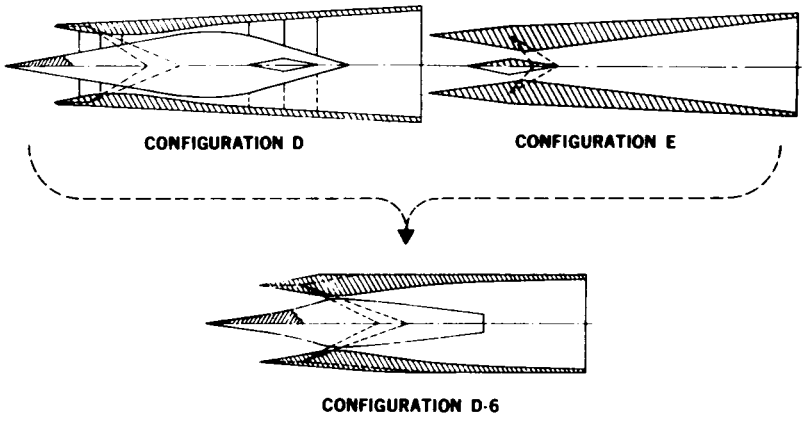

FIGURE 84. Configuration History of the MA-165 Hypersonic Ramjet Engine

V3392-64
2-3-66

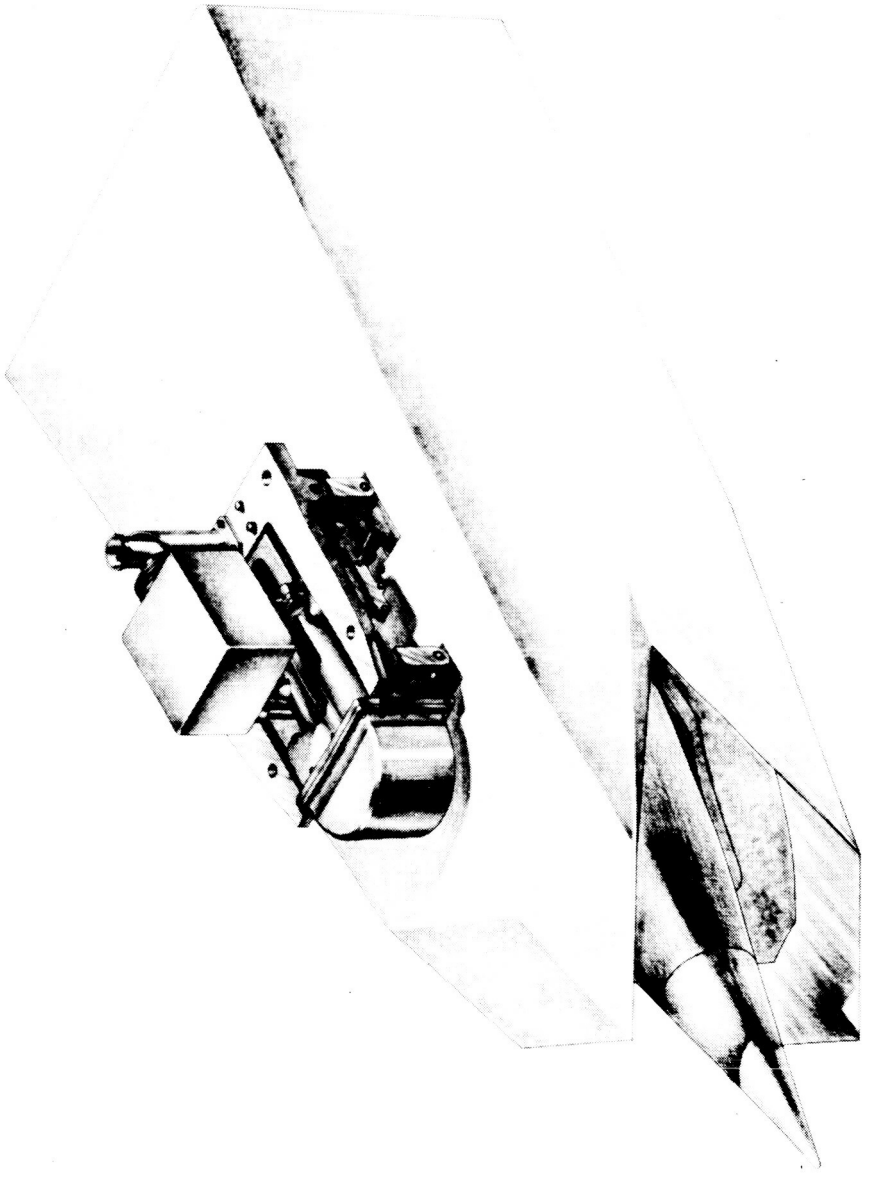

FIGURE 85. MA-165 Hypersonic Ramjet Engine (Configuration D-6)

DISTRIBUTION

Copy No.	Transmitted to
1 to 75 and Reproducible.	National Aeronautics and Space Administration Langley Research Center Langley Station Hampton, Virginia 23365 Mail Stop 126 Contract NAS-1-5117